# UNIVERSITÀ DEGLI STUDI DI TRIESTE

**XXII CICLO**

**SCUOLA DI DOTTORATO IN SCIENZE E TECNOLOGIE CHIMICHE E FARMACEUTICHE**

# CYCLIC POLYETHER PHYCOTOXINS *IN VITRO* STUDIES: EFFECTS OF YESSOTOXIN ON A PRIMARY CULTURE OF RAT CARDIOMYOCYTES-COMPARISON OF CIGUATOXINS AND BREVETOXINS POTENCY ON HUMAN VGSC OF BRAIN AND PERIPHERAL SENSORY NEURONS EXPRESSED IN HEK293 CELLS

**Settore scientifico-disciplinare Biologia Farmaceutica (BIO 15)**


*DOTTORANDO*
**Valeria Dell'Ovo**

*DIRETTORE DELLA SCUOLA*
**Prof. Enzo Alessio**

*RELATORE*
**Prof.ssa Aurelia Tubaro**

*CORRELATORE*
**Dott.ssa Chiara Florio**
**Dott. John S. Ramsdell**
**Dott.ssa Marie-Yasmine Dechraoui Bottein**


**ANNO ACCADEMICO 2008-2009**

# CONTENTS

**CYCLIC POLYETHER PHYCOTOXINS *IN VITRO* STUDIES: EFFECTS OF YESSOTOXIN ON A PRIMARY CULTURE OF RAT CARDIOMYOCYTES**


**Summary** ..... **1**

**Introduction** ..... **3**

Yessotoxin chemical structure ..... 3

Yessotoxin exposure ..... 4

Yessotoxin *in vitro* effects ..... 6

Ion channels: voltage gated sodium channels ..... 6

Ion channels: calcium channels ..... 6

Cyclic nucleotides: cyclic AMP ..... 7

Cyclic nucleotides: cyclic GMP ..... 8

Cytoskeleton: F-actin ..... 9

Cytoskeleton: E-cadherin ..... 9

Lysosomes ..... 10

Apoptosis and cell death ..... 10

Mitochondria ..... 11

Other effects ..... 12

Cardiomyocytes cultures ..... 13

**Aim of the study** ..... **15**

**Materials and Methods** ..... **17**

Isolation of heart cells and preparation of primary cultures ..... 17

Beating frequency experiments ..... 18

Electrophysiological recordings ..... 18

$Ca^{2+}$ imaging experiments ..... 19

Cyclic AMP quantification ..... 20

MTT viability assay ..... 21

Sulforhodamine B viability assay ..... 21

Cell nuclei fluorescent staining ..... 22

Glass coverslip preparation for fluorescent microscopy ..... 23

Mitochondrial membrane potential fluorometric measurement with JC-1 dye ..... 24

Caspase activity fluorometric quantification ..... 25

Cell necrosis fluorometric detection with PI dye ..... 25

Beating HL-1 atrial cardiomyocyte culture ....26
Mitochondrial membrane potential fluorometric measurement with TMRM dye ....27
Statistical analysis ....28
Chemicals ....28
**Results** ....**30**
Beating frequency observation after continuous exposure to YTX ....30
Membrane electrical activity and $Ca^{2+}$ release from intracellular stores in presence of YTX ....31
Intracellular cAMP accumulation in presence of YTX ....32
Cell viability assessment after continuous YTX exposure ....34
Cell viability assessment after a prolonged washout in YTX-free medium ....36
Nuclear morphology after continuous YTX exposure ....38
Nuclear morphology after prolonged washout in YTX-free medium ....40
Caspase activity after continuous exposure to YTX ....41
Cell necrosis after continuous exposure to YTX ....42
Short-term time course for YTX effect on mitochondrial membrane potential ....43
Time-course for YTX effect on mitochondrial membrane potential ....43
Effect of peripheral benzodiazepine receptor ligands on YTX mitochondrial effect ....45
**Discussion** ....**47**
**References** ....**54**

## SUMMARY

Yessotoxins (YTXs) are ladder-shaped polycyclic ether toxins, structurally related to brevetoxins and ciguatoxins (Ciminiello and Fattorusso, 2008). The parent compound of this class, yessotoxin, has been initially isolated from the scallop *Patinopecten yessoensis* (Murata *et al*., 1987). Only later their natural source has been identified in the phytoplanktonic dinoflagellates *Protoceratium reticulatum* (= *Gonyaulax grindley*) (Satake *et al*., 1997), *Lingulodinium polyedrum* (= *Gonyaulax polyedra*) (Tubaro *et al*., 1998; Paz *et al*., 2004) and *Gonyaulax spinifera* (Rhodes *et al*., 2006). When environmental conditions promote the growth of these species, their toxins accumulate in edible tissues of filter feeding shellfish exposed to these dinoflagellates, thus entering in the food chain. No human toxicity has been reported for YTXs, although YTXs contaminated-shellfish were worldwide recorded, thus, yessotoxin toxicological potential is still unknown.

Toxicological *in vivo* studies revealed high toxicity in mice after intraperitoneal administration ($LD_{50}$~μg/Kg), whilst very low toxicity (no lethality) was found after acute or repeated oral administration. Both routes are associated with clear evidence of ultrastructural cardiac alteration in rodent cardiac muscle, soon after toxin administration (Aune *et al*., 2002; Tubaro *et al*., 2003). Notwithstanding many *in vitro* studies highlighted numerous intracellular targets, YTX mechanism of action is unclear and the effects on the cardiac functional properties remain unknown. This study was performed on neonatal rat cardiomyocytes to study toxin effects on various fundamental aspects of cardiac muscle cells activity: cell beating, intracellular $Ca^{2+}$ and cAMP levels, cell vitality, mitochondrial membrane potential and type of cell death occurrence.

Results showed a time- and concentration-dependent reduction in the beating frequency (0.3 μM YTX, 1 h; $p<0.05$), neither associated to the uncoupling between the membrane electrical activity and $Ca^{2+}$ release from intracellular stores nor to the impairment of the mechanisms controlling the $Ca^{2+}$ homeostasis, nor to altered intracellular cyclic AMP levels. However, a decrease in the firing frequency (about 50%) occurred together with a 50% reduction of the number of beating cardiomyocytes.

A time- and concentration-dependent decrease in cell viability (0.1 μM YTX; 24 h) was observed, that evolved in two phases: at 24 h a significant ($p<0.001$) increase in mitochondrial activity (0.0001-1 μM YTX) together with membrane hyperpolarization (0.01-1 μM YTX;

*p*<0.001) occurred, with subsequent reduced cell viability and mitochondrial depolarization (0.01-1 μM YTX; *p*<0.001) starting from 48 h. YTX effect on mitochondrial potential wasn't affected by peripheral benzodiazepine receptor ligands PK-11195 and/or 4-chloro-diazepam (100 nM) after 24-48 h. Increasing concentrations of YTX induced the appearance of nuclear apoptotic bodies in a time-dependent way (0.001-0.1 μM YTX; 5-24 h), but no caspase activation (0.001-0.1 μM YTX; 5-72 h). Further viability experiments showed an irreversible cell damage, since no recovery occurred after up to 71 h in YTX-free medium. Moreover, 1 h exposure to 1 μM YTX was sufficient to inhibit beating activity and to cause irreversible reduction of cardiac cells viability. Propidium iodide uptake experiments showed a significant (*p*<0.01) increase of necrotic cells after 24 h (0.01 μM), but not after 5 h YTX exposure.
These results show a very cell-specific response to YTX if compared to previous studies, and a severe damage to *in vitro* cardiomyocytes. Thus, although no human intoxication due to YTX contamination has been reported so far, the toxicological potential of this compound should be better investigated.

Studying this toxin is limited by its non-commercial supply: YTX needed for this experiments was a kind gift of Professor T. Yasumoto.

# *INTRODUCTION*

## Yessotoxins chemical structure

Yessotoxins (YTXs) are ladder-shaped trans-fused ether rings toxins structurally related to brevetoxins and ciguatoxins (Ciminiello and Fattorusso, 2008). The parent compound of this class, yessotoxin, has been initially isolated in Japan from the scallop *Patinopecten yessoensis* (Murata *et al*., 1987) and thereafter detected in mussels throughout the world. Producing microalgae were detected in Japan, New Zealand, Norway, Italy, Scotland, and Chile (Howard *et al*., 2009). Toxins production takes places in the phytoplanktonic dinoflagellates *Protoceratium reticulatum* (*Gonyaulax grindley*) (Satake *et al*., 1997), *Lingulodinium polyedrum* (*Gonyaulax polyedra*) (Tubaro *et al*., 1998; Paz *et al*., 2004) and *Gonyaulax spinifera* (Rhodes *et al*., 2006). When environmental conditions promote the growth of these species, their toxins accumulate in edible tissues of filter feeding shellfish exposed to these dinoflagellates, thus entering in the marine food chain up to humans.

YTX is a disulfated polyether formed by 11 adjacent ether rings of different sizes and a terminal acyclic unsaturated side chain consisting of 9 carbons and 2 sulfate ethers.

About 100 yessotoxin analogues have been reported to date from both shellfish and dinoflagellates microalgae, although only the structure of 36 of them have been identified and characterized by NMR and /or LC-MS/MS techniques (Paz *et al*., 2008). As it is usually the case for marine toxins, some yessotoxins are directly produced by dinoflagellates, most of which derive from *P. reticulatum*, while a large number of derivatives is produced by the shellfish metabolism and differ in the oxidation state of the molecule, including hydroxilations, carboxylations, desulfatations, methylations, oxidations, amidations, changes in the length of the carbon chain, absence of the A ring, or glycosylation (Paz *et al*., 2008; Dominguez *et al*., 2009).

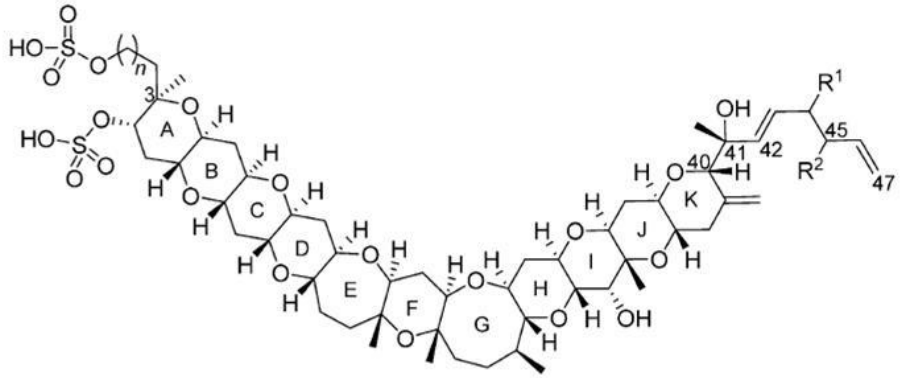

| toxin | $R_1$ | $R_2$ | n |
|---|---|---|---|
| YTX | $=CH_2$ | H | 1 |
| 45-hydroxyYTX | $=CH_2$ | OH | 1 |
| carboxyYTX | $CO_2H$ | H | 1 |
| homoYTX | $=CH_2$ | H | 2 |
| 45-hydroxihomoYTX | $=CH_2$ | OH | 2 |
| carboxyhomoYTX | $CO_2H$ | H | 2 |

**Figure 1: yessotoxins and main natural derivatives**
(Miles *et al*., 2005).

## Yessotoxin exposure

Yessotoxins are often co-present in shellfish contaminated with lipophilic marine toxins responsible of Diarrhetic Shellfish Poisoning (DSP) episodes, and bivalves extracts give positive results in the mouse bioassay traditionally employed to detect DSP toxins (Terao *et al*., 1990; Ogino *et al*., 1997). For this reasons, yessotoxins were initially included in the Diarrhetic Shellfish Poisoning (DSP) toxins group, but since neither *in vivo* diarrhea after oral administration (Ogino *et al*., 1997; Tubaro *et al*.,1998, 2003), nor *in vitro* inhibition of protein phosphatases (Ogino *et al*., 1997) occur, the European Commission classified YTX into a

separately regulated phycotoxin group (Directive 2002/225/EC), then derogated by Regulation Nº 853/2004/EC, which was amended by Regulation 2074/2005/EC of the European Commission (Paz *et al*., 2008).

Yessotoxin microalgae production is a worldwide phenomenon, with producing algae localization in Spain, United Kingdom, Italy, Ireland, Norway, United States (California, Florida, Washington), New Zealand, Canada, Japan, South Africa (Howard *et al*., 2009). Notwithstanding YTXs contaminated-shellfish were worldwide recorded and sometimes even at high concentrations up to several mg/kg (Munday *et al*, 2008; Paz *et al*, 2008) no reports of human poisoning induced by yessotoxins have been reported so far, thus human symptoms of intoxication are unknown.

To mice, either acute or repeated oral administration of yessotoxin, homoYTX and 45-hydroxy-homoYTX is not lethal, does not induce diarrhoea or provoke any evident symptom or sign of toxicity (Terao *et al*., 1990; Ogino *et al*., 1997; Munday *et al*., 2001; Aune *et al*., 2002; Tubaro *et al*., 2003, 2004, 2008a; Espenes *et al*., 2006). This could be due to a poor adsorption after oral intake: Tubaro *et al*. (2008a) reported a mean blood concentration of only 3.12 ng YTX equivalents/ml of blood 24 hours after the last 7 days-administration (1 mg/kg/day).

Histopathological studies revealed ultrastructural changes only at cardiac level 40 minutes to 24 hours after acute exposure (1-10 mg YTX/kg) (Aune *et al*., 2002; Tubaro *et al*., 2003) and daily repeated oral exposure to the toxin (1 and 2 mg/kg/day, for 7 days) (Tubaro *et al*., 2008a). Alterations were not detected at lower doses (0.5 mg YTX/kg) (Terao *et al*., 1990).

Ultrastructural alterations consist of swelling and cytoplasmic protrusions of cardiac muscle cells into the pericapillary space, package of rounded mitochondria and myofibrillar alterations (Aune *et al*., 2002; Tubaro *et al*., 2003). The cardiac tissue damage seems to be only temporary, since it was present 30 days after exposure (1 mg YTX/kg/day, for 7 days), while after 90 days a complete recovery occurred leaving no differences between control and YTX-treated mice were observed (Tubaro *et al*., 2008a). Moreover, non consecutive daily administration of YTX (1-5 mg YTX/kg twice a week within 21 days) resulted in no heart ultrastructural alteration 3 days after the last exposure (Espenes *et al*., 2006).

Acute intraperitoneal injection of YTX and some analogues was lethal to mice at doses between 0.08-0.1 and 1 mg/kg (Terao *et al*., 1990; Ogino *et al*., 1997; Aune *et al*., 2002; Tubaro *et al*., 2003; Franchini *et al*., 2004a and b). Similarly to oral administration, toxin

intraperitoneal injection affect cardiac tissue with ultrastructural changes such as swelling and separation of mitochondria and myofibrils (Terao *et al*., 1990; Aune *et al*., 2002).

YTX lethal doses cause restlessness, dyspnoea, jumping (Tubaro *et al*., 2003), shivering, and cramps (Aune *et al*., 2002) before death. Other alterations have been observed in mice cerebellar Purkinje cells and thymus (Franchini *et al*., 2004a and b).

Interestingly, di-desulfo-YTX showed a different target organ, by induction of mainly pancreas and liver alterations, with a severe fatty degeneration (300-500 µg/kg). Only a slight deposition of fat droplets was observed in cardiac muscle.

Notwithstanding the toxicological potential of yessotoxins is under debate, the few toxicological data pose for the possible risk for human health consequent to its exposure.

## Yessotoxin i*n vitro* effects

### *Ion channels*

*Voltage gated sodium channels*

Yessotoxin structure is very similar to brevetoxins and ciguatoxins, two neurotoxin groups that bind to receptor site 5 on voltage gated sodium channels increasing cell membrane permeability to sodium ions. Experiments performed to investigate on a common target in mediating YTX activity seem to rule out this hypothesis. Inoue *et al*. (2003) found both yessotoxin (1 µM) and di-desulfo yessotoxin (4.2 µM) unable to displace [$^3$H] PbTx-3 from rat brain synaptosomes channels, indicative of no binding on sodium channel site 5. Further experiments showed only a very small membrane potential depolarization in BE(2)-M17 human neuroblastoma cell line exposed to yessotoxin (1 µM) and in presence of veratridine no significant changes were detected, suggesting no interference of YTX on plasma membrane ion flux (Louzao *et al*., 2006).

Moreover, YTX induced rat cerebellar neurons cell death also in presence of saxitoxin and nefopam, two antagonists of voltage sensitive sodium channels (Pérez-Gómez *et al*., 2006).

*Calcium channels*

Some evidence of a modest and possibly indirect effect of YTX on calcium movements have been published on mammalian and mussel cells. de la Rosa *et al*. (2001a) studied YTX effect

on $Ca^{2+}$ homeostasis on freshly isolated human lymphocytes, founding a slight increase of intracellular $Ca^{2+}$ after YTX exposure (1 μM). This effect was abolished in calcium-free medium and in the presence of either nifedipine, a voltage-gated L-type calcium channel antagonist, or SKF96365, a receptor-mediated $Ca^{2+}$ entry inhibitor. YTX also exhibited a facilitatory effect on the influx of calcium induced by maitotoxin, a Ciguatera-related phycotoxin that activates $Ca^{2+}$-permeable, non-selective cation channels (de la Rosa *et al*., 2001b). On the other hand, YTX had an opposite, inhibitory effect in a calcium-free medium, reducing the $Ca^{2+}$ influx induced by the addition of 1 mM $CaCl_2$, and also inhibited the intracellular calcium increase evoked by the calcium-ATPase inhibitor thapsigargin (de la Rosa *et al*., 2001a).

On primary cultures of rat cerebellar neurons, 1 h exposure to YTX (25 nM) induced a slight but significant increase of intracellular calcium content, blocked by nifedipine and verapamil but not by TMB-8, an intracellular calcium antagonist (Pérez-Gómez *et al*., 2006).

Because of the modest increase in calcium influx, a direct interaction of YTX with voltage-sensitive L-type calcium channels was considered unlikely, as well as the role of calcium in YTX-induced cell damage, since in presence of channel blockers cell death still occurred.

YTX effect on L-type calcium voltage gated channels was also studied in the immunocytes from the mussel *Mytilus galloprovincialis* (Malagoli *et al*., 2006a), on which YTX (250 nM) doubled intracellular calcium concentration. The effect was totally abolished by verapamil, 2',5'-dideoxyadenosine, an inhibitor of adenylyl cyclase, and LY-83583, an inhibitor of soluble guanylyl cyclase. PKA involvement was excluded and it was thus hypothesized that YTX can influence both the activity of voltage-gated L-type calcium channel and cyclic nucleotide-gated cation channels. Recently, it has been reported that YTX (1 μM) did not alter the intracellular calcium transient in mouse skeletal muscle cells, but still caused a dramatic reduction of cell vitality (Tubaro *et al*., 2008b).

### *Cyclic nucleotides*

#### *Cyclic AMP*

Second messanger cyclic AMP (cAMP) involvement in YTX-induced cellular effects has been investigated on both human and mussel cells.

Experiments performed on human peripheral blood lymphocytes showed that YTX (1 µM) induced a dual effect on intracellular cAMP, dependent upon the presence or the absence of calcium in the culture medium. In the presence of extracellular $Ca^{2+}$, YTX induced a small and transient (within 90 seconds) increase of cyclic AMP soon followed by a decrease towards control levels, whereas a sustained and consistent increase was present in $Ca^{2+}$-free medium (Alfonso *et al*., 2003). YTX was then found to bind at least to $Ca^{2+}$-calmodulin-dependent PDE 1, cyclic GMP inhibited PDE 3, cyclic AMP-specific PDE 4, exonuclease PDE I (Alfonso *et al*., 2005; Pazos *et al*., 2006) and cGMP-stimulated phosphodiesterases PDE 2 together with desulfated yessotoxin (Mouri *et al*., 2009) but with low affinity (µM range).

In mussel immunocytes, a cAMP- and calcium-dependent effect of YTX on cell shape was found in cells activated by N-formyl-Met-Leu-Phe (fMLP), a chemotactic agent that promotes cellular changes and cell motility via both cAMP and phosphatidylinositol pathways. YTX (250 nM) induced a cell shape shift from a rounded inactive form to an ameboid active one, an effect that was counteracted by adenylyl cyclase inhibitor 2',5'-dideoxyadenosine and by verapamil. Inhibitors of protein kinase A (PKA), protein kinase C (PKC) and phosphoinositide 3-kinase (PI3K) (H-89, calphostin C and wortmannin, respectively), were ineffective (Malagoli and Ottaviani, 2004),

*Cyclic GMP*

As reported above, the only, and indirect, evidence of a role of cyclic GMP in the action of YTX has been obtained by Malagoli *et al* (2006a), on the basis of the ability of LY-83583, an inhibitor of soluble guanylyl cyclase, to impair YTX-induced intracellular calcium increase in mussel immunocytes (Malagoli *et al*., 2006a).

***Cytoskeleton***

After Franchini *et al*. (2004a) found by immunocytochemical technique some YTX-induced alterations to the cytoskeleton and the extracellular associated proteins of cerebellum Purkinje cells of mice intraperitoneally injected with YTX, several *in vitro* experiments on different cellular models confirmed the effect of YTX on cytoskeletal components, in particular F-actin and E-cadherin.

*F-actin*

A significant, time-dependent decrease in F-actin filaments was found in cerebellar granule cell cultures after 24 and 48 h of contact (25 nM YTX) (Pérez-Gómez *et al*., 2006), in insect fat body IPLB-LdFB and mouse fibroblast NIH3T3 cell lines after 24 h, that end up after 72 h of treatment with the complete lost of cytoskeletal integrity (Malagoli *et al*., 2006b), and in rat L6 and mouse BC3H1 myoblast cell lines up to 48 h (100 nM YTX) (Suárez Korsnes *et al*., 2007). Yessotoxin induced also the cleavage of tensin, a protein localized at the focal adhesion contacts that links F-actin filaments to the extracellular matrix, maybe as a consequence of the activation of caspase-3 (Suárez Korsnes *et al*., 2007). In accordance with a delayed effect on cytoskeleton, with respect to early events (see Suárez Korsnes *et al*., 2006b), a short time of incubation (1-4 h) with YTX had no effects on F-actin levels even at high concentration (1 µM YTX) (Leira *et al*., 2003; Ares *et al*., 2005).

Interestingly, 24 h of treatment (1 nM YTX) decreased F-actin levels in MCF-7 human breast adenocarcinoma cells, but not in Caco-2 human colon adenocarcinoma cells, indicating a specific cell-related phenomenon (Leira *et al*., 2003; Ronzitti *et al*., 2007).

Recent results showed YTX (1 nM)-affected cytoskeletal F-actin organization after 12 hours exposure without a detectable reduction in its content but leading to changing in cell shape of J774 murine macrophages (Orsi *et al*. 2010).

*E-cadherin*

YTX also affected the degradation pathway of E-cadherin, a cell adhesion molecule expressed in epithelial cells that is linked to F-actin through the binding proteins β- and γ-catenins (Stemmler, 2008).

Exposure of the epithelial cell line MCF-7 to YTX (0.2-1 nM) for 20 h resulted in a concentration-dependent accumulation of a 100 kDa E-cadherin fragment ($ECRA_{100}$) (Pierotti *et al*., 2003) with an $EC_{50}$ value of 0.55 nM (Ferrari *et al*., 2004). YTX effect was selective for epithelial E-cadherin, since it was induced in the epithelial cell lines human breast adenocarcinoma MCF-7 cells, human intestinal Caco-2 cells and Madin Darby canine kidney MDCK cells, but not in the rat pheochromocytoma PC12 cells, which express N-cadherin. Furthermore, YTX couldn't induce accumulation of fragments of one other member of the cadherin family, the K-cadherin (cadherin-6) in the three epithelial cell lines employed (Ronzitti *et al*., 2004; Ronzitti *et al*., 2007). Contrary to *in vitro* observations, a study

performed *in vivo* exposing mice to repeated oral doses (1 mg/kg/day, for 7 days) showed that extracts from colon, but not from lung, kidney or serum, contained a 90 kDa fragment of E-cadherin ($ECRA_{90}$), but the content was significantly higher in colon extracts from control mice than from YTX-treated animals (Callegari *et al*., 2006).

The exact mechanism by which YTX at nanomolar concentrations affects the degradation pathway of E-cadherin is still unknown, but involves inhibition of its internalization and degradation, possibly as a consequence of an altered turnover of plasma membrane proteins (Callegari and Rossini, 2008).

In accordance to inhibited endocytosis, Orsi *et al*. (2010) found YTX (1-10 nM) as inhibitor of J774 murine and mouse peritoneal macrophages phagocytosis in terms of internalization and phagosome maturation.

### *Lysosomes*

YTX has been found to cause a time- and concentration-dependent alteration of lysosomal vesicles in two different cell lines, the insect fat body IPLB-LdFB and the mouse fibroblast NIH3T3 cells. Within 24 h of incubation with YTX (100 nM), this subcellular component was no more detectable, indicating that the lysosomal content had changed or had been released into the cytoplasm. Since this effect has been observed both in the invertebrate and in the vertebrate model after the same exposure time and with the same concentrations, the authors suggested that the involvement of lysosomes as a general mechanism of YTX action (Malagoli *et al*., 2006b). Indeed, YTX (1 nM) interferes with the disposal of the degradation products of E-cadherin in MCF-7 human breast adenocarcinoma cells in a manner that resembled that of chloroquine, a drug known for its ability to hinder the function of lysosomes, causing extensive cell death (Callegari and Rossini, 2008).

### *Apoptosis and cell death*

The effects of YTX exposure on both apoptosis process and mitochondrial activity are perhaps the aspects that have been mostly investigated *in vitro* until now.

Several authors have investigated the ability of YTX to induce apoptotic cell death and the results highlighted differences in toxin sensitivity among cell lines and cell line-specificity in biochemical responses. The first study on the apoptotosis-inducing activity of YTX was

performed on the BE(2)-M17 neuroblastoma cell line, where the toxin induced morphological and biochemical changes typical of the apoptotic process. Starting from 12 h of incubation in the presence of YTX (10 nM), an increase of the Annexin-V binding was found, that is indicative of the translocation of phosphatidyl serine from the inner to the outer leaflet of the plasma membrane, characteristic of apoptotic cells. YTX also induced an increase of caspase-3 activity and a decrease of DNA content after 48 h of exposure. Only at high concentration (1 μM YTX) a reduction of mitochondrial membrane potential, morphological changes and DNA degradation after 12, 24 and 48 hours, respectively, were observed. The integrity of the plasma membrane was maintained throughout the whole period (up to 72 h) (Leira *et al*., 2002). Similarly, caspase activation, in particular of caspase-3 and -7, and DNA fragmentation have been demonstrated in HeLa $S_3$ cells exposed for 48 h to YTX (1 nM) (Malaguti *et al*., 2002), and DNA fragmentation, with condensation or fragmentation of chromatin, neurite fragmentation and appearance of apoptotic nuclei was observed in rat cerebellar neurons cultures exposed for 16 h to YTX (25 nM) (Pérez-Gómez *et al*., 2006). Caspase-3 and -9 activation, but not DNA fragmentation, was found by Suárez Korsnes *et al*. (2006a) in undifferentiated rat L6 and mouse BC3H1 skeletal muscle myoblast exposed for 48-72 h (100 nM YTX). Cells morphology also underwent to characteristic apoptotic sequential changes, such as cell shrinkage and plasma membrane blebbing, with a L6 cells higher sensitivity to YTX than BC3H1 cells.

On the contrary, YTX (10-100 nM) failed to induce a clear, unambiguous pro-apoptotic effect in both IPLB-LdFB insect fat body and NIH3T3 mouse fibroblast cells. Indeed, nuclear integrity was generally maintained with only a small percentage of insect cells showing DNA fragmentation (Malagoli *et al*., 2006b). Similarly, activation of caspase-3 and -7 or fragmentation of poly(ADP)ribose polymerase were not detected in Caco-2 and MCF-7 cells exposed to YTX (1 nM) (Callegari and Rossini, 2008).

Apoptotic phosphatidylserine exposure and necrotic cells were detected in HepG2 cell line after 12 and >24 hours exposure to YTX (1.4 μM), respectively (Young *et al*., 2009).

### *Mitochondria*

The involvement of mitochondrial permeability transition pore (PTP) in YTX toxic effects has been directly demonstrated in mitochondria isolated from livers of male Wistar rats (Bianchi *et al*., 2004). In this system, YTX acted as a potent pore opening reducing PTP

opening time ($K_{50}$ 197 nM) and leading to membrane depolarization. These effects were abolished by the PTP inhibitor cyclosporine A, demonstrating a direct effect of YTX on PTP. Notably, YTX was able to cross cell membrane and exerted a PTP-inducing effect in intact MH1C1 Morris Hepatoma cell line, where a concentration- and time-dependent depolarization of mitochondrial membrane occurred.

The involvement of the mitochondrial pathways in YTX-induced apoptosis has been confirmed in rat L6 and mouse BC3H1 skeletal muscle myoblasts, on which YTX (100 nM) induced loss of the mitochondrial membrane potential, opening of the PTP and release of cytochrome *c* and of the pro-apoptotic factor Smac/DIABLO (Suárez Korsnes *et al*., 2006b). Transmission electron microscope analysis confirmed the occurring of biochemical changes concomitantly to morphological changes such as swelling of mitochondria, increased density of the matrix space with loss or decrease of cristae number (Suárez Korsens *et al*., 2006b).

***Other effects***

Yessotoxin-treated cells increased cytokine release such as interleukin-2 in human lymphocytes after 20 hours exposure to 1 μM YTX (Alfonso *et al*., 2003), and such as TNF-α, MIP-1α and MIP-2 in J774 murine macrophages after 12 hours exposure to 0.1-10 nM YTX (Orsi *et al*., 2010).

A first proteomic analysis of YTX effects was performed by (Young *et al*., 2009) examining protein changes in HepG2 cells exposed for 3, 12.5, 18 and 24 h to YTX (1.4 μM). Results revealed a wide range of YTX-affected proteins, included molecular chaperones such as heat shock protein isoforms and protein disulphide isomerase precursors, nuclear proteins such as hnRNPs and lamins, the cathepsins and enzymes involved in cellular metabolism.

## Cardiomyocytes cultures

### *Neonatal rat cardiomyocytes primary cultures*

Since Harary and Farley first separated Wistar neonatal rat cardiomyocytes and succeeded in making spontaneously beating cardiomyocytes *in vitro* for 40 days, primary culture of cardiomyocytes has been widely applied in the basis cardiological research (Fu *et al*., 2005). Nowadays, the cultures of neonatal rat cardiomyocytes represent a well-established model for the observation and the understanding of cellular aspects of the electrophysiological, contractile, morphological, metabolic and molecular properties of the myocardium. A broad spectrum of experiments has been performed on these cultures, such as studies of contraction, ischemia, hypoxia, hypertrophy, cell death, toxicity and transport of drugs (Chlopcikovà *et al*., 2001; Athias *et al*., 2006). The advantage in doing experiments with neonatal rat cardiomyocytes is the lack of the influences of hemodynamic factors existing *in vivo*. In addition, in cell culture is feasible to control artificially other concomitant factors.

Because cardiomyocytes lose their ability to proliferate shortly after birth, growth of heart tissue is governed by cell growth rather than by proliferation. This cardiomyocytes feature doesn't allow cell propagation and requires repetitive primary cultures for multiple experiments (Fu *et al*., 2005). Rat heart cells can be obtained from either neonatal or adult rats, but the former are advantageous because of their lower sensitive to the concentration of calcium in the medium. Moreover, phenotype of cultured neonatal rat cardiomyocytes is very stable whilst cells from rats older than 5 days give poor quality of cardiomyocytes preparation, with less active cells that lose quickly contraction ability (Chlopcikovà *et al*., 2001).

### *HL-1 cardiomyocytes*

HL-1 cell line was derived from AT-1 mouse atrial tumor cells obtained from transgenic mice in which the expression of SV40 large T antigen is cardiac-directed (Claycomb *et al*., 1998). HL-1 cells spontaneously depolarize and express the necessary ion channels required for generating action potentials characteristic of primary cardiomyocytes. Cells contain highly organized sarcomeres necessary for mediating contraction and intracellular ANF granules characteristic of atrial myocytes. Analysis of gene expression revealed that they exhibit an adult cardiomyocyte-like gene expression profile. This differentiated cardiac phenotype is

maintained *in vitro* through the addition in the media of components such as retinoic acid, norephinephrine, insulin and essential lipids. Nowadays HL-1 cardiomyocytes have been used as a model system to investigate the effect of common pathophysiological conditions such as hypoxia, hyperglycemia and hyperinsulinemia, electrophysiology and various cellular signalling pathways, apoptosis and cardiomyocytes cell cycle studies (White *et al*., 2004) and mitochondrial dynamics (Beraud *et al*., 2009).

# AIM OF THE STUDY

Yessotoxin (YTX) is a food chain contaminating phycotoxin that accumulates in edible tissues of filter feeding shellfish exposed to toxin-producer dinoflagellates and may be ingested by humans through seafood consumption. Toxins production takes places in the phytoplanktonic dinoflagellates *Protoceratium reticulatum* (*Gonyaulax grindley*) (Satake *et al*., 1997), *Lingulodinium polyedrum* (*Gonyaulax polyedra*) (Tubaro *et al*., 1998; Paz *et al*., 2004) and *Gonyaulax spinifera* (Rhodes *et al*., 2006). These algae have been localized in several countries, included Spain, United Kingdom, Italy, Ireland, Norway, United States (California, Florida, Washington), New Zealand, Canada, Japan, South Africa (Howard *et al*., 2009), and contaminated-shellfish detection became a worldwide occurrence. No reports of human poisoning induced by yessotoxin have been reported so far, thus human symptoms of intoxication are unknown.

*In vivo* toxicological studies have been performed in mice to clarify YTX toxicological potential. Either acute or repeated oral administration of yessotoxin is not lethal, nor provokes any evident symptom or sign of toxicity (Terao *et al*., 1990; Ogino *et al*., 1997; Munday *et al*., 2001; Aune *et al*., 2002; Tubaro *et al*., 2003, 2004, 2008a; Espenes *et al*., 2006), probably due to a poor adsorption after oral intake (Tubaro *et al*., 2008a). On the contrary, acute intraperitoneal injection revealed high toxicity in mice ($LD_{50}$~μg/Kg) (Terao *et al*., 1990; Ogino *et al*., 1997; Aune *et al*., 2002; Tubaro *et al*., 2003; Franchini *et al*., 2004a and b). Both routes are associated with clear evidence of ultrastructural cardiac alteration in mice, with swelling of muscle cells, separation of mitochondria and myofibrillar alterations (Terao *et al*., 1990; Aune *et al*., 2002; Tubaro *et al*., 2003). These alterations showed a rapid onset, appearing 40 minutes (Aune *et al*., 2002) to 24 hours (Tubaro *et al*., 2003) after acute exposure.

This cardiac tissue damage seems to be only temporary, since it was present 30 days after exposure (1 mg YTX/kg/day, for 7 days), while after 90 days a complete recovery occurred leaving no differences between control and YTX-treated mice (Tubaro *et al*., 2008a).

Notwithstanding the cardiac tissue seems to represent the main toxin target, the effects on the functional cardiac properties remain unknown. Isolated cardiac cells are widely used to study the functional properties of the cardiac tissue at the single cell level. Hence, this study was performed on neonatal rat primary cultures of cardiomyocytes with the aim of investigate the effect of YTX on cell vitality and on some fundamental aspects of cellular activity by several techniques such as:

a) cardiomyocytes contractile activity by patch-clamp recordings, $Ca^{2+}$ imaging, cell beating and cyclic AMP levels evaluation;

b) cell viability by MTT and sulforhodamine B (SRB) tests;

c) mitochondrial membrane potential by JC-1 and TMRM fluorescent dyes;

d) apoptotic and necrotic occurrence by nuclei fluorescent staining, caspase assay and PI uptake experiments.

# MATERIALS & METHODS

**Isolation of heart cells and preparation of primary cultures**

Neonatal rat cardiomyocytes culture were prepared from one-three day old rat pups according to the method of Harary and Farley (1963) with some modifications. Experiments complied with the Italian D.L. n. 116 of 27 January 1992 and associates guidelines in the European Communities Council Directive of 24 November 1986 (86/609/ECC) concerning animal welfare.

For each culture isolation, twenty to forty Wistar rats obtained from a local conventional breeding colony were euthanized by decapitation and allowed to bleed. Hearts were aseptically removed by surgical dissection, taking ventricles only, placed in a 100 mm Petri dish containing 10 ml of ice-cold $Ca^{2+}$- and $Mg^{2+}$-free Hank's balanced salt solution (HBSS) and washed thoroughly to remove excess blood. Hearts were then minced into 1 $mm^3$ fragments, Hank's solution was replaced by 10 ml of 37 °C warm trypsin solution (0.1% w/v) and the preparation was stirred (MICROSTIRRER, VELP Scientifica) at 150-200 rpm for 10-15 minutes at 32-35 °C. Fragments were allowed to settle and supernatant was collected after each trypsinization, except for the first one which contains mainly cell debris, red blood cells, pericardial and endothelial cells and therefore should be discarded. Supernatant from subsequent trypsinizations was collected into 50 ml sterile tubes containing 20 ml of complete growth medium (Ham's F10 culture medium with 10% horse serum, 10% fetal bovine serum, 200.000 U/l penicillin, 0.2 g/l streptomycin and 1 mM L-glutamine) to inactivate trypsin enzyme. Tubes were centrifuged (ALC Refrigerated Centrifuge PK120R) at 150 x *g* for 10 min at 4 °C and resulting pellets were collected all together into one 50 ml tube with 2 ml of growth medium and stored on ice. Trypsinizations were repeated until all tissue fragments were dissociated (seven to nine trypsinizations). The final cell suspension obtained was filtered through 150 µm sterile mesh in order to exclude undissociated cells. Cells were pre-plated in two 100 mm Petri dishes with complete growth medium (20 ml/dish), and incubated at 37 °C in an atmosphere of 95% air and 5% $CO_2$. After one hour, medium was collected to harvest unattached cells and pre-plating was repeated a second time as above. Since non-muscular cells exhibit a more rapid attachment, this second pre-plating helps to exclude these cells and obtain a highly enriched myocyte preparation, as evidenced by cell morphology and spontaneous contraction. The myocyte cell suspension was then collected and cells were harvested by centrifugation (ALC Centrifuge 4222 MKII) at 102 x *g* for 5 minutes at room temperature (RT) and repeated twice. After pellet re-suspension in complete growth medium (10 ml), viable cells were counted in a hemacytometer by trypan blue test (0.4% trypan blue

in PBS saline solution) and plated as needed for experiments. Within 24 h of initial culture, cardiomyocytes started to exhibit spontaneous rhythmic contractions. Culture medium was renewed for the first time 24 h after plating, then every other day as well as the day before electrophysiological and $Ca^{2+}$ imaging measurements. All the cultures were employed within the fifth day of culture.

**Beating frequency experiments**

Cardiomyocytes were plated at a density of 1.2 x $10^6$ cells in 35 mm Petri dishes (2 ml/dish) and experiments were performed after 2-3 days of culture. Cultures were exposed to increasing YTX concentrations (0.01, 0.03, 0.1, 0.3 and 1 μM) and observed at different time points (0.5, 1, 5 and 24 h). Toxin vehicle control dishes were incubated with 1% ethanol. Cell beating frequency was evaluated by counting the number of cell contractions per unit time under the microscope. Optical fields were randomly chosen and observed for at least 3 minutes to ascertain the regular occurrence of spontaneous beats. For each experimental point 10 different fields per 35 mm Petri dish were observed and at least three different dishes were analyzed. Each experimental point was carried out with two different cell preparations.

**Electrophysiological recordings**

Cardiomyocytes were plated at a density of 1.2 x $10^6$ cells in 35 mm Petri dishes (2 ml/dish) and experiments were performed after 2-3 days of culture. Cell membrane potential changes were recorded in current-clamp, patch-clamp technique in a normal external solution (NES: 140 mM NaCl, 2.8 mM KCl, 2 mM $CaCl_2$, 5 mM $MgCl_2$, 10 mM glucose, 10 mM HEPES-NaOH, pH 7.4) both before and after a 1 h perfusion with 1 μM YTX. Access to the cytosolic compartment using the perforated patch clamp method was preferred to conventional whole-cell recording in order to provide exchange of small ions and to avoid intracellular second messenger washout. Membrane potentials were recorded with a pipette solution containing 10 mM NaCl, 0.005 mM $CaCl_2$, 1 mM $MgCl_2$, 10 mM HEPES, 140 mM K-aspartate, 0.1 mM EGTA, 2 mM MgATP, 5.6 mM glucose, pH 7.3 and were backfilled with the same solution containing amphotericin B (150 μg/ml) made fresh from a stock solution (20 mg/ml in dimethyl sulfoxide) kept at 4 °C. All data were acquired at room temperature (22-24 °C) with 4-6 MΩ patch pipettes using an Axopatch 200B (Axon Instruments, Foster City, CA)

amplifier, digitized through a Digidata 1321A interface (Axon Instruments) and stored on a PC-compatible hard disk. Currents were acquired at a sampling time of 10 µs and low-pass filtered at 2 KHz. For data acquisition and analysis, the pCLAMP software suite (version 8.0, Axon Instruments) and Origin 7 (Microcal Software, Northampton, MA) software were routinely used. To characterize cardiomyocyte firing properties, single-action potential amplitudes, resting potential and discharge frequency were measured. Only stable recordings were considered. Action potential amplitude was calculated from the baseline, and firing rate was obtained by averaging the instantaneous discharge frequency for at least 10 intervals in each recording.

### $Ca^{2+}$ imaging experiments

Cardiomyocytes were plated at a density of 1.2 x $10^6$ cells in 35 mm Petri dishes (2 ml/dish) and experiments were performed after 2-3 days of culture. As for membrane potential recordings, measurements of the intracellular $Ca^{2+}$ concentration ($[Ca^{2+}]_i$) were carried out by videoimaging technique before and after cell perfusion for 1 h with 1 µM YTX. Cell loading was performed with the fluorescent $Ca^{2+}$ dye fura-2 pentoacetoxymethylester (fura-2 AM) by incubation for 30 minutes at RT in NES solution supplemented with 10 mg/ml of bovine serum albumin and 5 µM fura-2 AM. During the experiments, cells were maintained in NES at a constant temperature of 37 °C. Videomicroscopy setup was composed of an inverted microscope (Zeiss, Oberkochen, Germany) equipped with an intensified charge-coupled device camera (Hammamatsu Photonics, Hammamatsu, Japan). Cells were alternately excited by a modified dual wavelength microfluorimeter (Jasco CAM-230, Tokyo, Japan) at 340 nm and 380 nm. Images were acquired at four frames per second. Calculation of 340/380 ratio images (pixel-by-pixel) and temporal plot of fluorescence changes were performed off-line. Mean fluorescence value was calculated for each cell observed. In temporal plots, fluorescent ratio at rest was assumed to be 1, and only fluorescence variations corresponding to a peak equal or higher than 1.5 were considered as a cell response. At least five optical fields were observed to estimate peak values of $[Ca^{2+}]_i$ transients and for each experimental condition the minimum number of analysed cells was 74.

**Cyclic AMP quantification**

Cardiomyocytes were seeded in 24-well tissue culture plates at a density of 0.3 x $10^6$ cells/well (1 ml/well) 72 h before experiments. Before experiments, cells were pre-incubated with warm serum-free medium (1 ml/well) for 10 minutes at 37 °C. Experiments began by replacing medium with warm serum free-medium (1 ml/well) containing test compounds and incubating cells for 10 minutes, 1, 5 or 24 hours. At the end of incubation time, extracellular medium was collected in Eppendorf tubes and stored at -20 °C until assayed. Ice-cold 0.1 N HCl was simultaneously added (0.25 ml/well) to stop cell reaction and wells were sonicated for 3 minutes each. Suspension pH was then neutralized by the addition of ice-cold 0.1 M Tris (0.25 ml/well), cells were collected in Eppendorf tubes to be centrifuged at 12,800*g* for 1 minute at RT (Eppendorf Centrifuge 5410) and stored at -20 °C until assayed. In each plate, two wells were kept for trypsinization (200 µl trypsin solution/well) at the end of experiments to determine viable cell number in a hemacytometer by trypan blue test (0.4% trypan blue in PBS saline solution).

Cell cyclic AMP production was determined by displacement of [$^3$H] cyclic AMP bound to a bovine adrenal extract rich in protein kinase A enzyme as described by Nordstedt and Fredholm (1990), with slight modifications (Florio *et al*., 1999). Different aliquots of each sample were added in duplicate in a 96-well MultiScreen-FB microtiter plate (50, 100 or 150 µl/well) together with the kinase binding protein solution (50 µl/well), 2 nM [$^3$H] cyclic AMP (37 MBq/ml, 50 µl/well) and different volumes of buffer (50 mM Tris-HCl, 250 mM NaCl and 10 mM EDTA, pH 7.4) up to a final volume of 250 µl/well. Plate filter membranes were wetted with ice-cold 50 mM Tris-HCl buffer (200 µl/well) for 5-10 minutes before loading samples. In each plate, a standard curve with known increasing quantities of unlabeled cyclic AMP (0.25, 0.5, 1, 2, 4, 8 and 16 nM final concentration) was run, and maximum (total) bound counts were determined in two wells in the absence of non-radiolabeled cAMP. After 150 min at 4 °C, the incubation was stopped by vacuum filtration using a MultiScreen Vacuum Manifold (Millipore Corporation, Bedford, MA) and empty well filters were quickly rinsed once with ice-cold 50 mM Tris-HCl buffer (200 µl/well) with vacuum still running to remove non-bound cAMP. Plate filters were air-dried under a lamp for 5-10 minutes and Optiphase SuperMix liquid scintillation cocktail was then added (25 µl/well). The microplate was placed in a counting cassette and allowed to sit overnight at RT before counting in a MicroBeta Trilux liquid scintillation counter (Wallac, Turku, Finland). The amount of cell cyclic AMP was calculated by interpolation of samples

counts per minute (cpm) from the linear portion of the standard curve by nonlinear regression. Experiments were performed in triplicate and quadruplicate with different cardiomyocyte preparations.

**MTT viability assay**

The cytotoxic effect of yessotoxin was quantified by the tetrazolium-dye assay introduced by Mosmann (1983) based on the ability of yellow soluble 3-[4,5-dimethylthiazol-2-yl]-2,5-diphenyl tetrazolium bromide (MTT) to form violet formazan crystals when reduced by mitochondrial dehydrogenase enzyme. Product quantity absorbance is linearly proportional to cell viability.

Cells were seeded into 96-well plates at a cell density of 0.2 x $10^6$ cells/ml (200 µl/well) in complete growth medium. After 24 h, cells were exposed to increasing concentrations of YTX (0.0001, 0.001, 0.01, 0.1 and 1 µM) for 24, 48 and 72 h. Toxin vehicle control wells were incubated with absolute ethanol for a final concentration of 1%. In a separate set of experiments, cells were treated with the same YTX concentrations as above for 1, 5 and 24 h, then washed with fresh medium without the toxin to continue cell culture up to 72 h.

YTX effect on mitochondrial dehydrogenase activity was evaluated also in presence of peripheral benzodiazepine receptor ligands PK-11195 and 4-chlorodiazepam. In these experiments, cells were exposed for 24 h to YTX, PK-11195 and 4-chlorodiazepam (0.1 µM) either alone or associated. When cells were treated with a ligand in presence of YTX, a pre-treatment with the ligand alone was performed for 1 h.

MTT solution (5 mg/ml PBS) was added (20 µl/well) 5 hours before the end of incubation time. Medium was then removed by vacuum aspiration and cellular formazan crystals were solubilized with dimethyl sulfoxide (200 µl/well). Absorbance was measured on an Automated Microplate Reader EL 311s (Bio-Tek Instruments, Inc., Winooski, VT) with a reference wavelength of 630 nm and a test wavelength of 540 nm. Each set of experiments was performed in 12 replicate wells for each toxin concentration and repeated at least three times with different cardiomyocyte preparations.

**Sulforhodamine B viability assay**

The SRB-based spectrophotometric assay was introduced by Skehan *et al*. (1990) and its excellent linear relationship between staining intensity and cell number as well as cellular

protein has been well demonstrated (Haselsberger *et al*., 1996; Keepers *et al*., 1991; Voigt, 2005). Sulforhodamine B (SRB) is a protein dye that under mild acidic conditions electrostatically binds to basic amino acid residues of fixed cells and under mild basic conditions can be extracted from cells and solubilised for measurement (Voigt, 2005).

Cells were seeded into 96-well plates at a cell density of 0.2 x $10^6$ cells/ml (200 µl/well) in complete growth medium and exposed after 24 h to increasing concentrations of YTX (0.01, 0.1 and 1 µM) for 24, 48 and 72 h. Toxin vehicle control wells were incubated with absolute ethanol for a final concentration of 1%. In a separate set of experiments, cells were treated with the same YTX concentration as above for 1, 5 and 24 h, then washed with fresh medium without the toxin to continue cell culture up to 72 h. At the end of incubation time, plates were centrifuged at 300*g* for 5 min at RT (Sigma 3K30 Celbio centrifuge), rinsed twice with warm calcium- and magnesium-free PBS (100 µl/well) and cells were fixed with ice-cold 50% (w/v) trichloroacetic acid solution (50 µl/well). After 1 h at 4 °C, wells were rinsed twice with bi-distilled water (100 µl/well), and cell proteins were stained with 0.4% sulforhodamine B in 1% acetic acid solution (100 µl/well). After 30 min at RT, plates were rinsed three times with 1% acetic acid (100 µl/well) to eliminate excess colorant and were allowed to air-dry for 5 minutes. Protein-bound dye was solubilised by repetitive pipetting of 10 mM tris(hydroxymethyl)aminomethane (Tris) solution (200 µl/well) and sample absorbance was determined on an Automated Microplate Reader EL 311s (Bio-Tek Instruments, Inc., Winooski, VT) with a single wavelength of 570 nm. Each experiment was performed in 8-12 replicate wells for each toxin concentration and repeated two to three times with different cardiomyocytes preparations.

**Cell nuclei fluorescent staining**

Cell nuclear DNA was stained to detect toxin-induced morphological alterations by fluorescence microscopy. Fluorochrome of choice was 4',6-diamidino-2'-phenylindole dihydrochloride (DAPI), which strongly binds to adenine-thymine, adenine-uracil and inosine-cytosine base pairs and emits in blue/cyan when excited with ultraviolet light.

Cells were seeded in 24-well plates aseptically pre-loaded with rounded 13 mm-glass coverslips at a seeding density of 0.5 x $10^6$ cells/well in complete growth medium (1 ml/well). After 24-48 hours cells were exposed for either 24, 48 and 72 hours to 0.01, 0.1 and 1 µM YTX or for 1, 5 and 24 hours to 0.001, 0.01 and 0.1 µM YTX followed thereafter by up to 71

additional hours of culture in fresh medium without the toxin. Negative controls and toxin vehicle control wells (1% ethanol final concentration) were set up for the same incubation times. Positive controls were incubated with 0.5 mM hydrogen peroxide for 1-24 h. Prior to cell staining, the wells were washed once with warm 0.1 M PBS (0.5 ml/well) and cells were fixed by overlaying with 2% paraformaldehyde in PBS (0.5 ml/well) for 30 minutes at RT. The solution was then removed and wells were washed three times with ice-cold 0.1 M PBS (0.5 ml/well). Cells were then stored at 4 °C with 0.1 M PBS (0.5 ml/well) until the fluorescent staining day. Cell staining began with three rinses for 5 minutes each, with ice-cold 0.1 M PBS (0.5 ml/well) while rocking plates on a shaker at RT. Non-specific binding sites were then saturated by incubation with 0.1 M glycine in PBS (0.5 ml/well) on a plate shaker for 5 minutes at RT. Wells were then rinsed three times for 5 minutes each with PBS as described above and cell membranes were permeabilized by incubating cells for 5 minutes with freshly prepared 0.1% Triton X-100 in 0.1 M PBS (0.5 ml/well). After three additional 5 minute-washes with PBS as above, cells were stained in the dark for 5 minutes with fresh-diluted DAPI (1 µg/ml PBS) (100 µl/coverslip). Wells were then washed three times with PBS as above and cells were dehydrated with decreasing dilutions of ice-cold ethanol (70, 90 and 100%) for three minutes each (0.5 ml/well). Glass coverslips were finally harvested and mounted onto glass microscope slides (76x26 mm) by pouring a few microliters of 1,4-diazabicyclo[2.2.2]octane (DABCO)-glycerol directly on the cell side surface. Coverslip borders were sealed with the application of clear nail polish and samples were stored at -20 °C in the dark. Pictures were acquired at 60x magnification with a NIKON Eclipse E800 fluorescence microscope equipped with DMX 1200 digital camera.

**Glass coverslip preparation for fluorescent microscopy**

Coverslips were first washed with xylene in a closed glass box by repeated shaking for 1 hour, then rinsed two times with acetone and left in an acetone bath for 2-3 hours, changing the solvent each hour. Acetone was then replaced by absolute ethanol and the bath was repeated as above. Cleaned coverslips were then stored in 100% ethanol until use.

**Mitochondrial membrane potential ($\Delta\Psi_m$) fluorometric measurement with JC-1 dye**

The fluorescent dye of choice was 5,5',6,6'-tetrachloro-1,1',3,3'-tetra-ethylbenzimidazolocarbocyanine iodide (JC-1), a lipophilic cation that produces two fluorescence emission peaks according to its physical form: at low concentration or at low $\Delta\Psi_m$ value it is principally present as a monomer and emits green fluorescence with an emission maximum at 527 nm. Conversely, at high dye concentration or high $\Delta\Psi_m$ value a multimeric form is predominant that emits orange-red fluorescence with an emission maximum at 590 nm (Mathur *et al.*, 2000). Thus, since the amount of cationic dye taken up by the mitochondrion depends on its transmembrane potential, at low $\Delta\Psi_m$ values the fluorescence emission will be mostly green, whereas at high $\Delta\Psi_m$ values it will shift to orange-red, providing a useful tool to observe the cell mitochondrial polarization state.

Cardiomyocytes were seeded at a density of 40.000 cells/well into 96-well plates in complete growth medium (100 µL/well) and exposed after 24 h to increasing concentrations (0.0001, 0.001, 0.01, 0.1 and 1 µM) of YTX for 24, 48 and 72 h. In a separate set of experiments, cells were treated for 24 and 48 h with 0.1 µM YTX either alone or in the presence of peripheral benzodiazepine receptor modulators 4-chlorodiazepam and/or PK-11195 at a concentration of 0.01 or 0.1 µM. Wells treated with either YTX and these compounds were pre-treated for 1 hour with inhibitors alone to ensure receptor occupancy before YTX addition. JC-1 kit solutions were prepared according to manufacturer protocol: 200 µM dye stock solution (25 µl) was diluted in a tube with 4 ml of bi-distilled water and gently mixed. The solution sat for 2 minutes at RT to ensure dye dissolution and 1 ml of 5x staining buffer was then added to the tube and mixed by inversion. In a separate tube, 1 mg/ml valinomycin stock solution (1 µl) was added to 770 µl of prepared dye solution, and an equal volume of serum-free medium was then added to both tubes (4.3 ml and 770 µl), pipetting well to mix. Afterwards, 1 µM valinomycin was used as a positive control for its ability to act as a potassium ionophore through lipid membranes dissipating membrane potential (Cossarizza, 1997). At the end of toxin exposure time, the medium was removed by vacuum aspiration and replaced with a dye solution (0.2 ml/cm$^2$ growth surface) to incubate for 20 minutes in a cell incubator at 37 °C. The medium was then removed by vacuum aspiration and wells were rinsed two times with warm serum-free medium (50 µl/well). Cold medium was then added (50 µl/well) and fluorescence was immediately measured. JC-1 aggregates' red fluorescence was detected with a 535 nm excitation filter and 595 nm emission filter combination whilst the monomers' green fluorescence was detected with 485 nm excitation filter and 535 nm emission filter

combination by an Infinite F200 fluorometer (Tecan Group Ltd, Männedorf, Swizerland). Results were expressed as a ratio between red and green fluorescence values and reported as a percentage relative to the mean control values. Each YTX concentration was tested in 3 to 12 replicates and experiments were repeated three to four times with different cardiomyocyte preparations.

**Caspase activity fluorometric quantification**

A Sensolyte® AFC Caspase Substrate Sampler Kit was used to determine cell caspase activity. Seven AFC-based peptide substrates (for caspase-1, -2, -3/7, -6, -8, -9 and -10) were chosen. Enzymatic activity profiling is based upon the fluorescent shift of free AFC (7-amino-4-trifluoromethyl coumarin conjugated at C-terminal) after cleavage from the caspase peptide substrate molecule using a fluorescence reader.

Cardiomyocytes were plated at a density of 40.000 cells/well into 96-well plates in complete growth medium (100 µL/well) and, starting 24 h after seeding, were then exposed to increasing concentrations of YTX (0.001, 0.01 and 0.1 µM) for 5, 24, 48 and 72 h. Positive control wells were exposed to 10 µM camptothecin and 0.1% DMSO was used as vehicle control wells. Both no cell- and negative-control wells were set up. Kit solutions were prepared according to manufacturer protocol: 1 M DTT was added to kit provided buffer (20 µl/ml buffer), and used to dilute AFC-based caspase substrate stock solutions to 100 µM as the final concentration. At the end of plate incubation time, prepared substrate solutions were added to each well (50 µl) and plates incubated for 60 minutes at RT rocking on a plate shaker at 100-200 rpm in the dark. An AFC standard curve was prepared by serial dilution of 10 mM AFC stock solution to 30, 15, 7.5, 3.75, 1.9, 0.9 and 0.5 µM final concentration in the same assay plate (100 µl/well). Fluorescence was measured with 360/35 nm excitation filter and 460/35 nm emission filter combination in a Microplate Fluorometer (Packard Instrument Co., Meriden, CT, USA. Each sample was tested in duplicate and the assay was performed two to three times with different cardiomyocyte preparations.

**Cell necrosis fluorometric detection with PI dye**

Propidium iodide (PI) is a nuclear staining-fluorescent impermeant dye normally excluded from healthy cells, but which penetrates damaged cell membranes of dying or dead cells and intercalates into double-stranded nucleic acids. Once bound, its fluorescence is enhanced 20-

to 30-fold, with a shift of ~30-40 nm in fluorescence excitation maximum to the red and a shift of ~15 nm in fluorescence emission maximum to the blue.

Cardiomyocytes were plated at a density of 40.000 cells/well into 96-well plates in complete growth medium (100 μL/well) and, starting 24 h after seeding, exposed to increasing concentrations (0.0001, 0.001, 0.01, 0.1 μM) of YTX for 5, 24, 48 and 72 h. At the end of the incubation time, plates were centrifuged (Sigma 3K30 Celbio centrifuge) at 170*g* for 1 minute at RT, medium was removed by vacuum aspiration and replaced with 3 μM propidium iodide in PBS (200 μL/well). In positive control wells, cells were lysed by the addition of 10% Triton X-100 in PBS (4 μL/well). Plates were incubated for 30 minutes in a cell incubator at 37 °C. Fluorescence was measured with 530/25 nm excitation filter and 590/20 nm emission filter combination in a FluoroCount Microplate Fluorometer (Packard Instrument Co., Meriden, CT, USA). 10% Triton X-100 in PBS was then added (4 μL/well) to measure the maximum fluorescence value for each well and the plate was incubated for an additional 30 minutes in a cell incubator at 37 °C. Fluorescence values were measured again with the same reading settings. Results were calculated as ratio between fluorescence measured from each well relative to its fluorescence maximum, and then expressed as a percentage of negative control mean values. Each YTX concentration was tested in 5 replicates and experiments were repeated four times with different cardiomyocyte preparations.

**Beating HL-1 atrial cardiomyocyte culture**

HL-1 cardiomyocytes were a kind gift of Dr. W. C. Claycomb (Department of Biochemistry and Molecular Biology, Louisiana State University Health Science Center, New Orleans, LA) and cultured as recommended. Cells were fed every day with Claycomb medium supplemented with 10% FBS, 100U/ml penicillin, 100 μg/ml streptomycin, 0.1 mM norepinephrine, 2 mM L-glutamine (10 ml/T75-flask). Cultures were passaged twice a week, one day after fully confluent, with a dilution factor of three. For each culture flask, 3 new flasks were pre-coated by overnight incubation with 0.02% Bacto-gelatin solution with fibronectin (0.005 mg/ml) (6 ml/T75-flask) in a cell incubator at 37 °C. To split cultures, each flask was gently rinsed with warm 0.05% trypsin/EDTA solution (5 ml/T75-flask), the rinse was vacuum aspirated and the solution was added again (3 ml/T75-flask) and left to sit for 2 minutes at 37 °C. The solution was discarded again and fresh trypsin/EDTA solution was added and left for an additional 2-3 minutes. An equal volume of soybean trypsin inhibitor

solution (0.25 mg/ml Dulbecco's $Ca^{2+}$- and $Mg^{2+}$- free PBS) was then added to inactivate the enzyme, using a pipet to dislodge cells from the surface. the cell suspension was collected into a 15 ml tube and the empty flask was rinsed once with wash medium (Claycomb medium containing only 5% FBS and penicillin/streptomycin) (5 ml/T75-flask). This rinse was added to the tube and the suspension was centrifuged (Thermo IEC Centra CL2, Thermo Fisher Scientific Inc.) at 170*g* for 5 minutes at RT. Meanwhile, the three newly pre-coated T75-flasks were empted from the gelatin/fibronectin solution by vacuum aspiration and filled with complete Claycomb growth medium (8 ml/T75-flask). Centrifuged supernatant was discarded and the cell pellet was gently resuspended in 3 ml of complete growth medium. One ml of cell suspension was transferred into each of three coated flasks and cells were grown in a cell incubator in a humidified atmosphere of 5 % $CO_2$, 95 % air, at 37 °C. To freeze cultures, cells were harvested with the same trypsinization protocol as above, and the pellet resulting from centrifugation was re-suspended in freezing medium (95% FBS with 5% DMSO) (1.5 ml/T75-flask). The contents of each fully confluent T75-flask was collected into one cryovial. Cryovials were placed at -80 °C into a Nalgene freezing jar filled with RT isopropanol and transferred 6 to 12 hours later into a liquid nitrogen dewar. When cells were needed, one cryovial was thawed into one T75-flask. To do this, cells were quickly thawed in a 37 °C water bath for about 2 minutes and transferred into a 15 ml tube containing warm wash medium (10 ml), then centrifuged (Thermo IEC Centra CL2, Thermo Fisher Scientific Inc.) at 170*g* for 5 minutes at RT. The supernatant was discarded and the pellet was re-suspended with complete growth medium (5 ml) and placed in a coated T75-flask pre-filled with 10 ml of warm growth medium. Medium was replaced soon after cells had attached (4 hours later). Cultures employed for experiments were between 63rd and 73rd passage number.

**Mitochondrial membrane potential ($\Delta\Psi_m$) fluorometric measurement with TMRM dye**

Tetramethylrhodamine methyl ester (TMRM) is a fluorescent derivative of rhodamine 123 and accumulates as a lipophilic cation into the mitochondrial matrix in proportion to the electrical potential across the inner mitochondrial membrane. Upon accumulation, a red shift occurs in both excitation and emission fluorescence spectra and its extent is used to determine dye distribution (Scaduto and Grotyohann, 1999). Carbonyl cyanide 4-(trifluoromethoxy)phenylhydrazone (FCCP) was used as a positive control for its effect as a

proton ionophore causing an altered ion distribution and a depolarized mitochondrial membrane.

Cells were seeded at a density of 50.000 cells/well (100 µl/well). First, cells were loaded with 50 nM TMRM dye dissolved in medium (35 µl/well), and sat at RT for 30 minutes in the dark. Incubation began by exposing cells to 1 µM YTX, 4 or 40 µM FCCP, or 1% methanol as a toxin vehicle control, for a final volume of 70 µl/well. Negative controls and no-cell wells to quantify background signal were also present. As soon as the incubation started, fluorescent measurements were recorded every minute for 60 minutes with an automated microplate-based plate reader NOVOstar (BMG Labtechnologies) at an excitation wavelength of 544 nm and at an emission wavelength of 570-10 nm. Each treatment was performed in duplicate and experiments were repeated two times.

## Statistical analysis

Statistical analysis was performed with GraphPad Prism® software version 4.03 (GraphPad Software, Inc., San Diego, CA) and a value of $p<0.05$ was considered significant. One-way ANOVA tests were performed for statistical analyses of one variable, followed by either a Dunnett post test, post test for linear trend or Bonferroni post test to compare column pairs. A Two-way ANOVA test followed by Bonferroni post test was performed for statistical analyses with two variables. Student's unpaired *t*-test was performed by Microsoft Office Excel software.

## Chemicals

YTX, a kind gift of Prof. Takeshi Yasumoto (Japan) was isolated from *P. reticulatum* collected in Mutsu Bay (Japan), following the method of Murata *et al*. (1987). The purity of YTX was confirmed by mass spectrometry and by liquid chromatographic methods (Satake *et al*., 1997; Yasumoto and Takizawa, 1997). A stock solution of 100 µM YTX in 95% aqueous ethanol was prepared.

**NEN™ Life Science Products:** [$^3$H] cyclic AMP (37 MBq/ml);

**Perkin Elmer:** Optiphase SuperMix liquid scintillation cocktail;

**Backer:** 37% chloridric acid, potassium chloride;

**Carlo Erba:** Sodium chloride;

**Euro€lone:** Dulbecco's phosphate buffered saline, Penicillin/Streptomycin (10.000 U/ml-10.000 μg/ml), 200 mM L-Glutamine, Ham's F10; amphotericin B;

**Merck:** Triton X-100;

**Sigma-Aldhrich:** Tetramethylrhodamine methyl ester (TMRM); carbonyl cyanide 4-(trifluoromethoxy)phenylhydrazone (FCCP); methanol; propidium iodide; acetone; 4-chlorodiazepam; PK-11195; glycine; 1,4-diazabicyclo[2.2.2]octane-glycerol; 4',6-diamidino-2'-phenylindole dihydrochloride; sulforhodamine B; ethanol; trichloroacetic acid; acetic acid; tris(hydroxymethyl)aminomethane; trypan blue; hydrogen peroxide; fura-2 AM; bovine serum albumine; glucose; HEPES; forskolin; Claycomb medium, F10 Ham's nutrient mixture, fetal bovine serum (Lot #8A0177 for HL-1 cardiomyocytes), horse serum, norepinephrine [(±)-Arterenol], L-ascorbic acid sodium salt, fibronectin, Trypan blue, Sulforodamina B, dimethyl sulfoxide; potassium chloride; calcium chloride; magnesium chloride; K-aspartate; Hank's balanced salt solution calcium-and magnesium-free (HBSS); horse serum; trypsin (T4424); sodium hydroxide; MagnesiumATP; Ethylene glycol-bis(2-aminoethylether)-*N,N,N',N'*-tetraacetic acid; mitochondria staining kit (CS0390);

**AnaSpec Corporate:** SensoLyte AFC caspase sampler kit, fluorimetric (71117);

**Millipore Corporation:** 96-well MultiScreen-FB microtiter plate;

**Life Technologies:** Penicillin-streptomycin ($10^4$ U/ml-$10^4$ μg/ml), 200 mM L-glutamine, trypsine/EDTA (25300-054), soybean trypsin inhibitor, cell culture-grade distilled water;

**Invitrogen:** Dulbecco's $Ca^{2+}$- and $Mg^{2+}$- free PBS;

**Fisher Scientific:** Bacto-gelatin.

# RESULTS

**Beating frequency observation after continuous exposure to YTX**

Yessotoxin-exposed cardiomyocytes showed a concentration- and time-dependent reduction of beating frequency. Cells were observed at different time points (0.5, 1, 5, 24 h) after exposure to increasing YTX concentrations (0.01 up to 1 µM). Results are shown in figure 2 as YTX concentration on the X axis and as corresponding beating frequency value expressed as a percentage relative to control values on the Y axis. After 0.5 h exposure no reduced beating activity was observed (data not shown). After 1 h, its decrease was observed in a time- and concentration-manner at all toxin concentrations tested, becoming significant at 0.3 µM YTX. After 5 hours the pattern was similar, while at 24 hours beating frequency reduction was significant starting from 0.1 µM YTX.

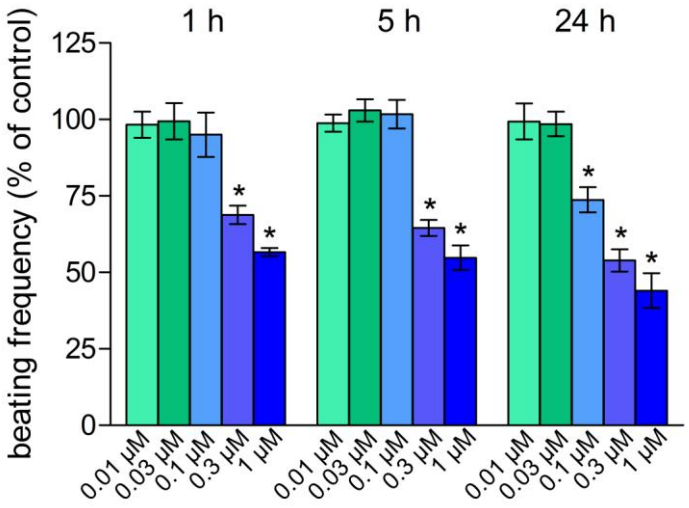


**Figure 2: YTX effect on cardiomyocyte beating frequency**
Data are reported as mean ±SEM (*n*= 40-50 fields) of samples assayed in triplicate. Experiments were repeated two times with two different cell preparations.
* $p<0.05$ vs control (Two-way ANOVA with Bonferroni post test).

Among cardiomyocyte cells, 86.4 ±6.8% were regularly beating (*n*=60 fields). A >50% reduction in number of beating cells was observed after a 24 hour exposure to 1 µM YTX.

Results are shown in figure 3 as a percentage of beating cells with respect to total cell number.

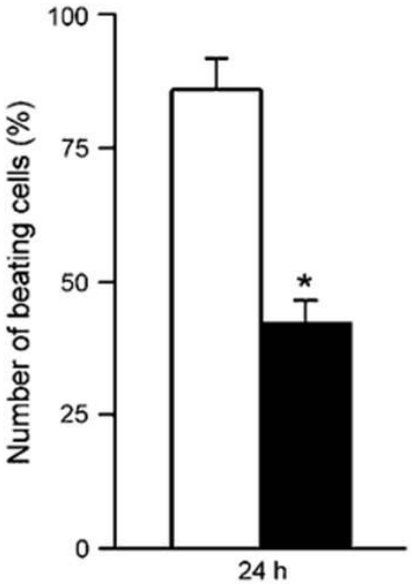


□ before 1 μM YTX exposure

■ after 1 μM YTX exposure

**Figure 3: YTX effect on number of beating cardiomyocytes**
Data are reported as mean ±SEM (*n*=30 fields).
* $p<0.05$ *vs* control (Student *t*-test).

**Membrane electrical activity and $Ca^{2+}$ release from intracellular stores in presence of YTX**

Cardiomyocyte firing frequency was affected by YTX treatment. Patch-clamp and calcium imaging technique recordings were performed on cells before and after 1 h perfusion with 1 μM YTX. Changes in both membrane potential and calcium transients were measured in the same cell. Results are shown in figure 4 as membrane potential (mV) in the upper panel and the corresponding $[Ca^{2+}]_i$ pick in the lower panel. The pattern for control cells is shown on the left half of the figure and for YTX-exposed cells on the right half. A decrease in the firing frequency of about 50% with respect to untreated cells was observed without any corresponding change in either resting or action membrane potential amplitude (from 50.3 ±0.1 mV to 51.6 ±0.1 mV, *n*=30 cells). Similarly, both basal and peak $[Ca^{2+}]_i$ transient values

were not affected by toxin exposure (from 1.9 ±0.1 mV to 1.8 ±0.2 mV; *n*=80 cells, 15 fields). As in control conditions, in the presence of YTX each action potential always remained associated to a $[Ca^{2+}]_i$ transient.

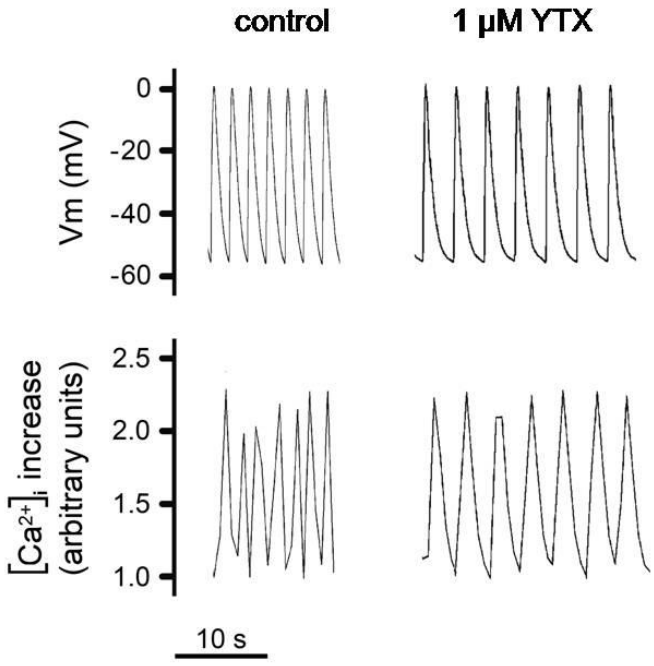


**Figure 4: YTX effect on cardiac cells electromechanical coupling**
Results are reported as changes in membrane potential voltage (*n*=30 cells) and corresponding $[Ca^{2+}]_i$ transient (*n*=80 cells).

### Intracellular cAMP accumulation in presence of YTX

Cardiomyocyte intracellular cyclic AMP levels were significantly affected by YTX. Adenylyl cyclase enzyme activity was directly stimulated with 10 µM forskolin simultaneously with exposure to increasing toxin concentrations (0.0001, 0.001, 0.01 and 1 µM). Experiments were performed at 10 minutes, a time point determined by preliminary time-course experiments (data not shown). Results are shown in figure 5 as intracellular cyclic AMP pmol produced per million of cells on the Y axis. A significant reduction ($p$<0.01) of cAMP levels was observed only in 1 µM YTX exposed cells (-33 ±11% *vs* control cells).

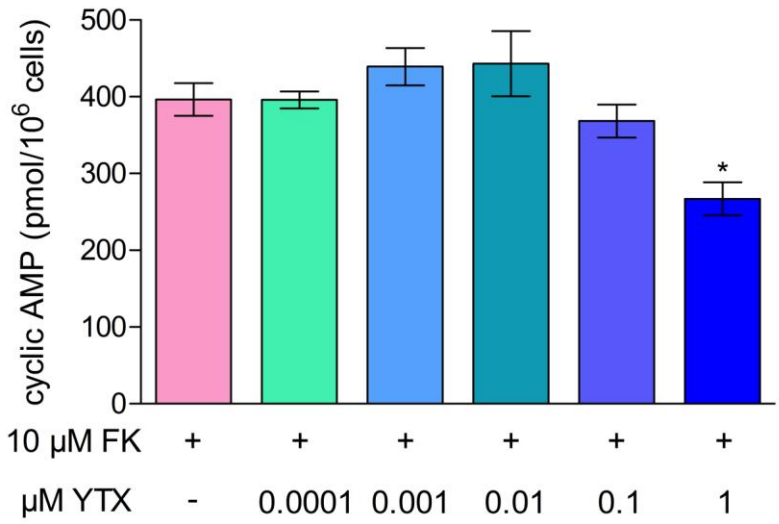


**Figure 5: YTX effect on intracellular cAMP accumulation in presence of forskolin (FK)**
Data are reported as mean ±SEM of samples assayed in triplicate or quadruplicate. Experiments were repeated two times with two different cell preparations.
* $p<0.01$ *vs* control (One-way ANOVA with Dunnet post test).

On the contrary, when adenylyl cyclase activity was not stimulated, YTX did not alter cyclic nucleotide levels. Cells were exposed for 10 minutes or 1, 5, and 24 hours to 1 µM YTX and compared to control cells. Results are shown in figure 6 as pmol of intracellular cAMP produced per million of cells on Y axis and each group of bars represents a different time point measurement of both control and YTX-exposed cells. YTX did not caused appreciable variations of cAMP content with respect to controls at any time point. A progressive increase in cAMP content was found in both treated and untreated cells, but no significant difference between the two groups was found.

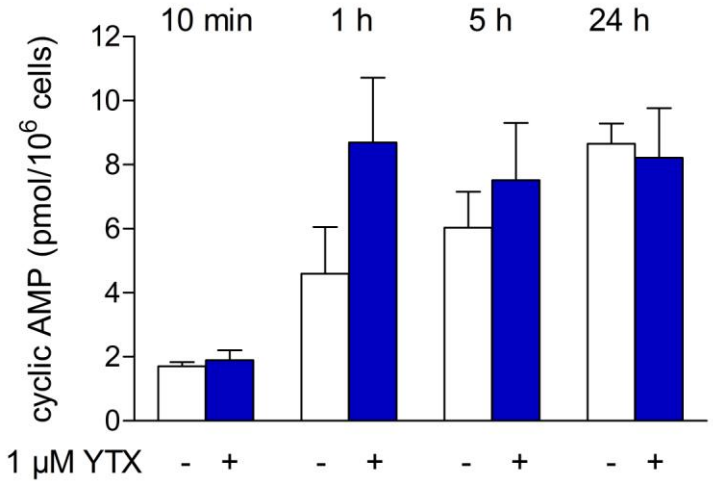


**Figure 6: YTX effect on intracellular cAMP accumulation in basal condition**
Data are reported as mean ±SEM of samples assayed in triplicate or quadruplicate with two different cell preparations. No significant difference between control and treated cells was calculated (Two-way ANOVA with Bonferroni post test).

**Cell viability assessment after continuous YTX exposure**

Cardiomyocytes exposed to increasing concentrations of YTX showed a reduced viability in a concentration- and time-dependent way. Cells were exposed to increasing concentrations of YTX (0.0001, 0.001, 0.01, 0.1 and 1 µM) for 24, 48 and 72 hours. Results are shown in figure 7 as a percent viability of treated cells with respect to control. After 48 hours of incubation, a significant ($p$<0.001) decrease of mitochondrial activity was observed starting from 0.01 µM YTX and after 72 h a similar pattern was observed. Two-way ANOVA evidenced a significant ($p$<0.001) influence of incubation time, toxin concentration and their interaction (accounting for 49.4%, 19.3% and 22.3% of total variance, respectively). On the contrary, cells treated for 24 h resulted in a significant increase in mitochondrial activity at all concentrations of YTX tested.

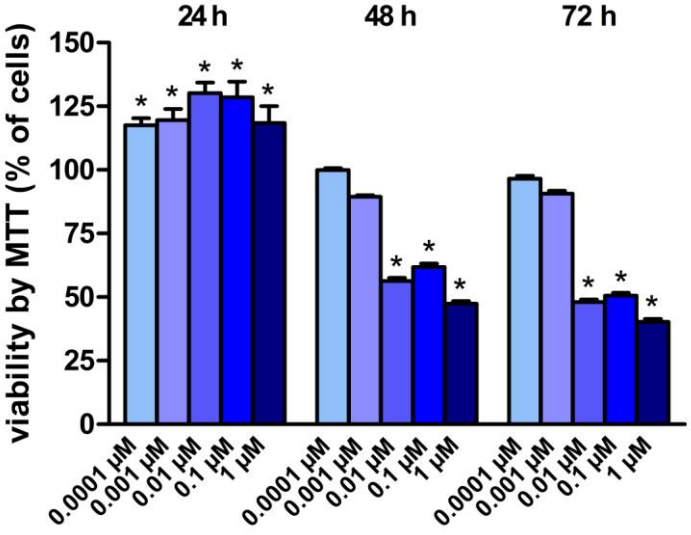


**Figure 7: YTX effect on cardiomyocyte viability by MTT assay**
Data are reported as mean ±SEM (*n*=12) of viability percentage with respect to control cells. Experiments were repeated three times with different cell preparations.
* $p<0.001$ *vs* control (Two-way ANOVA with Bonferroni post test).

Under the same experimental conditions, results obtained by MTT assay were confirmed by the SRB assay that determines cell number by protein content. After 48 and 72 h, a time- and concentration-dependent viability reduction occurred at all toxin incubation time. Cells were exposed to 0.01, 0.1 and 1 µM YTX for 24, 48 and 72 hours and results are shown in figure 8 as cell number percentage with respect to control. After 24 hours, a significant decrease in cell number was observed starting from 0.1 µM YTX ($p<0.01$), and after 48 h of incubation the effective concentration lowered to 0.01 µM YTX ($p<0.001$). Similar results were obtained after 72 hours exposure.

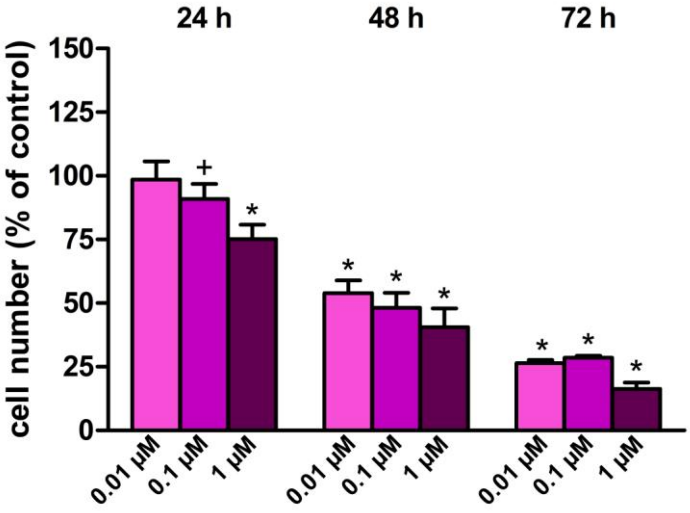


**Figure 8: YTX effect on cardiomyocyte cell number by SRB assay**
Data are reported as mean ±SD (*n*=8-12) of cell number percentage with respect to control. Experiments were repeated three times with different cell preparations.
+ $p<0.01$ *vs* control (Two-way ANOVA with Bonferroni post test);
* $p<0.001$ *vs* control (Two-way ANOVA with Bonferroni post test).

**Cell viability assessment after a prolonged washout in YTX-free medium**

In a second set of experiments, cells were exposed to increasing YTX concentrations up to 24 hours. Medium was then replaced by YTX-free medium and cell cultures were maintained up to the fifth day of culture. These experiments were performed in order to evaluate the potential recovery of toxin-exposed cells. Results obtained showed a time-dependent reduced viability even after a short time exposure such as 1 hour with no recovery of viability after up to 71 h. Cells were exposed to increasing concentrations of YTX (0.0001, 0.001, 0.01, 0.1 and 1 µM) for 1, 5 and 24 hours and maintained thereafter in YTX-free medium up to 71, 67 and 48 hours, respectively. Results are shown in figure 9 as percent viability of treated cells with respect to control. After 1 h exposure a significant ($p<0.001$) reduction in viability was found starting from 0.1 µM YTX. After 24 hours of treatment, 0.01 µM YTX was the lowest

effective concentration. With analysis by Two-way ANOVA, a significant ($p$<0.001) effect of YTX concentration, length of exposure and their interaction was observed, accounting for 87.0%, 2.9% and 4.7% of total variance, respectively.

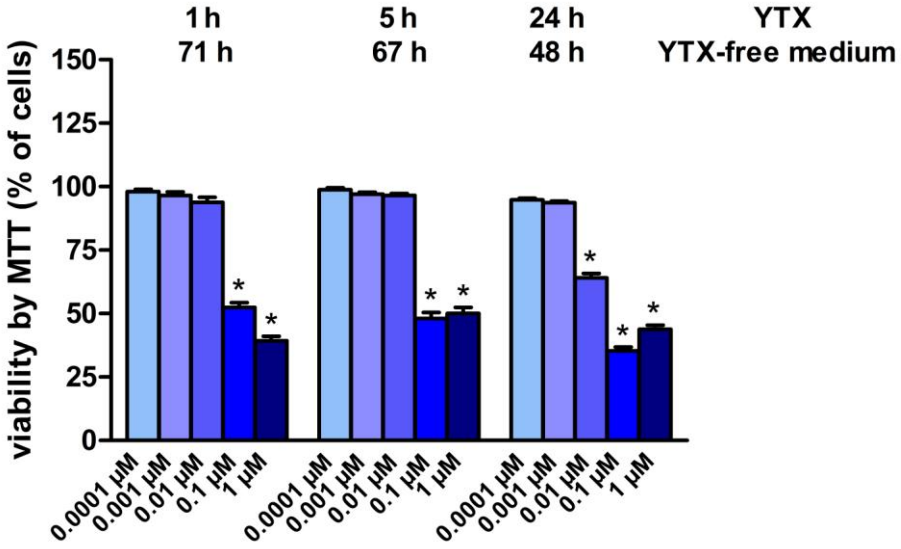


**Figure 9: YTX effect on cardiomyocyte viability by MTT assay**
Data are reported as mean ±SEM ($n$=12) of viability percentage with respect to control cells. Experiments were repeated two times with different cell preparations.
* $p$<0.001 *vs* control (Two-way ANOVA with Bonferroni post test).

Comparable results were obtained performing the SRB test under similar experimental conditions. Cells were exposed to 0.01, 0.1 and 1 µM YTX for 1, 5 and 24 hours and maintained thereafter in YTX-free medium up to the fifth day of culture. Results are shown in figure 10 as cell number percentage with respect to control. One hour exposure to 0.1 µM YTX was sufficient to dramatically reduce cell number ($p$<0.001), and a similar pattern was observed after 5 hours. 24 hours of exposure to the toxin followed by 48 hours in toxin-free medium resulted in a decrease of cell number at all concentrations tested. Under this condition, the percentage of living cells was lower than after 24 h of continuous contact to the toxin (-80.45 ±8.13% *vs* -24.85 ±5.64%, respectively, after 1 µM YTX treatment).

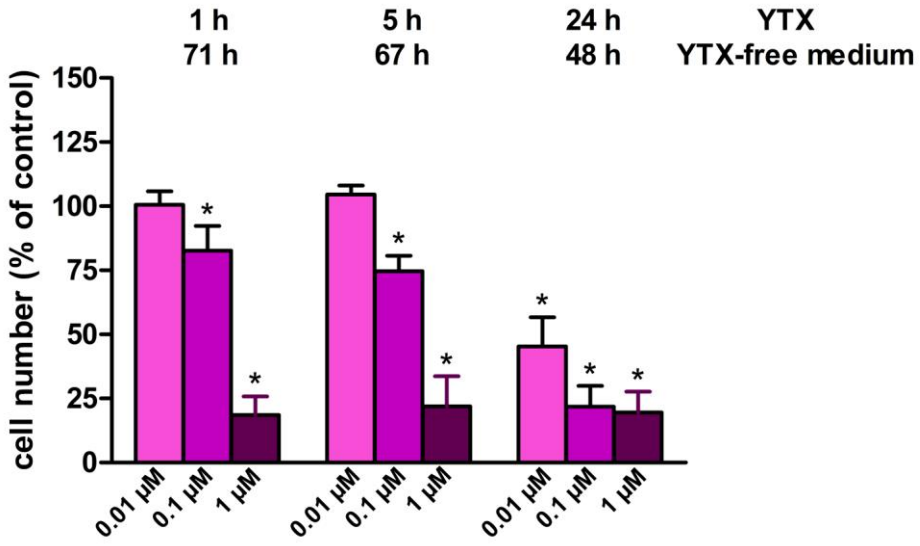


**Figure 10: YTX effect on cardiomyocyte cell number by SRB assay**
Data are reported as mean ±SD ($n$=12) of cell number percentage with respect to control. Experiments were repeated two times with different cell preparations.
* $p$<0.001 *vs* control (Two-way ANOVA with Bonferroni post test).

**Nuclear morphology after continuous YTX exposure**

Increasing concentrations of YTX induced the appearance of nuclear apoptotic bodies in cardiomyocytes. In DAPI-stained cells, nuclei are considered to have a normal phenotype when glowing bright and homogenously. Apoptotic alterations present as either condensed chromatin gathering at the periphery of the nuclear membrane or a total fragmented morphology of nuclear bodies.

Cells were exposed to 0.001, 0.01 and 0.1 µM YTX for 1, 5 and 24 h and cultures were fixed at the end of the treatment. Positive control wells were exposed to 0.5 mM hydrogen peroxide for 1, 5 and 24 h. Pictures were acquired with 60x magnification. YTX had a time-dependent effect (see figure 11). A percentage quantification was not possible because of the cluster nature of the culture.

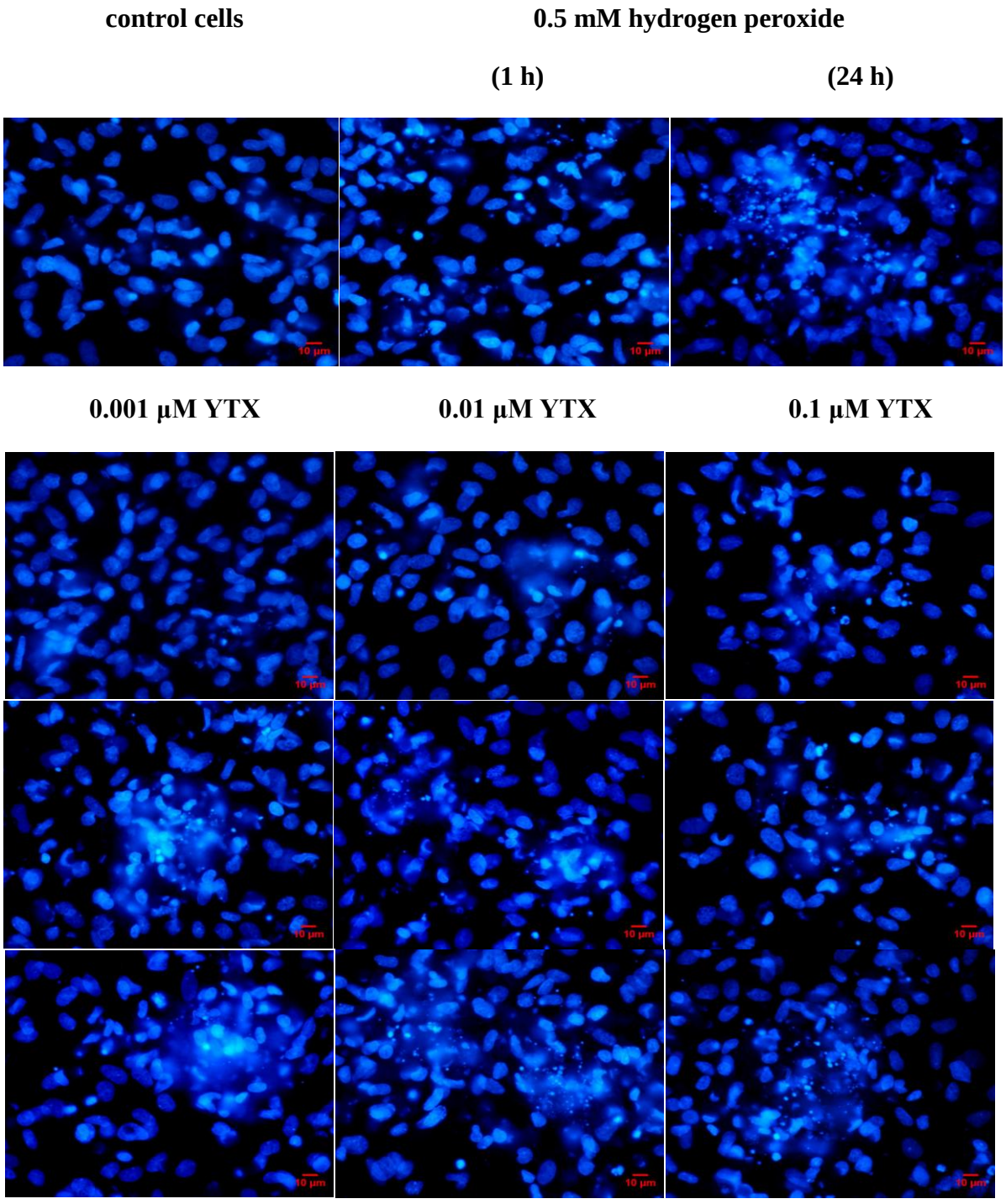


**Figure 11: Cardiomyocytes nuclear morphology after continuous YTX exposure for 1 h (first row), 5 h (second row) or 24 h (third row)**

**Nuclear morphology after prolonged washout in YTX-free medium**

In a second set of experiments, cells were exposed to 0.01, 0.1 and 1 µM YTX for 1, 5 and 24 h. Cultures were then maintained up to the fifth day of culture in YTX-free medium and then fixed. Pictures were acquired with 60x magnification. A percentage quantification was not possible because of the cluster nature-behaviour of the culture. Both concentration- and time-dependent effects of the toxin are observable in figure 12, together with a significant loss in cell number.

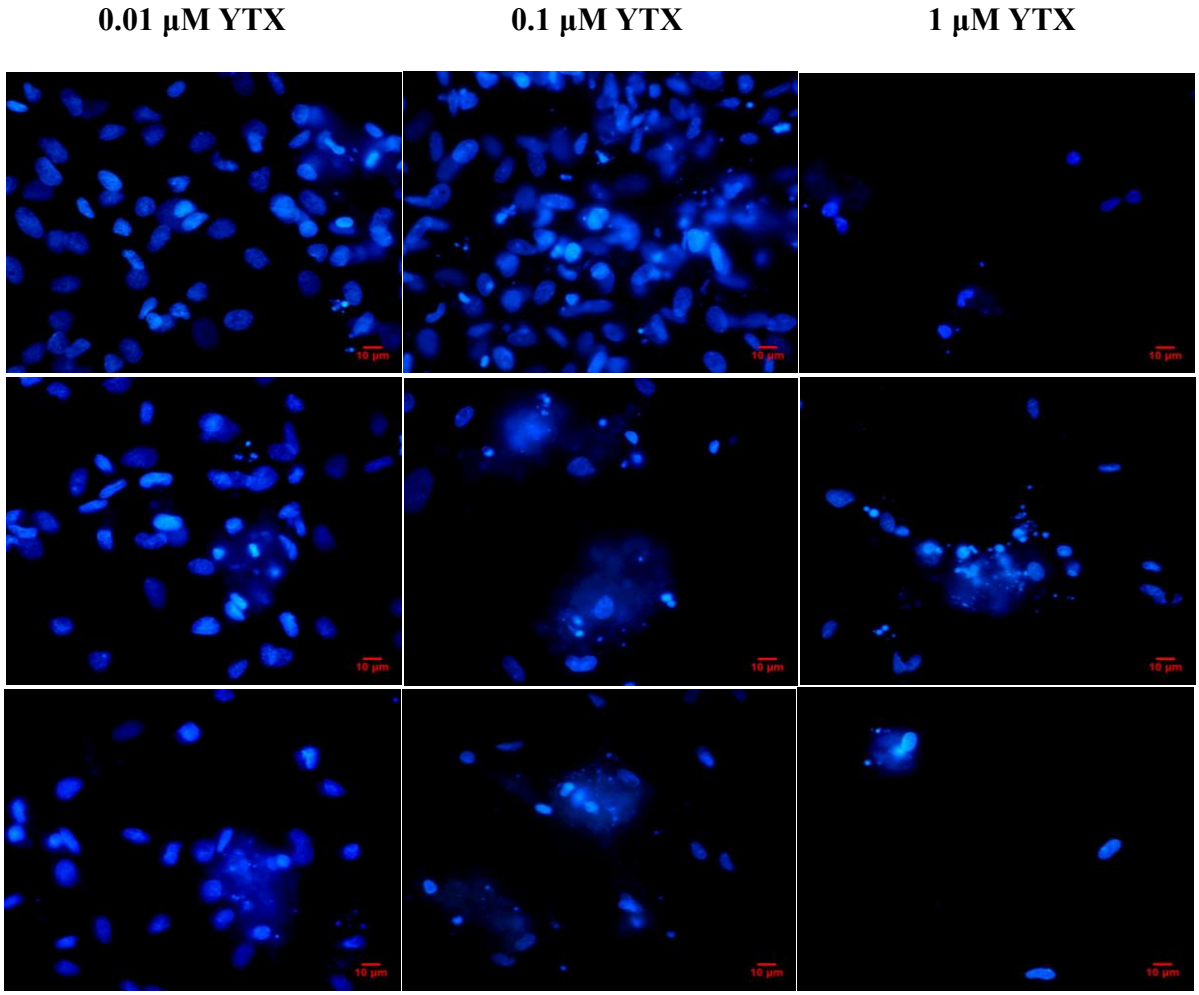


**Figure 12: Cardiomyocytes nuclear morphology after 1 h (first row), 5 h (second row) or 24 h (third row) exposure to YTX, followed by 71, 67 and 48 h, respectively, in YTX-free medium**

**Caspase activity after continuous exposure to YTX**

No caspase activation was found in YTX-treated cardiomyocytes. Cardiomyocytes were exposed to increasing concentrations of YTX (0.001, 0.01 and 0.1 μM) for 5, 24, 48 and 72 h. Positive control wells were exposed to the apoptosis inducer 10 μM camptothecin for 24 hours. Results are reported only for the highest YTX concentration employed (0.1 μM) after 72 h. In table 1 are grouped data for initiators of the apoptosis pathway and in table 2 are grouped data for executors of the apoptosis pathway as well as for caspase 1, an isoform involved in cytokine activation. Data are reported as fluorescence units (mean ±SD) of free AFC fluorochrome released by caspase hydrolysis of AFC-peptide complexes. Results after 5, 24, and 48 h were equally ineffective at all YTX concentrations tested.

**Table 1: YTX effect on apoptosis initiator caspases 2, 8, 10 and 9 activity**

| | caspase 2 | caspase 8 | caspase 10 | caspase 9 |
|---|---|---|---|---|
| | (fluorescence units) | | | |
| **control** | 3.462 ±1 | 3.235 ±59 | 4.827 ±33 | 2.279 ±16 |
| **10 μM camptothecin (24 h)** | 19.731 ±56 | 19.763 ±380 | 21.080 ±162 | 18.553 ±82 |
| **0.1 μM YTX (72 h)** | 3.374 ±0 | 3.176 ±30 | 4.362 ±306 | 2.188 ±6 |

**Table 2: YTX effect on caspase 1 and on apoptosis executor caspases 3/7 and 6 activity**

| | caspase 1 | caspase 3/7 | caspase 6 |
|---|---|---|---|
| | (fluorescence units) | | |
| **control** | 2.448 ±12 | 5.525 ±38 | 3.790 ±16 |
| **10 μM camptothecin (24 h)** | 18.613 ±76 | 21.826 ±128 | 19.930 ±354 |
| **0.1 μM YTX (72 h)** | 2.334 ±1 | 5.221 ±26 | 3.647 ±32 |

**Cell necrosis after continuous exposure to YTX**

Propidium iodide (PI) experiments were performed in order to investigate YTX effect on cell viability. YTX induced concentration- and time-dependent cell death. Cardiomyocytes were exposed to 0.0001, 0.001, 0.01 and 0.1 µM YTX for 5, 24, 48 and 72 h. Results are reported in figure 13 and were calculated for each well as a ratio between YTX-induced PI fluorescence above PI fluorescence maximum, and then expressed as a percentage of negative control values. After a 5 h exposure no significant increase was detected in any of the YTX concentrations. A significant increase of PI uptake was detected after 24 h exposure starting from 0.01 µM YTX ($p$<0.01). After 48 hours exposure, the lowest effective concentration was 0.001 µM YTX ($p$<0.01), increasing the uptake value from 20 ±6% to 64 ±3% at 72 hours ($p$<0.001). 48 hour and 72 hour treatments resulted in a similar pattern. Two-way ANOVA revealed a significant ($p$<0.001) effect of YTX concentration, length of exposure and their interaction, accounting for approximately 36.5%, 29.2% and 25.6% of total variance, respectively. One-way ANOVA with post test for linear trend performed for each exposure time revealed a significant linear trend at all times tested ($p$<0.0001). 0.01 µM YTX *vs* 0.1 µM YTX values were not significantly different at all times tested (One-way ANOVA with Bonferroni post test for column pairs).

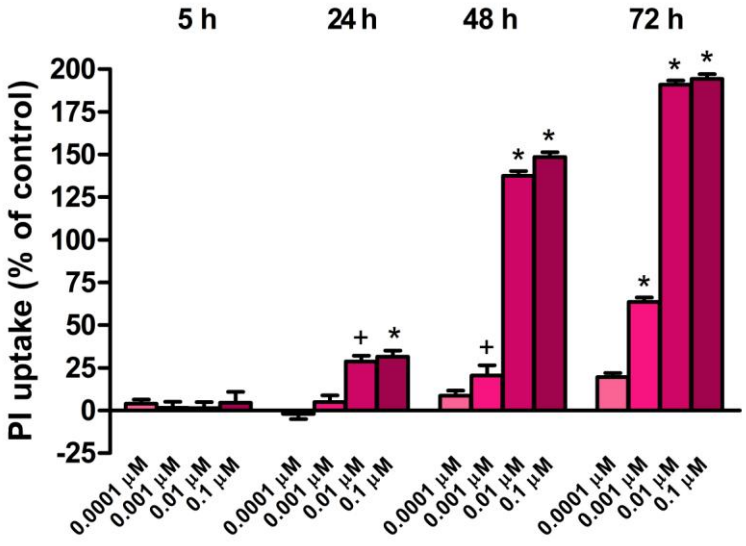


**Figure 13: YTX effect on cardiomyocyte viability by PI uptake**
Data are reported as mean ±SEM ($n$=16-24) Experiments were repeated four times with three different cardiomyocyte preparations.
+ $p$<0.01 *vs* control (Two-way ANOVA with Bonferroni post test);
* $p$<0.001 *vs* control (Two-way ANOVA with Bonferroni post test).

**Short-term time course for YTX effect on mitochondrial membrane potential**

In HL-1 cardiomyocytes exposed to 1 µM YTX up to 60 minutes, no mitochondrial membrane potential ($\Delta\Psi_m$) depolarization occurred. Cells were exposed to 1 µM YTX or to the depolarizing agent carbonyl cyanide 4-(trifluoromethoxy)phenylhydrazone (FCCP) (4 or 40 µM) as a positive control. TMRM dye fluorescence readings were acquired every minute for 1 h, beginning as soon as incubation started (figure 14). No significant difference was foundbetween control and YTX-treated cells by Two-way ANOVA with Bonferroni post test analysis.

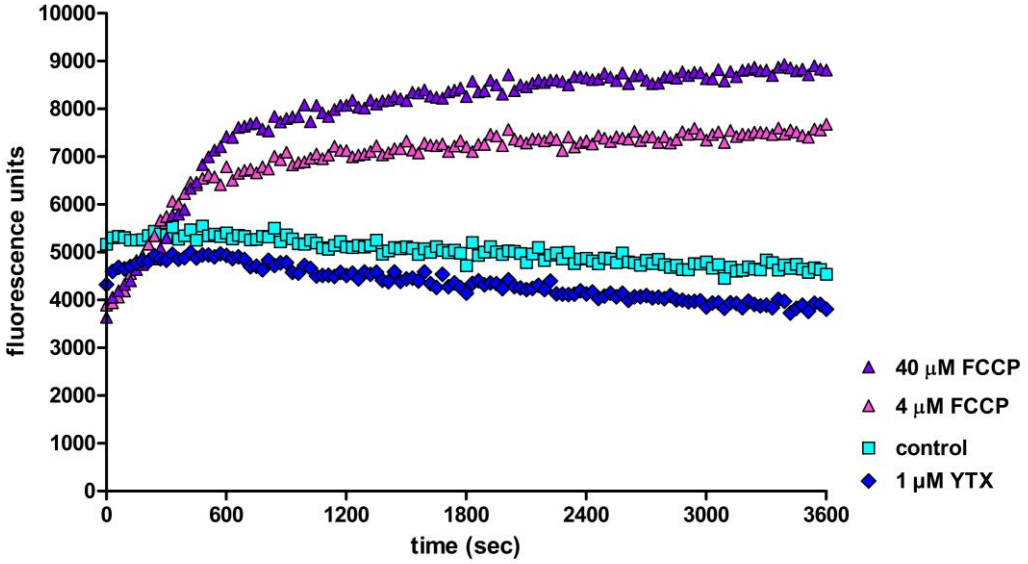


**Figure 14: YTX effect on $\Delta\Psi_m$ by TMRM dye**
Data are reported as mean of fluorescence units of one representative experiment. Experiments were performed in duplicate and repeated two times.

**Time course for YTX effect on mitochondrial membrane potential**

In neonatal rat cardiomyocytes, altered mitochondrial membrane potential ($\Delta\Psi_m$) was found by JC-1 dye. Cells were exposed to 0.0001, 0.001, 0.01, 0.1 and 1 µM YTX for 24, 48 and 72 hours. The depolarizing agent valinomycin 1 µM was used as a positive control. Data are

reported in figure 15 as a percentage relative to control of the ratio between fluorescence units emitted in red and above green wavelengths.

Data analysis by Two-way ANOVA found a significant ($p$<0.0001) effect of concentration, exposure time and their interaction, accounting for approximately 13.5%, 31.2% and 25.8% on total variance, respectively. Bonferroni post test calculated a significant effect of toxin treatment on $\Delta\Psi_m$ at 24 h starting from a concentration equal to 0.01 μM ($p$<0.001). After 48 h, all YTX concentrations showed a modified $\Delta\Psi_m$, with a significance equal to $p$<0.05 for 0.0001 μM and 0.001 μM YTX, and $p$<0.001 for 0.01, 0.1 and 1 μM YTX. At 72 h a similar pattern was observed.

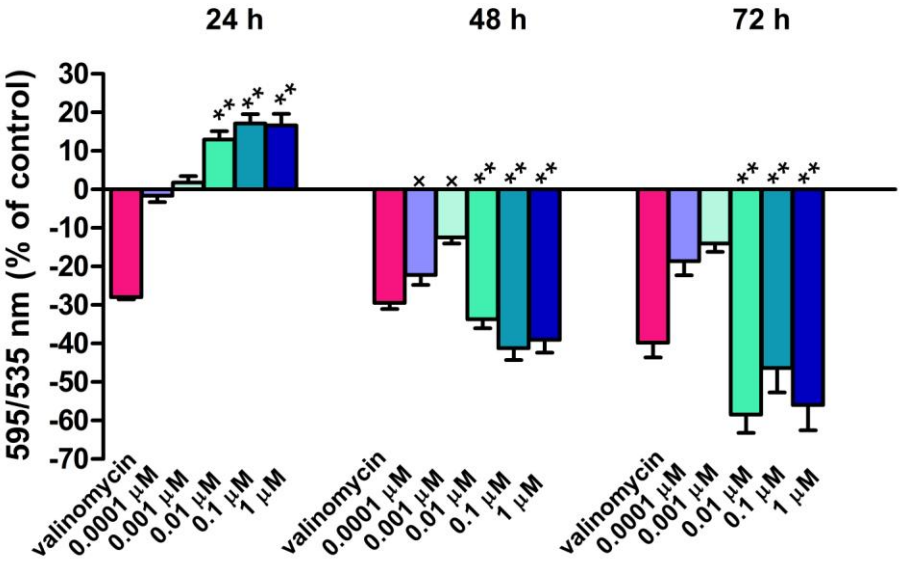


**Figure 15: YTX effect on $\Delta\Psi_m$ by JC-1 dye**
Data are reported as mean ±SEM. Experiments were performed in 5-12 replicates for each treatment and repeated two to six times with different cardiomyocyte preparations.
x $p$<0.05 *vs* control (Two-way ANOVA with Bonferroni post test);
** $p$<0.001 *vs* control (Two-way ANOVA with Bonferroni post test).

**Effect of peripheral benzodiazepine receptor ligands on YTX mitochondrial effect**

By MTT assay, the effect of YTX on mitochondrial dehydrogenase activity was not affected by the modulation of peripheral benzodiazepine receptor activity. Neonatal rat cardiomyocytes were exposed for 24 hours to 0.1 μM YTX either alone or in the presence of 0.1 μM peripheral benzodiazepine receptor modulators 4-chloro-diazepam and/or PK-11195. Results are reported in table 3 as mean ±SD of percentage relative to control values for mitochondrial dehydrogenase activity. Data analysis by One-way ANOVA with the Tukey-Kramer post test showed no significant effect.

**Table 3**
**PBdzR modulators effect on 24 hYTX-exposed cells by MTT assay**

| compound | viability (% of control) |
|---|---|
| **YTX 0.1 μM** | 29.1 ±5.6 |
| **PK-11195 0.1 μM** | 11.3 ±6.3 |
| **PK+YTX** | 36.8 ±8.7 |
| **4-chloro-diazepam 0.1 μM** | 7.1 ±3.7 |
| **4-chloro-diazepam+YTX** | 33.5 ±5.6 |
| **PK-11195+4-chloro-diazepam** | 7.3 ±9.4 |
| **PK-11195+4-chloro-diazepam+YTX** | 31.6 ±5.4 |

In a separate set of experiments, the effect of YTX on the mitochondrial membrane potential ($\Delta\Psi_m$) in the presence of peripheral benzodiazepine receptor ligands was tested by JC-1 dye. Neonatal rat cardiomyocytes were exposed for 24 or 48 hours to 0.1 μM YTX, either alone or in the presence of one or both peripheral benzodiazepine receptor modulators 4-chloro-diazepam and/or PK-11195 (0.1 or 0.01 μM). Results after both 24 and 48 h incubation are shown in table 4 as mean ±SEM of the percent relative to control of the ratio between JC dye fluorescence units emitted in red and above green wavelengths. Data analysis with One-way ANOVA with Tukey-Kramer post test did not found any significant difference between YTX alone and YTX with one or both receptor ligands.

**Table 4**
**PBdzR modulators effect on 24 and 48 h YTX-exposed cells by JC-1 dye**

| compound | 595/535 nm (% of control) | |
|---|---|---|
| | 24 h | 48 h |
| **valinomycin 1 μM** | -35.5 ±2.5 | -32.4 ±1.9 |
| **YTX 0.1 μM** | 24.3 ±2.2 | -43.6 ±3.0 |
| **PK-11195 0.1 μM** | -16.7 ±2.5 | -15.1 ±5.1 |
| **PK+YTX** | 13.0 ±4.6 | -48.5 ±4.1 |
| **4-chloro-diazepam 0.1 μM** | -14.4 ±2.8 | -22.3 ±4.2 |
| **4-chloro-diazepam+YTX** | 18.1 ±2.4 | -47.2 ±4.0 |
| **PK-11195+4-chloro-diazepam** | -11.1 ±1.6 | -8.7 ±2.3 |
| **PK-11195+4-chloro-diazepam+YTX** | 10.2 ±1.4 | -50.0 ±5.2 |

# DISCUSSION

Cardiomyocytes exposed to YTX showed a concentration- and time-dependent reduction of beating frequency starting from 1 h exposure to 0.3 µM YTX. No reduced beating activity was observed after 0.5 h exposure. Cardiac contraction and relaxation activity rely on the processes of excitation-contraction coupling. These processes start with the initial cell membrane depolarization through voltage-gated sodium channels activation, the consequent voltage-dependent opening of L-type voltage-gated calcium channels, the $Ca^{2+}$-induced $Ca^{2+}$-release through ryanodine receptors located on sarcoplasmic reticulum, and finally the binding of cytosolic calcium to the myofilaments and cell contraction. A major deficit in failing myocytes is the reduced $Ca^{2+}$ content of the sarcoplasmic reticulum (SR), that together with related altered mechanisms, lead to smaller and dyssynchronous SR calcium release (Maack and O'Rourke, 2007). In cardiomyocytes exposed to YTX, a 50% reduction of fire frequency occurred after 1 h perfusion (1 µM YTX), but no change was found in both resting and action membrane potential amplitude. Moreover, both $[Ca^{2+}]$i basal and peak values were not affected by toxin exposure: as in control conditions, YTX-exposed cells showed action potentials always associated to a $[Ca^{2+}]$i transient. These results exclude a YTX-induced impairment of excitation-contraction coupling, calcium release or action potential amplitude. Literature data from previous *in vitro* studies reported already only a modest effect of YTX on calcium movements in mammalian cells, also with high concentration (1 µM YTX) (de la Rosa *et al*., 2001a; 2001b). Moreover, the presence of calcium channel blockers did not prevented rat cerebellar neurons cell death (Pérez-Gómez *et al*., 2006).

Another second messenger regulating heart rate is cyclic AMP (cAMP), that through cAMP-dependent kinase A (PKA) could mediate several fundamental processes in the heart, including cardiac contractility and action potential duration (DiFrancesco, 2006). YTX has been previously found to slightly affect intracellular cAMP levels on human lymphocytes (Alfonso *et al*., 2003), an effect related to toxin ability to bind to several phosphodiesterases (Alfonso *et al*., 2005; Pazos *et al*., 2006; Mouri *et al*., 2009). In the present study, cardiomyocytes intracellular cyclic AMP levels were significantly reduced ($p<0.01$) only at the highest concentration employed (1 µM YTX) and with a modest effect (-33 ±11% *vs* control cells). Moreover, this effect could be observed only in presence of a direct activator of adenylyl cyclase: in non-stimulated condition, YTX did not altered cyclic nucleotide levels, even after longer exposure time such as 24 hours. These results lead to exclude a highly affected cAMP pathway at the bases of cardiomyocytes reduced firing activity.

Since in beating cells number observations a ~50% reduction of beating cardiomyocytes was found after a 24 hours exposure to 1 µM YTX, the possible correlation to a reduced cell viability was investigated. Cardiomyocytes were exposed to increasing concentrations of YTX for 24, 48 and 72 hours and MTT and SRB assays were performed. A concentration- and time-dependent reduction of viability was found after 48 h of incubation, with a significant ($p$<0.001) decrease of mitochondrial activity observed starting from 0.01 µM YTX. After 72 h a similar pattern occurred.

Interestingly, 24 h exposure caused a significant ($p$<0.001) increase in mitochondrial dehydrogenase activity at all YTX concentrations tested (0.0001-1 µM). This effect could be due to an increased cell number, but adhered cells quantification by SRB assay excluded this possibility, founding a significant decrease in cell number starting from 0.1 µM YTX ($p$<0.01). An influx of $Ca^{2+}$ into the cytosol and its consequent sequestering into the mitochondria has been reported to activate respiratory dehydrogenases and oxidative phosphorylation (Lemasters *et al*., 2009). Previous studies reported a slight YTX-induced increase of intracellular $Ca^{2+}$ content in human lymphocytes (de la Rosa *et al*., 2001a and 2001b), rat cerebellar neurons (Pérez-Gómez *et al*., 2006) and immunocytes from the mussel *Mytilus galloprovincialis* (Malagoli *et al*., 2006a). On the contrary, similarly to the findings of the present study, no altered calcium homeostasis in mouse skeletal muscle seem to occur (Tubaro *et al*., 2008b). In cardiac myocytes, both cytosolic and mitochondrial $Ca^{2+}$ levels increase transiently during the contractile cycle, as part of excitation-contraction coupling, and possibly stimulate mitochondrial ATP production on a beat to beat basis (Lemasters *et al*., 2009). Because cardiac myocytes, as well as skeletal muscle, experience constant fluctuations of free $Ca^{2+}$, ion level control could be more efficient than other cell types, and a small YTX-induced calcium increase could not affect calcium transients or excitation-contraction coupling.

Mitochondria occupy a central position in cell survival/cell death decision. Mitochondrial membrane potential is a key factor for a functional organelle and whilst a transient loss of mitochondrial membrane potential is physiological, a long lasting dissipation is associated with cell death (Korichneva *et al*., 2003; Iijima *et al*., 2003), although available literature data still didn't identified an exact cause-consequence sequence and several different pathways are possible. In the heart, mitochondria occupy about 30% of myocyte cell volume: their high number is related to the high metabolic demand of heart tissue and their role as buffer of cytosolic calcium levels (Baskin, 1991). YTX effects on both mitochondrial activity and

apoptosis are perhaps the aspects that have been mostly investigated *in vitro* until now, showing different sensitivity among cell lines and cell line-specificity in biochemical responses. A reduction of mitochondrial membrane potential in the BE(2)-M17 neuroblastoma cell line has been found at high concentration (1 μM YTX) starting after 12 hours incubation (Leira *et al*., 2002) and similar results were found in rat L6 and mouse BC3H1 skeletal muscle myoblasts after 24 or 48 hours exposure (100 nM YTX), respectively (Suárez Korsnes *et al*., 2006b). In cardiomyocytes culture, a significantly reduced mitochondrial membrane (mitochondrial depolarization) occurred after 48-72 hours exposure to 0.01-1 μM YTX ($p<0.001$). On the contrary, a significant ($p<0.001$) increase in mitochondrial membrane polarization (hyperpolarization) occurred at the same toxin concentrations after 24 hour incubation. This could be in agreement with MTT results obtained after 24 h exposure. In neurons, the hyperpolarization produced by specific inhibition of the mitochondrial $Na^+/Ca^{2+}$ exchanger has been correlated to the increase in matrix $Ca^{2+}$ and the consequent $Ca^{2+}$-dependent increased metabolic activity. An important role for matrix $Ca^{2+}$ in matching ATP production with cellular activity has been proposed, since two key enzymes of the tricarboxylic acid cycle as well as the overall activity of the electron transport chain are upregulated by matrix $Ca^{2+}$ levels achieved in stimulated cardiac myocytes (White and Reynolds, 1996). However, contrasting opinions are described in literature (see below).

The mitochondrial permeability transition is the consequence of causes such as calcium overload, reactive chemicals and oxidative stress. This process activates a large conductance permeability transition pore that makes the mitochondrial inner membrane permeable to all solutes of molecular weight up to about 1500 Da, with consequent mitochondrial depolarization, uncoupling of oxidative phosphorylation and mitochondrial swelling driven by colloid osmotic forces that ends in the rupture of mitochondrial outer membrane. Pore composition remains controversial: a multicomponent protein complex assembles at contact sites of inner and outer mitochondrial membranes and its constituents comprehend the voltage-dependent anion channel, adenine nucleotide translocase, hexokinase, creatine kinase, cyclophilin D and peripheral benzodiazepine receptor (Kroemer *et al*., 2007; Lemasters *et al*., 2009). This latter component is a receptor for benzodiazepines abundantly expressed in mitochondrial membranes of most peripheral tissues. Its pharmacology is distinct from the central receptor subtype and it is selectively inhibited by the benzodiazepine Ro5-4864 (4'-chlorodiazepam) as well as the nonbenzodiazepine isoquinoline carboxamide derivative PK-

11195. These ligands block the mitochondrial inner membrane anion channel stabilizing the inner membrane potential, and can block or prevent if beforehand mitochondrial inner membrane potential depolarizations triggered by metabolic stress. Moreover, a peculiar heart protective role has been shown for 4'-chlorodiazepam (Akar *et al*., 2005).

In the present study, YTX-altered mitochondrial potential in neonatal rat cardiomyocytes wasn't affected by either PK-11195 and/or 4-chlorodiazepam after 24-48 h exposure. When cells were incubated with receptor ligand only, the membrane depolarization occurred, for an averaged value of ~16% for PK-11195, ~18% for R5-4864 and 10% for their association. This could be related to the depressing effects on cardiac activity of these compounds, such as the significant reduction in indices of contractility, aortic flow, stroke work and total pressure-volume area in isolated working rat heart model (Edoute *et al*., 1993), negative inotropic and chronotropic effects (Gesi *et al*., 1999).

Results obtained at 24 hours were confirmed by MTT assay, with no altered YTX-induced mitochondrial dehydrogenase activity in presence of peripheral benzodiazepine receptor ligands Ro5-4864 and/or PK-11195.

Mitochondrial permeability transition occurs in several forms of cell death, included necrosis, apoptosis and autophagy (Lemasters *et al*., 1998). Several authors already reported a YTX-induced apoptotic effect, DNA fragmentation and caspase 3-7-9 activation with great difference in sensitivity among cell lines (Leira *et al*., 2002; Malaguti *et al*., 2002; Pérez-Gómez *et al*., 2006; Suárez Korsnes *et al*., 2006a). On the contrary, YTX failed to induce DNA fragmentation in rat and mouse skeletal muscle myoblast (Suárez Korsnes *et al*., 2006a); a pro-apoptotic effect in both IPLB-LdFB insect fat body and NIH3T3 mouse fibroblast cells (Malagoli *et al*., 2006b), activation of caspase-3 and -7 or fragmentation of poly(ADP)ribose polymerase in both Caco-2 and MCF-7 cells have also been reported (Callegari and Rossini, 2008).

To test whether cardiomyocytes depolarization was concomitant to an apoptotic event, treated cells were stained with nuclear fluorochrome DAPI. A YTX-induced appearance of nuclear apoptotic bodies was observable after both continuous exposure for 1, 5 and 24 h, with a time-dependent effect, and after 1, 5 and 24 h treatment observing cells after up to 71 hours in culture without the toxin, with a concentration- and time-dependent effect.

To confirm the apoptotic effect of YTX, caspase activity was measured after 5, 24, 48 and 72 h exposure to YTX (0.001 up to 0.1 μM). In contrast to expectations, results obtained showed no caspase activation for initiator caspases 2, 8, 10 and 9; as well as for executor caspases 3, 6

and 7 and caspase 1, involved in cytokine activation. These results are in contrast to some of previous studies performed on different cell lines, whilst are in agreement with no apoptotic DNA fragmentation occurrence found in mice heart tissue sections from *in vivo* studies by TUNEL staining (Tubaro *et al*., 2003; 2004).

Moreover, these findings can be related to mitochondrial membrane potential observations. Since proton re-entry during ATP production in complex V normalizes mitochondrial membrane potential and prevents hyperpolarization, this alteration could mean a disturbance of the electron transport system (Iijima *et al*., 2003). ATP is essential for cell apoptosis: the so-called apoptosome complex formed after cytochrome c release from mitochondria finally activates procaspase 9 to caspase 9 in an ATP or dATP dependent fashion. When ATP is depleted, apoptosis is blocked (Kim *et al*., 2003). It would be useful to monitor cardiomyocytes ATP levels in the first 48 hours of exposure to YTX for a better understanding.

A morphological damage due to insufficient amount of ATP has been described when the coronary flow is re-established after a prolonged ischemic episode: the partial recovery of mitochondrial function generates an amount of ATP sufficient for contraction but not for relaxation, resulting in hyper-contracture and sarcolemma rupture. This effect can be prevented by respiratory chain inhibitors or mitochondrial uncouplers as well as by inhibition of myosin ATPase (Bernardi *et al*., 2006). This could explain the ultrastructural alterations such as separation of bundles of myofibrils, sarcoplasmic reticulum and T-systems observed in tissue preparations from mice treated with YTX (J.S. Ramsdell, personal communication) in several *in vivo* studies (Terao *et al*., 1990; Aune *et al*., 2002; Tubaro *et al*., 2003; 2004; 2008a).

A separate set of cytotoxicity experiments was performed by both MTT and SRB assays to evaluate both the entity and the reversibility of cytotoxic damage in YTX-exposed cardiomyocytes. Results obtained showed a time-dependent reduced viability even after a short time of exposure such as 1 hour (0.1 µM YTX) with no recovery of viability after up to 71 h in YTX-free culture. After 24 hours of exposure, 0.01 µM YTX was the lowest effective concentration. These results suggest a cell damage consequent to toxin exposure that once triggered leads irreversible to cell death.

Since no caspase activation occurred, the apoptosis pathway seems to be improbably involved in YTX cytotocicity on cardiomyocytes, and two other cell death mechanisms could be considered: necrosis and autophagy. Necrosis causes disruption of the plasma membrane

leading to lactate dehydrogenase leakage from cells. Autophagy results in formation of an autophagosome that could destroy major portions of the cytoplasm and organelles, with no nuclear chromatin condensation, no caspase activation or DNA degradation, mitochondrial and endoplasmic reticulum swelling (Ellis *et al*., 2010). From *in vivo* studies performed in mice, no autophagic response has been observed in mice heart ultrastructure. On the contrary, desulfated yessotoxin induced the clear appearance of small autophagosomes in a very short time, but the target organs were liver and pancreas, with no cardiac alteration (Terao *et al*., 1990).

Subsequent experiments were then performed on cardiomyocytes by propidium iodide uptake to detect dye-permeable necrotic cells. Cells were exposed for 5, 24, 48 and 72 h to increasing YTX concentrations (0.0001 up to 0.1 μM). Experiments showed a significant ($p$<0.01) increase of dye uptake after 24 h (0.01 μM), that was stronger at 48 h ($p$<0.001). No uptake was found after 5 h YTX exposure. These results are in contrast with those of Leira *et al*. (2002) in neuroblastoma cells, but are in agreement with a recent study performed in HepG2 cell line (Young *et al*., 2009).

The occurrence of apoptotic bodies with no detection of apoptosis is object of recent studies. It seems either that apoptotic pathways activated can be interrupted downstream by concomitant upregulation of endogenous caspase inhibitors and repressors, as well as by the lack of ATP needed to complete the active process of apoptosis. Moreover, this condition impairs cardiac contractile performance without myocytes drop-out. Another possible outcome of apoptosis interrupts is caspase-independent apoptosis, characterized by DNA cleavage into ~50 Kbp fragments much larger than the 200 bp fragments seen after conventional apoptosis. The critical mediators of caspase independent apoptosis are normally located in the mitochondrial intermembranous space and are released by permeabilization of outer mitochondrial membrane. Once released into the cytosol, these activators directly cause apoptosis by translocating from the cytosol to the nucleus where cause DNA fragmentation without caspase activation. This apoptosis way is thought to play significant roles in programmed cell death occurring with ischaemia-reperfusion and oxidant injury (Dorn, 2009). Thus, in cardiomyocyte culture, a first apoptotic feature such as nuclear apoptotic bodies could be followed by necrotic cell death correlated to the lost mitochondrial functionality.

An additional experiment was performed on HL-1 atrial cardiomyocytes. Cells were exposed to the highest concentration of YTX employed in experiments (1 μM) and mitochondrial membrane potential was monitored as soon as incubation started up to 60

minutes. In this experimental system, no mitochondrial membrane potential depolarization was detectable. Previously, Bianchi *et al*. (2004) demonstrated an immediate and potent effect of YTX as a direct pore opener of mitochondrial permeability transition pore in both mitochondria isolated from adult rat livers and in intact MH1C1 Morris Hepatoma cell line. This could be tentatively explained because of cardiac myocytes constant fluctuations of free $Ca^{2+}$: their mitochondria may adapt to become resistant to $Ca^{2+}$ induction of the MPT. This adaptation may not occur in non excitable tissues such as liver, which is also vulnerable to MPT-dependent ischemia-reperfusion injury as well as heart (Lemasters *et al*., 2009). Results obtained show a high cytotoxicity in cardiomyocytes as well as a very cell specific response consequent to YTX exposure. The toxicological potential of this toxin needs to be further investigated to better understand the health risk to the humans.

# *REFERENCES*

Akar F.G., Aon M.A., Tomaselli G.F., O'Rourke B. 2005. The mitochondrial origin of postischemic arrhythmias. J Clin Invest 115: 3527-3535.

Alfonso A., de la Rosa L., Vieytes M.R., Yasumoto T., Botana L.M. 2003. Yessotoxin, a novel phycotoxin, activates phosphodiesterase activity. Effect of yessotoxin on cAMP levels in human lymphocytes. Biochem Pharmacol 65: 193-208.

Alfonso, C., Alfonso, A., Vieytes, M.R., Yasumoto, T., Botana, L.M. 2005. Quantification of yessotoxin using the fluorescence polarization technique and study of the adeguate extraction procedure. Anal Biochem 344: 266-274.

Ares, I.R., Louzao, M.C., Vieytes, M.R., Yasumoto, T., Botana, L.M. 2005. Actin cytoskeleton of rabbit intestinal cells is a target for potent marine phycotoxins. J Exp Biol 208: 4345-4354.

Athias P., Vandroux D., Tissier C., Rochette L. 2006. Development of cardiac physiological models from cultured cardiomyocytes. Ann Cardiol Angeiol (Paris) 55: 90-99.

Aune, T., Sorby, R., Yasumoto, T., Ramstad, H., Landsverk, T. 2002. Comparison of oral and intraperitoneal toxicity of yessotoxin towards mice. Toxicon 40: 77-82.

Baskin S.I. 1991. Principles of cardiac toxicology. CRC Press, Boca Raton Ann Arbor, Boston London, pp13-20.

Beraud N., Pelloux S., Usson Y., Kuznetsov A.V., Ronot X., Tourneur Y., Saks V. 2009. Mitochondrial dynamics in heart cells: Very low amplitude high frequency fluctuations in adult cardiomyocytes and flow motion in non beating Hl-1 cells. J Bioenerg Biomembr 41: 195-214.

Bernardi P., Krauskopf A., Basso E., Petronilli V., Blachly-Dyson E., Di Lisa F., Forte M.A. 2006. The mitochondrial permeability transition from *in vitro* artifact to disease target. FEBS J 273(10): 2077-99.

Bianchi C., Fato R., Angelin A., Trombetti F., Ventrella V., Borgatti A.R., Fattorusso E., Ciminiello P., Bernardi P., Lenaz, G., Castelli G.P. 2004. Yessotoxin, a shellfish biotoxin, is a potent inducer of the permeability transition in isolated mitochondria and intact cells. Biochim Biophys Acta 1656: 139-147.

Callegari F., Rossini G.P. 2008. Yessotoxin inhibits the complete degradation of E-cadherin. Toxicology 244: 133-144.

Callegari F., Sosa S., Ferrari S., Soranzo M.R., Pierotti S., Yasumoto T., Tubaro A., Rossini G.P. 2006. Oral administration of yessotoxin stabilizes E-cadherin in mouse colon. Toxicology 227: 145-155.

CEE, 2002. Commission decision of 15 March 2002. Official J. Eur. Commun. 16.3.2002.

Chlopcikova S., Psotova J., Miketova P. 2001. Neonatal rat cardiomyocytes-a model for the study of morphological, biochemical and electrophysiological characteristics of the heart. Biomed Papers 145: 49-55.

Ciminiello P., Fattorusso E. 2008. Chemistry, metabolism and chemical analysis. In: Botana, L.M. Ed., Seafood and Freshwater Toxins. Pharmacology, Physiology and Detection, 2nd ed., CRC Press, Taylor & Francis Group, Boca Raton, pp. 287-314.

Ciminiello P., Fattorusso E., Forino M., Magno S., Poletti R., Viviani R. 1998. Isolation of adriatoxin, a new analogue of yessotoxin from mussels of the Adriatic Sea. Tetrahedron Lett 39: 8897-8900.

Claycomb W.C., Lanson N.A., Stallworth B.S., Egeland D.B., Delcarpio J.B., Bahinski A., Izzo N.J. 1998. HL-1 cells: A cardiac muscle cell line that contracts and retains phenotypic characteristics of the adult cardiomyocytes. Cell Biol 95: 2979-2984.

Cossarizza A. 1997. Measure of mitochondria membrane potential with the fluorescent probe JC-1 (http://www.cyto.purdue.edu/flowcyt/research/cytotech/amfc/data/page13.htm).

de la Rosa L.A., Alfonso A., Vilariño N., Vieytes M.R., Botana L.M. 2001a. Modulation of cytosolic calcium levels of human lymphocytes by yessotoxin, a novel marine phycotoxin. Biochem Pharmacol 61: 827-833.

de la Rosa L.A., Alfonso A., Vilariño N., Vieytes M.R., Yasumoto T., Botana L.M. 2001b. Maitotoxin-induced calcium entry in human lymphocytes: modulation by yessotoxin, $Ca^{2+}$ channel blockers and kinases. Cell Signal 13: 711-716.

DiFrancesco D. 2006. Funny channels in the control of cardiac rhythm and mode of action of selective blockers. Pharmacol Res 53: 399-406.

Dominguez H.J., Paz B., Daranas A.H., Norte M., Franco J.M., Fernandez J.J. 2009. Dinoflagellate polyether within the yessotoxin, pectenotoxin and okadaic acid toxin groups: characterization, analysis and human health implications. Toxicon doi: 10.16/j.toxicon.2009.11.005.

Dorn G.W. 2009. Apoptotic and non-apoptotic programmed cardiomyocyte death in ventricular remodelling. Cardiovasc Res 81: 465-473.

Edoute Y., Giris J., Ben-Haim S.A., Lochner A., Weitzman A., Hayam G., Katz Y., Gavish M. 1993. Ro5-4864 and PK11195, but not diazepam, depress cardiac function, in an isolated worling rat heart model. Pharmacol 46: 224-230.

Ellis C.E., Naicker D., Basson K.M., Botha C.J., Meintjes R.A., Schults R.A. 2010. Cytotoxicity and ultrastructural changes in H9c2(2-1) cells treated with pavetamine, a novel polyamine. Toxicon 55: 12-19.

Espenes A., Aasen J., Satake M., Smith A., Eraker N., Aune T. 2006. Toxicity of yessotoxin in mice after repeated oral exposure. In: Henshilwood, K., Deegan, B., McMahon, T., Cusack, C., Keaveney, S., Silke, J., O'Cinneide, M., Lyons, D., Hess, P. Eds., Molluscan Shellfish Safety. Proceedings 5th International Conference on Molluscan Shellfish Safety, 14-18 June 2004, Galway, Ireland, pp. 419-423.

Ferrari S., Ciminiello P., Dell'Aversano C., Forino M., Malaguti C., Tubaro A., Poletti R., Yasumoto T., Fattorusso E., Rossini G.P. 2004. Structure-activity relationships of yessotoxins in cultured cells. Chem Res Toxicol 17: 1251-1257.

Florio C., Frausin F., Vertua R., Gaion R. M. 1999. Involvement of P1 receptors in the effect of forskolin on cyclic AMP accumulation and export in PC12 cells. Biochem Pharmacol 57: 355-364.

Franchini A., Marchesini E., Poletti R., Ottaviani E. 2004a. Acute effect of the algal yessotoxin on Purkinje cells from the cerebellum of Swiss CD1 mice. Toxicon 43: 347-352.

Franchini A., Marchesini E., Poletti R., Ottaviani E. 2004b. Lethal and sublethal yessotoxin dose-induced morpho-functional alterations in intraperitoneal injected Swiss CD1 mice. Toxicon 44: 83-90.

Fu J., Gao J., Pi R., Liu P. 2005. An optimized protocol for culture of cardiomyocyte from neonatal rat. Cytotech 49: 109-116.

Gesi M., Riva A., Soldani P., Fornai F., Natale G., Lenzi P., Pellegrini A., Paparelli A. 1999. Central and peripheral benzodiazepine ligands prevent mitochonrial damage induced by noise exposure in the rat myocardium: an ultrastructural study. Anat Rec 255: 334-341.

Harary I., and Farley B. 1963. *In vitro* studies on single beating rat heart cells I: Growth and organization. Exp Cell Res 29: 451-465.

Haselsberger K., Peterson D.C., Thomas D.G., Darling J.L. 1996. Assay of anticancer drugs in tissue culture: comparison of a tetrazolium-based assay and a protein binding dye assayin short-term cultures derived from human malignant glioma. Anticancer Drugs 7: 331-338.

Howard M.D., Smith G.J., Kudela R.M. 2009. Phylogenetic relationships of yessotoxin-producing dinoflagellates, based on the large subunit and internal transcribed spacer ribosomal DNA domains. Appl Environm Microbiol 75: 54-63.

Iijima T., Mishima T., Akegawa K., Iwao Y., 2003. Mitochondrial hyperpolarization after transient oxygen-glucose deprivation and subsequent apoptosis in cultured rat hippocampal neurons. Brain Res 993: 140-145.

Inoue, M., Hirama, M., Satake, M., Sugiyama, K., Yasumoto, T. 2003. Inhibition of brevetoxin binding to the voltage-gated sodium channel by gambierol and gambieric acid-A. Toxicon 41: 469-474.

Keepers Y.P., Pizao P.E. Peters G.J., van Ark-Otte J., Winograd B., Pinedo H.M. 1991. Comparison of the sulforhodamine B protein and tetrazolium (MTT) assays for *in vitro* chemosensitivity testing. Eur J Cancer 27: 897-900.

Kim J.S., He L., Lemasters J.J. 2003. Mitochondrial permeability transition: a common pathway to necrosis and apoptosis. Biochem Biophys Res Comm 304: 463-470.

Korichneva I., Waka J., Hammerling U. 2003. Regulation of the cardiac mitochondrial membrane potential by retinoids. J Pharmacol Exp Ther 305: 426-433.

Kroemer G., Galluzzi L., Brenner C. 2007. Mitochondrial Membrane Permeabilization in Cell Death. Physiol Rev 87: 99-163.

Leira F., Alvarez C., Vieites J.M., Vieytes M.R., Botana L.M. 2002. Characterization of distinct apoptotic changes induced by okadaic acid and yessotoxin in the BE(2)-M17 neuroblastoma cell line. Toxicol In Vitro 16: 23-31.

Leira F., Alvarez C., Cabado A.G., Vieites J.M., Vieytes M.R., Botana L.M. 2003. Development of a F actin-based live-cell fluorimetric microplate assay for diarrhetic shellfish toxins. Anal Biochem 317: 129-135.

Lemasters J.J., Qian T., Elmore S.P., Trost L.C., Nishimura Y., Herman B., Bradham C.A., Brenner D.A., Nieminen A.L. 1998. Confocal microscopy of the mitochondrial permeability transition in necrotic cell killing, apoptosis and autophagy. Biofactors. 8: 283-285.

Lemasters J.J., Nieminen A.L., Qian T., Trost L.C., Elmore S.P., Nishimura Y., Crowe R.A., Cascio W.E., Bradham C.A., Brenner D.A., Herman B. 2009. The mitochondrial permeability transition in cell death: a common mechanism in necrosis, apoptosis and autophagy. 1366: 177-196.

Louzao M.C., Cagide E., Vieytes M.R., Sasaki M., Fuwa H., Yasumoto T., Botana L.M. 2006. The sodium channel of human excitable cells is a target for gambierol. Cell Physiol Biochem 17: 257-268.

Maack C., O'Rourke B. 2007. Excitation-contraction coupling and mitochondrial energetic. Basic Res Cardiol 102(5): 369-392.

Malagoli D., Ottaviani E. 2004. Yessotoxin affects fMLP-induced cell shape changes in *Mytilus galloprovincialis* immunocytes. Cell Biol Int 28: 57-61.

Malagoli D., Casarini L., Ottaviani E. 2006a. Algal toxin yessotoxin signalling pathways involve immunocyte mussel calcium channels. Cell Biol Int 30: 721-726.

Malagoli D., Marchesini E., Ottaviani E. 2006b. Lysosomes as the target of yessotoxin in invertebrate and vertebrate cell lines. Toxicol Lett 167: 75-83.

Malaguti C., Ciminiello P., Fattorusso E., Rossini G.P. 2002. Caspase activation and death induced by yessotoxin in HeLa cells. Toxicol In Vitro 16: 357-363.

Mathur A., Hong Y., Kemp B., Barrientos A.A., Erusalimisky J.D. 2000. Evaluation of fluorescent dyes for the detection of mitochondrial membrane potential changes in cultured cardiomyocytes. Cardiovasc Res 46: 126-138.

Miles C.O., Wilkins A.L., Hawkes A.D., Selwood A.I., Jensen D.J., Munday R., Cooney J.M., Beuzenberg V. 2005. Polyhydroxylated amide analogs of yessotoxin from *Protoceratium reticulatum*. Toxicon 45: 61-71.

Mosmann, T. 1983. Rapid colorimetric assay for cellular growth and survival: application to proliferation and cytotoxicity assays. J Immunol Methods 65: 55–63.

Mouri R. Oishi T., Torikai K., Ujiara S., Matsumori N., Murata M., Oshima Y. 2009. Surface plasmon resonance-based detection of ladder-shaped polyethers by inhibition detection method. Bioorg Med Chem Lett. 19: 2824-2828.

Munday R., Finch S., Miles C., Munday C., Towers N. 2001. Yessotoxin toxicity studies. Gordon Research Conference on Mycotoxins and Phycotoxins. Williamstown (USA), June 24-29, 2001.

Munday R., Aune T., Rossini G.P. 2008. Toxicology of the yessotoxins. In: Botana, L.M. (Ed.), Seafood and Freshwater Toxins. Pharmacology, Physiology and Detection, 2nd ed., CRC Press, Taylor & Francis Group, Boca Raton, pp. 329-339.

Murata M., Kumagai M., Lee J.-S., Yasumoto T. 1987. Isolation and structure of yessotoxin, a novel polyether compound implicated in diarrhetic shellfish poisoning. Tetrahedron Lett. 28: 5869-5872.

Nordstedt C., Fredholm B.B. 1990. A modification of a protein-binding method for rapid quantification of cAMP in cell-culture supernatants and body fluid. Anal Biochem 189: 231-234.

Ogino H., Kumagai M., Yasumoto T. 1997. Toxicologic evaluation of yessotoxin. Nat Toxins 5: 255-259.

Orsi C.F., Colombari B., Callegari F., Todaro A.M., Ardizzoni A., Rossini G.P., Blasi E., Peppoloni S. 2010. Yessotoxin inhibits phagocytic activity of macrophages. Toxicon 55: 265-273.

Paz B., Riobó P., Fernández M.L., Fraga S., Franco J.M. 2004. Production and release of yessotoxins by the dinoflagellates *Protoceratium reticulatum* and *Lingulodinium polyedrum* in culture. Toxicon 44: 251-258.

Paz B., Daranas A.H., Norte M., Riobó P., Franco J.M., Fernández J.J. 2008. Yessotoxins, a group of marine polyether toxins: an overview. Mar Drugs 6: 73-102.

Pazos M.J., Alfonso A., Vieytes M.R., Yasumoto T., Botana L.M. 2006. Study of the interaction between different phosphodiesterases and yessotoxin using a resonant mirror biosensor. Chem Res Toxicol 19: 794-800.

Pérez-Gómez A., Ferrero-Gutierrez A., Novelli A., Franco J.M., Paz B., Fernández-Sánchez M.T. 2006. Potent neurotoxic action of the shellfish biotoxin yessotoxin on cultured cerebellar neurons. Toxicol Sci 90: 168-177.

Pierotti S., Malaguti C., Milandri A., Poletti R., Rossini G.P. 2003. Functional assay to measure yessotoxins in contaminated mussel samples. Anal Biochem 312: 208-216.

Rhodes L., McNabb P., de Salas M., Briggs L., Beuzenberg V., Gladstone M. 2006. Yessotoxin production by *Gonyaulax spinifera*. Harmful Algae 5: 148-155.

Ronzitti G., Callegari F., Malaguti C., Rossini G.P. 2004. Selective disruption of the E-cadherin-catenin system by an algal toxin. Br J Cancer 90: 1100-1107.

Ronzitti G., Hess P., Rehmann N., Rossini G.P. 2007. Azaspiracid-1 alters the E-cadherin pool in epithelial cells. Toxicol Sci 95: 427-435.

Satake M., MacKenzie L., Yasumoto T. 1997. Identification of *Protoceratium reticulatum* as the biogenetic origin of yessotoxin. Nat Toxins 5: 164-167.

Scaduto R.C. and Grotyohann L.W. 1999. Measurement of mitochondrial membrane potential using fluorescent rhodamine derivatives. Biophys J 76: 469-477.

Skehan P., Storeng R., Scudiero D., Monks A., McMahon J., Vistica D., Warren JT, Bokesch H, Kenney S., Boyd MR, 1990. New colorimetric cytotoxicity assay for anticancer-drug screening. J Natl Cancer Inst 82: 1107-12.

Stemmler M.P. 2008. Cadherins in development and cancer. Mol Biosyst 4: 835-850.

Suárez Korsnes M.S., Hetland D.L., Espenes A., Tranulis M.A., Aune T. 2006a. Apoptotic events induced by yessotoxin in myoblast cell lines from rat and mouse. Toxicol In Vitro 20: 1077-1087.

Suárez Korsnes M., Hetland D.L., Espenes A., Aune T. 2006b. Induction of apoptosis by YTX in myoblast cell lines via mitochondrial signalling transduction pathway. Toxicol In Vitro 20: 1419-1426.

Suárez Korsnes M.S., Hetland D.L., Espenes A., Aune T., 2007. Cleavage of tensin during cytoskeleton disruption in YTX-induced apoptosis. Toxicol In Vitro 21: 9-15.

Terao K., Ito E., Yanagi T., Yasumoto T. 1990. Histopathological studies on experimental marine toxin poisoning. 5. The effects in mice of yessotoxin isolated from *Patinopecten yessoensis* and of a desulfated derivative. Toxicon 28: 1095-1104.

Tubaro A., Sidari L., Della Loggia R., Yasumoto T. 1998. Occurrence of homoyessotoxin in phytoplankton and mussels from Northern Adriatic Sea. In: Reguera, B., Blanco, J., Fernández M. L., Wyatt T. Eds., Harmful

Algae, Xunta de Galicia and Intergovernmental Oceanographic Commission of UNESCO, Grafisant, Santiago de Compostela, pp. 470-472.

Tubaro A., Sosa S., Carbonatto M., Altinier G., Vita F., Melato M., Satake M., Yasumoto T. 2003. Oral and intraperitoneal acute toxicity studies of yessotoxin and homoyessotoxins in mice. Toxicon 41: 783-792.

Tubaro A., Sosa S., Altinier G., Soranzo M.R., Satake M., Della Loggia R., Yasumoto T. 2004. Short-term oral toxicity of homoyessotoxins, yessotoxin and okadaic acid in mice. Toxicon 43: 439-445.

Tubaro A., Giangaspero A., Ardizzone M., Soranzo M.R., Vita F., Yasumoto T., Maucher J.M., Ramsdell J.S., Sosa S., 2008a. Ultrastructural damage to heart tissue from repeated oral exposure to yessotoxin resolves in 3 months. Toxicon 51: 1225-1235.

Tubaro A., Bandi E., Sosa S., Soranzo M.R., De Ninis V., Yasumoto T., Lorenzon P. 2008b. Effects of YTX on the skeletal muscle: an update. Food Addit Contam 25: 1095-1100.

Voigt W. 2005. Sulforhodamine B assay and chemosensitivity. Methods Mol Med. 110: 39-48.

White R.J. and Reynolds I.J. 1996. Mitochondrial depolarization in glutamate-stimulated neurons: an early signal specific to excitotoxins exposure. J Neurosci 16: 5688-5697

White S.M., Constantin P.E., Claycomb W.C. 2004. Cardiac physiology at the cellular level: use of cultured HL-1 cardiomyocytes for studies of cardiac muscle cell structure and function. Am J Physiol Heart Circ Physiol 286: H823-H829.

Yasumoto T, Takizawa A. 1997. Fluorometric measurement of yessotoxins in shellfish by high-pressure liquid chromatography. Biosci Biotechnol Biochem 61(10): 1775-1777.

Young C., Truman P., Boucher M., Keyzers R.A., Northcote P., Jordan T.W. 2009. The algal metabolite yessotoxin affects heterogeneous nuclear riboproteins in HepG2 cells. Proteomics 9: 2529-2542.

# CONTENTS

# CYCLIC POLYETHER PHYCOTOXINS *IN VITRO* STUDIES: COMPARISON OF CIGUATOXINS AND BREVETOXINS POTENCY ON HUMAN VGSC OF BRAIN AND PERIPHERAL SENSORY NEURONS EXPRESSED IN HEK293 CELLS


**Summary** ..... **60**

**Introduction** ..... **62**

Brevetoxins chemical structure ..... 62

Ciguatoxins chemical structure ..... 64

Brevetoxins and ciguatoxins intoxication ..... 65

Brevetoxins and ciguatoxins molecular target ..... 67

Brevetoxins and ciguatoxins *in vitro* effects ..... 69

Voltage-gated sodium channels ..... 70

Structure ..... 70

Distribution and classification ..... 72

Voltage-gated sodium channel and pain ..... 73

Voltage-gated sodium channel neurotoxins ..... 75

**Aim of the study** ..... **78**

**Materials and Methods** ..... **79**

HEK-293 cell line culture ..... 79

Stable cell transfection ..... 79

RNA extraction and clean-up ..... 80

Reverse transcription ..... 81

Real Time PCR ..... 82

Real Time PCR products bio sizing and quantification ..... 83

Real Time PCR products clean up ..... 83

Real Time PCR products sequencing ..... 84

Cytotoxicity assay ..... 84

Amino acid sequence comparison ..... 84

Data analysis ..... 85

Chemicals ..... 85

**Results** ..... **87**

Expression of $Na_V1.2$ and $Na_V1.8$ VGSC alpha subunit mRNA in HEK clones ..... 87

Real Time PCR .....87
Real Time PCR products bio sizing and quantification .....88
Real Time PCR product sequencing .....88
Brevetoxin and ciguatoxins toxicity on HEK clones and on HEK-non transfected cells .....89
Dose-response curves .....89
Comparison of brevetoxin and ciguatoxin $EC_{50}$ values in $Na_V$ clones .....91
Amino acid sequence comparison .....92
**Discussion** .....**94**
**Conclusions** .....**97**
**References** .....**98**

## SUMMARY

Brevetoxins (BTXs) and ciguatoxins (CTXs) are two classes of algal neurotoxins produced by the dinoflagellates *Karenia brevis* and *Gambierdiscus toxicus*, and in humans are responsible of Neurotoxic Shellfish Poisoning and Ciguatera Fish Poisoning, respectively. Both intoxications are mainly characterized by neurological and gastro-intestinal symptoms and, in more severe cases, cardiovascular symptoms. Pharmacological studies have shown that molecular target for the CTXs and BTXs is the site-5 on the voltage-gated sodium channel ($Na_V$). Toxin binding modifies channel activation and inactivation mechanisms to a terminal excitotoxicity and cell swelling via continuous sodium influx, membrane depolarization and spontaneous action potentials.

$Na_V$ are responsible for action potential generation and propagation in excitable cells, playing a fundamental role in many higher processes such as cognition, cardiac conduction and sensitive perception. Mammalian $Na_V\alpha$-subunits have been identified in excitable tissues and named $Na_V1.1$ through $Na_V1.9$ as products of different genes and with different primary tissue distributions, cDNA sequences, protein structures, gating kinetics and pharmacological properties. This study focused on the $Na_V1.8$ isoform, highly expressed in sensory dorsal root ganglion neurons and the $Na_V1.2$ isoform, broadly expressed in neurons in the central nervous system, with the aim to better understand central and peripheral nervous system effects of these toxins in human poisoning episodes. The activity of BTXs (PbTx-1, PbTx-7, PbTx-3), and CTXs (P-CTX-1, C-CTX-1 and P-CTX-3C) was screened on the human embryonic kidney cell line (HEK293) stably expressing either $Na_V1.2$ or $Na_V1.8$ human isoforms.

Cells were transfected by a chemical approach with $Na_V\alpha$ subunits cDNA gene inserted in a TrueClone pCMV6-Neo plasmid and complexed in a liposome transfection reagent. The mRNA level analysis using Real Time PCR technique showed the specific presence of both isoforms only in transfected cells. Product specificity was confirmed by bio-sizing and sequencing techniques. The cytotoxic effects of neurotoxin BTX and CTX were assessed by exposing cells to increasing toxin concentrations in presence of the sodium channel activator veratridine and the sodium-potassium ATPase inhibitor ouabain. Results showed for BTX A and BTX B types, as well as for P- and C-CTX, a dose-dependent toxic effect on both HEK-$Na_V1.2$ and HEK-$Na_V1.8$ clones while no observable effects were measured on the non-transfected cells. For both clones, $EC_{50}$ values of either P-CTX-1 and PbTx-7 were one order

of magnitude lower than those of other CTXs tested ($10^{-13}$ *vs* $10^{-12}$ M) and other BTXs tested ($10^{-10}$ *vs* $10^{-9}$ M).

Overall the toxic response of the peripheral $Na_V1.8$ to the polyether toxins was similar to that of the $Na_V1.2$ suggesting the absence of a tissue selectivity of the polyether toxins for the peripheral channel. A better understanding of the particular sensory abnormalities associated to CFP and NSP will require further isoform studies.

# *INTRODUCTION*

**Brevetoxins chemical structure**

Brevetoxins (BTXs) are complex multi-ring methylated polyether neurotoxins produced by strains of the marine dinoflagellates *Karenia brevis* (formerly *Ptychodiscus brevis* or *Gymnodinium breve*). Two backbone type A and type B are known. The BTX type A backbone is formed by 10 contiguous ether rings (A-J) with the A-F and H-J rings forming two essentially independent planar portions of the backbone. This type can exist in solution in two stereochemical conformations relative to the G ring: a boat chair conformation and a crown conformation, with thermodynamics favouring the former. The BTX type B backbone consists of a long carbon chain forming 11 contiguous ether rings, all fused trans to one another. This ladder-like structure is essentially planar and rigid (Lin *et al*., 1981; Baden, 1989).

Both backbones originate a myriad of congeners (>15 toxins are known), including parent molecules and their biometabolites (figure 17). Initially, brevetoxins have been classified under several nomenclature that were unified by Poli *et al*. (1986) with the proposal for a unique notation system to correlate the toxins isolated from all the laboratories, with the numbering system proposed by Shimizu preceded by the letters PbTx denoting *Ptychodiscus brevis* toxin. As new brevetoxin metabolites are identified, the inclusion of the backbone type (type A or type B) in the nomenclature of brevetoxins has been more recently used. The brevetoxin chemical structures named with the 2 nomenclatures are reported in figure 16.

Brevetoxin derivatives result from epoxidation across the double bond in the H-ring or derivatization at the C-37 hydroxyl in PbTx-2 (Baden *et al*., 2005). Some other natural brevetoxins isolated so far include PbTx-11, characterized by a shortened side chain, PbTx-12, the only natural ketone brevetoxin known, and PbTx-tmb, PbTx-2 without the side chain tail. Other derivatives presumably non natural include PbTx-8, artefact of aqueous chloroform extraction of PbTx-2; PbTx-13 and -14, both believed to be extraction artefacts.

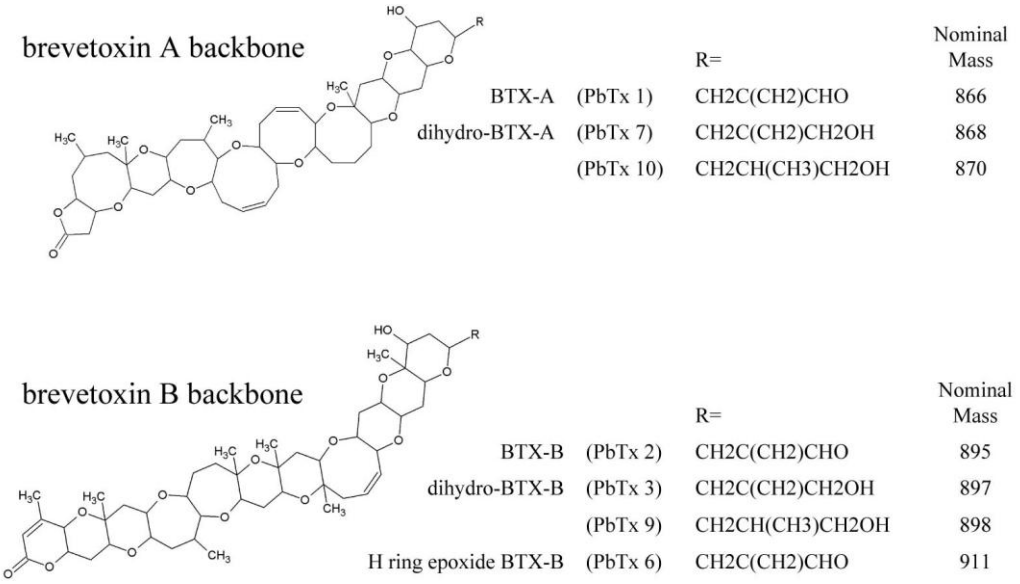


**Figure 16: brevetoxin neurotoxins structure**
(Modified from Plakas and Dickey, 2009).

Several biometabolites have been identified in shellfish and other living animals naturally or laboratory exposed to *K. brevis* brevetoxins. These metabolites included a desoxyBTX-B2, as well as glycinilcysteine, glutathione, and gamma-glutamylcysteine conjugates, and a series of fatty acids derivatives.

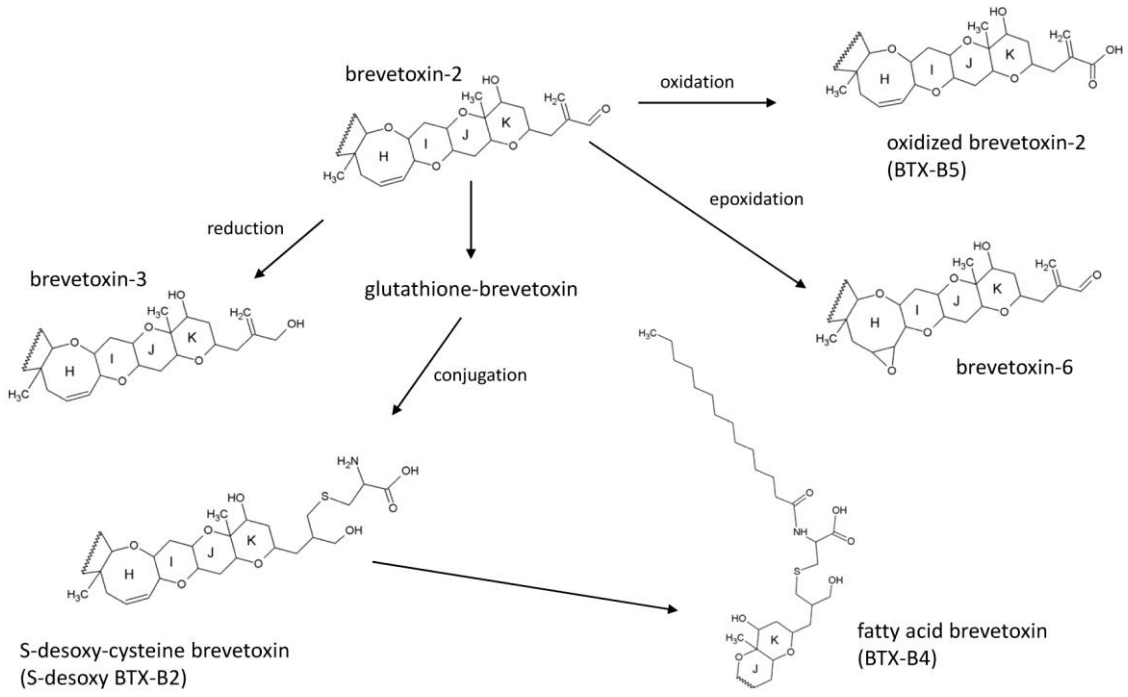


**Figure 17: Oxidative and conjugative pathways of B-type brevetoxin metabolism** (rings H through K with R groups shown).
(Modified from Radwan and Ramsdell, 2006).

## Ciguatoxins chemical structure

Ciguatoxins (CTXs) are a family of complex highly oxygenated cyclic polyether compounds produced by the benthic dinoflagellate of the genus *Gambierdiscus spp* which adhere to dead coral surfaces and bottom-associated algae (Bagnis *et al*., 1980). Toxins produced by algae are transmitted through marine food chain to herbivorous and carnivorous fishes, and ultimately to man (Vernoux *et al*., 1986). *Gambierdiscus* have been reported in Caribbean Sea, Indian and Pacific Ocean, (Pottier *et al*., 2002; Pottier and Vernoux, 2003) and more recently in the Western Africa Atlantic ocean and the eastern Mediterranean sea (Bentur and Spanier, 2007). Chemical structures of CTX have been found to vary with geographical origin (Vernoux and Lewis, 1997). Pacific Ocean ciguatoxins (P-CTX) and Caribbean ciguatoxins (C-CTX) have been isolated in different sources (*Gambierdiscus spp.*, herbivorous or carnivorous fishes) and their structure determined (figure 18), whilst four Indian Ocean CTXs have been isolated and characterized, however their instability during late stages of purification did not allow their structural characterization (Lewis, 2006). P-CTX and C-CTX backbone consist of 13-14 contiguous ether rings trans-fused in a ladder-like manner (Lin *et al*., 1981; Shimizu *et al*., 1986; Murata *et al*., 1989; Satake *et al*., 1993; Satake *et al*., 1998).

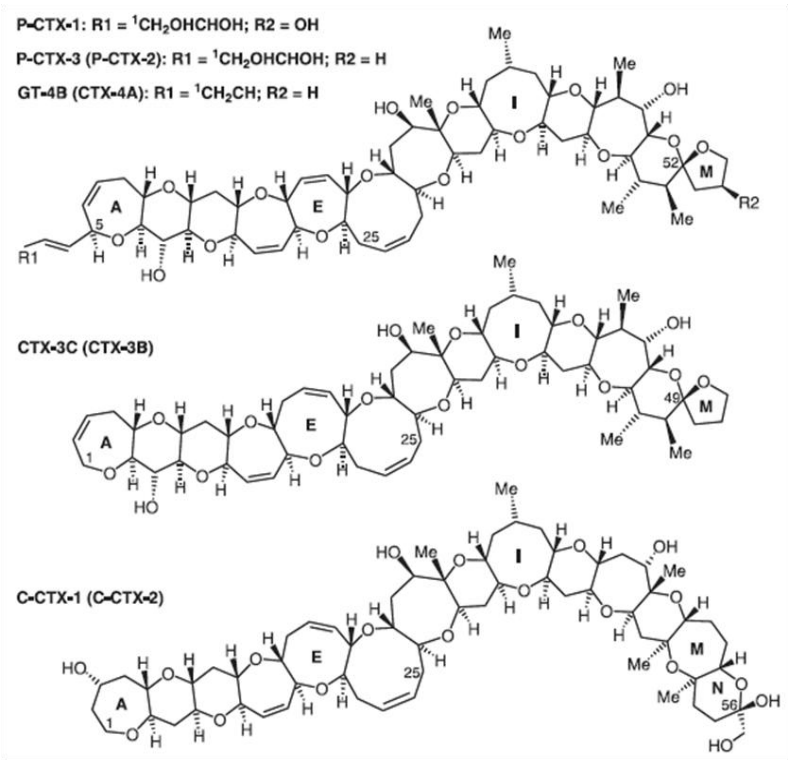


**Figure 18: Pacific and Caribbean ciguatoxin structure**
(Lewis, 2006).

Ciguatoxins and brevetoxins share similar structure, with trans/syn-fused ether rings of various sizes (see figure 19), lacking in nitrogen, with similar molecular weight (~1112 *vs* ~895, respectively) and common physical properties, in particular as non-polar compounds that are highly lipid-soluble.

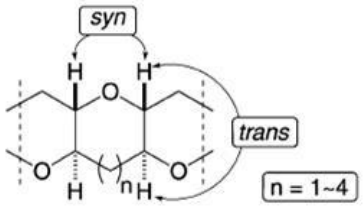


**Figure 19: common structural feature of ladder shaped polyethers like brevetoxins, ciguatoxins and yessotoxin**
(Inoue *et al*., 2003).

**Brevetoxin and ciguatoxin intoxication**

Brevetoxins are transferred and accumulated in fish through marine food web (Flewelling *et al*., 2005; Naar *et al*., 2007) responsible for massive fish kills in the gulf of Mexico (Poli *et al*., 1986; Dortch *et al*., 1998; Dickey *et al*., 1999). Brevetoxins are also responsible for birds, marine mammal mortalities and other marine species (Dickey *et al*., 1999; Trainer and Baden, 1999). Toxicity to humans is through a non-fatal foodborne illness named neurotoxic shellfish poisoning (NSP) that occurs after ingestion of shellfish (Johnson *et al*., 1985; Baden, 1989). Its symptoms include gastrointestinal effects, neurologic effects on both central and peripheral nervous system and cardiac effects. Gastrointestinal effects include abdominal pain and cramping, nausea, vomiting and diarrhoea. Common neurological symptoms include face, throat, fingers, toes and possibly total body paresthesias; ataxia; loss of coordination and/or balance; cramping limb pain; convulsions; paralysis; respiratory arrest up to coma; burning sensation of mucous membranes; distortion of oral and peripheral temperature sensation with reversal of temperature sensation (paradoxical dysaesthesia), i.e. warm drinks taste cold, a peripheral feeling like ‘cold rain’ (Johnson *et al*., 1985; Sims, 1987). Only in most severe cases also disturbances of cardiac function have been reported, but usually intoxications are characterized by severe gastrointestinal disorders, paresthestia and locomotory problems, and no human fatalities have been reported so far (Baden, 1989; David *et al*., 2003).

Other brevetoxins effects in humans are the consequence of skin exposure or through inhalation of aerosolized toxin formed from wave action during a red tide event. Consequences of inhalation are severe inflammatory response, with skin and upper-lower

airway irritation, with a non-productive cough, shortness of breath, bronchoconstriction, burning sensation of conjunctiva, rhinorrhea, sneezing, and eventually wheezing in persons predisposed to asthma (Huang *et al.*, 1984; Lombet *et al.*, 1987; Abraham *et al*., 2005).

Ciguatoxins are responsible for ciguatera fish poisoning (CFP), a human seafood intoxication caused by the ingestion of contaminated fish species from tropical and subtropical coral reefs. Ciguatoxins are transferred from the benthos to herbivorous, macroalgae-feeding species (fish and invertebrates) and then to carnivorous fish via marine food web (Lewis and Holmes, 1993). Ciguatera is the most frequently reported toxin related seafood illness in the world, with at least 50,000 cases reported annually worldwide (Lewis, 2001; Friedman *et al*., 2008). Onset of symptoms can vary from 30 minutes for severe intoxications to 24-48 hours and can be either gastrointestinal or neurological. Gastrointestinal symptoms include acute gastroenteritis (vomiting, diarrhoea, nausea and abdominal pain) only for a few days, while some neurological effects can take several days to develop. Ciguatera can last for several weeks to several months, in particular for peripheral neurologic symptoms, with a small percentage of cases (<5%) with symptoms persisting for years. Neurological symptoms occur within first days of illness, often becoming prominent after GI symptoms, particularly for C-CTXs. They include paresthesias (numbness, tingling), in extremities (lips, hands, feet) and oral region, generalized pruritus (itching), myalgia (muscle pain), arthralgia (joint pain), and severe feeling of fatigue. A distinctive symptom, as in NSP, is an alteration or reversal of hot/cold temperature perception, in which cold surfaces are perceived as hot to the patient, or dysesthesia (unpleasant abnormal sensation). Most severe intoxications develop cardiac symptoms with hypotension, bradycardia, respiratory difficulties and paralysis. Deaths are rare, probably because rarely do fish accumulate lethal CTXs levels at a single meal. Some patients develop allergy-like reactions to the consumption of certain proteinaceus food (fish, peanuts, chicken, pork) and alcohol, associated with re-occurring ciguatera neurological symptoms (Lombet *et al*., 1987; Mattei *et al*., 1999; Lewis, 2006; Friedman *et al*., 2008).

Ciguatera intoxication differs in symptomatology depending on the geographical area of toxin production. Ciguatoxins from the Pacific Ocean cause more severe intoxication with predominantal neurological symptoms, including rare cases of coma and death (Hamilton *et al*., 2009). Ciguatera in the Caribbean Sea is characterized by gastrointestinal symptoms in the acute phase (i.e. 12 hours) with subsequent prominence of, mainly peripheral, neurologic symptoms. Ciguatoxins from Indian Ocean cause intoxication with neurological and mental

status alterations, with hallucinations, incoordination, loss of equilibrium, mental depression, nightmares. Ciguateric fish in Indian Oceans are also more frequently contaminated by lethal levels of CTXs (Lewis, 2006; Friedman, 2008).

For both NSP and CFP there is no official treatment available, except for symptomatic therapies.

**Brevetoxins and ciguatoxins molecular target**

So far, *in vitro* studies have been performed and the interaction of both brevetoxins and ciguatoxins with voltage-gated sodium channel alpha subunit ($Na_V$) has been well demonstrated. Neurotoxin site-5 on $Na_V$ was identified as the brevetoxin and ciguatoxin binding site, with toxins acting as competitive inhibitors. Structurally, site-5 is formed by transmembrane segments S6 and S5 of homology domains I (IS6) and IV (IVS5) of α-subunit, respectively (Lombet *et al*., 1987; Trainer *et al*., 1991; Trainer *et al*. 1994; Hogg *et al*., 1998; Dechraoui *et al*., 1999; Strachan and Nicholson, 1999). Toxin interaction with this receptor has been demonstrated to occur for brevetoxin molecule with a 1:1 stoichiometry PbTx-3:$Na_V$ (Trainer *et al*., 1991).

Toxin binding to site-5 results in the prolonged depolarization of excitable membranes (cardiac cells, brain synaptosomes, nodose ganglia) and excitotoxicity by a) a shift in $Na^+$ channel activation potential in the hyperpolarizing direction leading to channel opening at membrane potential where they are normally closed; b) the prolongation of channel mean open times by a destabilization of inactivated conformation of the protein; c) the inhibition of fast channel inactivation process, by destabilization of inactivated conformation; and d) the occurrence of subconductance states in addition to the normal conducting state, with slowed kinetics of ion transport (Schreibmayer and Jeglitsch, 1992; Gawley *et al*., 1995; Jeglitsch *et al*., 1998). By increasing the sodium ion permeability of excitable cell membranes, toxins affect various sodium-dependent signalling processes such as neurotransmitter release (Bidard *et al*., 1984; Molgó *et al*., 1992). Binding of brevetoxins has been shown to be independent of membrane potential, binding equally well to both active and inactive channels (Poli *et al*., 1986; Baden, 1989). In mammals, CTXs are the most potent $Na_V$ specific neurotoxin known, being similarly potent in mice by oral or i.p. administration (Lewis, 2006). Ciguatoxins affinity for sodium channels is at least 20-50 times higher than that of brevetoxins, and their effects are probably due to other cellular mechanisms than sodium channel modulation (Lombet *et al*., 1987; Gawley *et al*., 1992; Dechraoui *et al*., 1999). As such recent studies

demonstrated an inhibition of potassium channels at low nanomolar concentrations for ciguatoxins and related compounds (Hidalgo *et al*., 2002; Ghiaroni *et al*., 2005; Birinyi-Strachan *et al*., 2005; Cuypers *et al*., 2008; Mattei *et al*., 2009; Schlumberger *et al*., 2009; Kopljar *et al*., 2009).

On $Na_V$ both brevetoxins and ciguatoxins act as allosteric modulators. Toxins bind with high affinity to sites distinct from the pore or the voltage sensor and activate channels by shifting conformational equilibrium toward the activated state. Active brevetoxins share common structural requisites: a relatively rigid H-K ring thought to be involved in site binding; an electrophilic A ring, in most cases a 5- or 6-membered lactone (so called 'head region'); several ring 'spacer regions' between these two sites; and a side chain called the 'tail' located at the K-ring of the molecule (Rein *et al*., 1994; Baden *et al*., 2005).

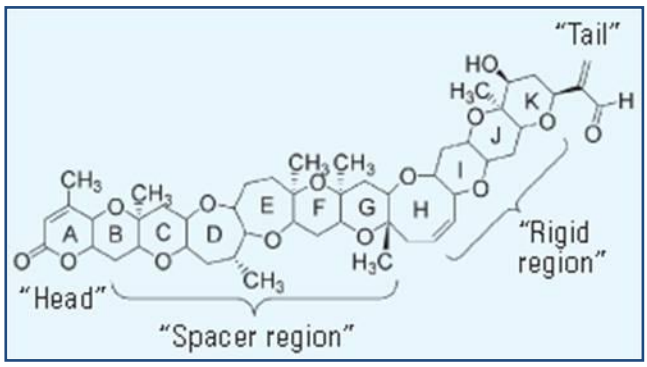


**Figure 20: active brevetoxins structure features**
(Baden *et al*., 2005).

Gawley *et al*. (1995) proposed the model of interaction between toxins and the open (conducting) conformation of the channel protein, with toxin head physically obstructing the normal motion of inactivation gate (IIIS6-IVS1 intracellular loop) that blocks ion conduction. Photoaffinity experiments showed the 'tail' of brevetoxin B backbone lay next to S5-S6 extracellular loop of domain IV.

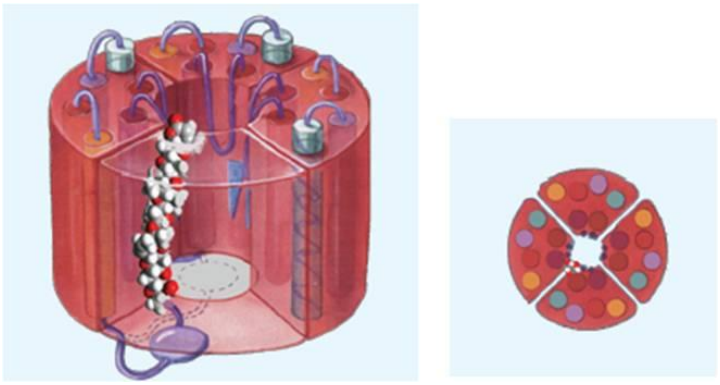

**Figure 21: 'head-down' brevetoxin binding to VGSC site 5 model proposed by Gawley *et al*. (1995)**
(Baden *et al*., 2005).

Possible altered interactions of transmembrane segments within and between adjacent homologous domains, result in the alteration of voltage-gated activation and coupling to inactivation (Cestèle and Catterall, 2000).

Brevenal, a derivative of brevetoxin, is characterized as an antagonist able to counteract the effect of brevetoxins (Purkerson-Parker *et al*., 2000; Bourdelais *et al*., 2004) and P-CTX-1B-induced catecholamine release from chromaffin cells (Mattei *et al*., 2008; Nguyen-Huu *et al*., 2009), opening the possibility to develop therapeutics to prevent or reverse brevetoxins intoxication.

**Brevetoxins and ciguatoxins *in vitro* effects**

The *in vitro* effects of brevetoxin and ciguatoxins have been well studied using on different tissue preparation and using a variety of methods.

Brevetoxins induced *in vitro* effects include swelling of myelinated axons (Mattei *et al*., 1999), depolarization of nerves and muscle (Sasner, 1965; Shinnick-Gallagher, 1980; Huang *et al*., 1984; Richards and Bourgeois, 2010), repetitive firing in nerve cells (Westerfield *et al*., 1977; Parmentier *et al*., 1978; Shoukimas *et al*., 1979; Huang *et al*., 1984; Wu *et al*., 1985), increased release of catecholamine and acetylcholine transmitters (Ellis *et al*., 1979; Gallagher and Shinnick-Gallagher, 1980; Vogel *et al*., 1982; Risk *et al*., 1982; Atchinson *et al.*, 1986), neuromuscular block (Baden *et al*., 1984), muscles fasciculation (Baden and Mende, 1982; Johnson *et al*., 1985), and ventricular fibrillation (Music *et al*., 1973; Johnson *et al*., 1985).

Ciguatoxins induced *in vitro* effects included swelling of myelinated axons (Mattei *et al*., 1999), the depolarization of muscle and neuroblastoma cells membrane (Rayner and Kosaki, 1970; Rayner, 1972; Bidard *et al*., 1984; Brock *et al*., 1995), of cardiac muscle (Lewis and Endean, 1986), the stimulated release of neurotransmitters such as GABA, dopamine and acetylcholine (Ohizumi *et al*., 1982; Molgó *et al*., 1992; Molgó *et al*., 1993; Bidard *et al*., 1984; Brock *et al*., 1995; Marquais and Sauviat, 1999; Sauviat *et al*., 2002; Mattei *et al*., 2009), contraction of the guinea pig vas deferens (Ohizumi *et al*., 1981) and ileum (Lewis and Endean, 1984; Lewis and Hoy, 1993), and positive chronotropy-inotropy in isolated atria (Ohshika, 1971; Miyahara *et al*., 1979; Lewis *et al*., 1992; Lewis and Hoy, 1993). Inotropic effect on isolated guinea pig atria consists of two components, one indirect neurogenic action, at low concentration, through induction of noradrenaline release from

adrenergic nerve endings, and one direct myogenic action, at higher concentration, through direct interaction with sodium channels (Lewis and Endean, 1986; Seino *et al*., 1988).

## VOLTAGE GATED SODIUM CHANNELS

Voltage gated sodium channels ($Na_V$) form a family of membrane proteins expressed at low level in non-excitable cells such as glia, lymphocytes, osteoblasts, fibroblasts, endothelial cells, metastatic cancer cells of epithelial origin (Diss *et al*., 2004), and at higher level in excitable cells such as muscles (skeletal and cardiac), neurons (central nervous system, peripheral nervous system and sensory neurons), and neuroendocrine cells. $Na_V$ respond to depolarization of the membrane by opening a sodium ion-selective pore that permits ions flow down their electrochemical gradient into the cell, thereby contributing to the generation and conduction of action potentials (Shah *et al*., 2004, Chancey *et al*., 2007). For these reasons, $Na_V$ play an indispensable role in many higher processes such as cognition, cardiac conduction and locomotion and sensitive perception. Their physiological role in nonexcitable cells remains unclear (Catterall *et al*., 2005).

### Structure

Voltage-gated $Na^+$ channels are formed by one large α-subunit (220-260 kDa) and one or more smaller β-subunits (33-36 kDa). Pore-forming α-subunit is sufficient for channel functional expression, but kinetics, voltage dependence of channel gating and channel cellular localization are modified by auxiliary β-subunits (Catterall *et al*., 2002).

The structure of α-subunit is organized in four homologous domains (I-IV), each containing six transmembrane α helices (S1-S6) and an additional membrane re-entrant pore loop (P-loop) located between S5 and S6 segments, with internal and external connecting polypeptide loops.

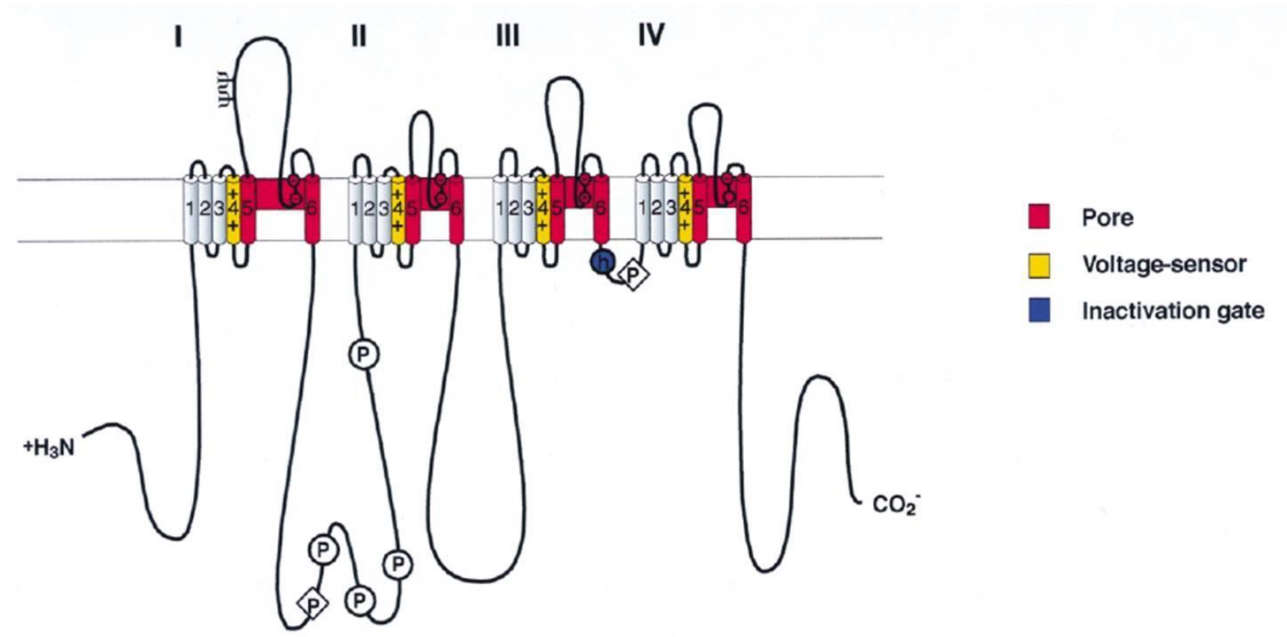


**Figure 22: $Na_V$ α-subunit structure**
(Cestèle and Catterall, 2000).

Membrane re-entrant pore loops between S5 and S6 line the outer, narrow extracellular end of the pore, and each P-loop repeats and shares one critical residue forming a ring of four amino acid residues responsible for ion selectivity and permeation across the pore (Cestèle and Catterall, 2000; Sun *et al*., 2008). The inner wider intracellular end of the pore is formed by S6 segments.

In each of the four domains, there is a S4 segment containing positively charged amino acid residues at every third position. These residues serve as gating charges and move outward under the influence of the membrane electric field when the membrane is depolarized, to initiate a conformational change that opens the pore (Catterall *et al*., 2007) through an activation gate hypothesized to be located at the cytoplasmic end of the S6 segments (Wang and Wang, 2003). A short intracellular loop connecting homologous domains III and IV serves as the inactivation gate, folding into the channel structure and blocking the pore from the inside during sustained depolarization of the membrane (Catterall *et al*., 2002). Both

voltage sensors and inactivation gate are considered to be inaccessible to binding of hydrophilic polypeptide toxins (Catterall *et al*., 2007).

Four auxiliary subunits of sodium channels have been defined thus far: $Na_V\beta1$, $Na_V\beta2$, $Na_V\beta3$, and $Na_V\beta4$, encoded by gene SCN1B, SCN2B, SCN3B and SCN4B, respectively. β subunits proteins contain a large N-terminal extracellular domain, a single transmembrane segment and a short C-terminal intracellular segment. β subunits proteins are fundamental for VGSC protein interaction with cell adhesion molecules, extracellular matrix proteins, and cytoskeletal linker proteins. They also enhance channel pore expression levels at plasma membrane and modulate its physiological properties (McCormick *et al*., 1999; Meadows and Isom, 2005). The molecular basis for sodium current diversity among the isoforms depends partly on subunit composition (Aman *et al*., 2009).

**Distribution and classification**

In mammals, at least nine isoforms ($Na_V$-1.1 to $Na_V$-1.9) of α-subunit have been characterized by cDNA cloning, sequencing and electrophysiological recording and functionally expressed. The majority of these subtypes are expressed in neurons, except for $Na_V$-1.4 and $Na_V$-1.5 isoforms, typically expressed in skeletal and cardiac muscle, respectively. Proteins differences in amino acid sequences result in specialized electrophysiological function (e.g. single channel conductance) and pharmacological properties (e.g. sensitivity to pharmacological agents) (Catterall *et al*., 2002, 2007; Baden, 2005).

All isoforms show greater than 50% identical amino acid sequence in extracellular domains, and greater than 70% amino acid sequence identity in their transmembrane segments (Goldin *et al*., 2000; Catterall *et al*., 2002; Catterall *et al*., 2007). $Na_V1.1$, $Na_V1.2$, $Na_V1.3$, and $Na_V1.7$ are broadly expressed in neurones. $Na_V1.5$, $Na_V1.8$, and $Na_V1.9$ are tetrodotoxin-resistant to varying degrees due to changes in amino acid sequence at a single position in domain I, and they are highly expressed in heart ($Na_V1.5$) and dorsal root ganglion neurons ($Na_V1.8$ and $Na_V1.9$). Isoforms $Na_V1.4$ is expressed primarily in skeletal muscle, and $Na_V1.6$ is expressed primarily in the central nervous system.

**Table 4:**
**Classification of voltage-gated sodium channel, names encoding the channels, auxiliary β subunits and primary tissue in which they are located**
*(nd not determined)*

| $Na_V$ α subunit (gene) | Auxiliary subunits | TTX Sensitivity | tissue localization |
|---|---|---|---|
| $Na_V1.1$ (SCN1A) | β1-β2-β3 | + ($EC_{50}$ nM) | CNS, cardiac myocytes, SA node |
| $Na_V1.2$ (SCN2A) | β1-β2-β3 | + ($EC_{50}$ nM) | CNS, primarily un-, pre-myelinated axons |
| $Na_V1.3$ (SCN3A) | nd | + ($EC_{50}$ nM) | CNS, cardiac myocytes |
| $Na_V1.4$ (SCN4A) | β1 | + ($EC_{50}$ nM) | skeletal muscle |
| $Na_V1.5$ (SCN5A) | β1-β2-β3 | - | cardiac myocytes |
| $Na_V1.6$ (SCN8A) | β1-β2 | + ($EC_{50}$ nM) | cerebellum, hippocampus, Purkinje cells, astrocytes, Schwann cells, DRG, CNS nodes of Ranvier |
| $Na_V1.7$ (SCN9A) | β1-β2 | + ($EC_{50}$ nM) | all types DRG neurons, sympathetic neurones, Schwann cells, neuroendocrine cells |
| $Na_V1.8$ (SCN10A) | nd | - | small & medium-sized DRG neurons and their axons |
| $Na_V1.9$ (SCN11A) | nd | - | c-type DRG neurones, trigeminal neurones and their axons |

**Voltage-gated sodium channel and pain**

In sensory nerves, $Na_V$ mediates perception of touch, temperature and pain. Neuropathic pain results from damage to components of the nervous system such as primary afferent nerves, spinal cord, and central nervous system regions with altered electrical excitability of neurons (Ueda, 2006; Cummins *et al.*, 2007). Its onset may be delayed after nerve injury, then pain sensation may persist after complete healing. Neuropathic pain is often characterized by stimulus-independent persistent pain, abnormal pain sensory perception as allodynia (pain sensation in response to innocuous tactile stimuli) and hyperalgesia (exaggerated pain sensation in response to mildly noxious stimuli) (Ueda, 2006). Nociceptors are located at

terminal of thinly myelinated Aδ-fiber and unmyelinated C-fiber of primary afferent neurons and transduce noxious chemical, mechanical or thermal stimuli into depolarizing currents that ultimately induce action potentials conducted to CNS (Ueda, 2006). $Na_V1.7$ (tetrodotoxin TTX-sensitive), 1.8 and 1.9 (TTX-resistant) are the isoforms primarily expressed in nociceptive neurons (Liu *et al*., 2006). $Na_V1.7$ play a crucial role in perceiving pain sensations, but seems to be not involved in proprioception, touch, warmth and cold (Cummins *et al*., 2007), whilst TTX-resistant $Na_V1.8$-1.9 are both primarily expressed in the subpopulation of small-diameter unmyelinated nociceptive C-fibers of sensory neurons thought to be important in nociception (Ueda, 2006; Cummins *et al*., 2007). Unlike most neurones, small-diameter sensory neurons generate tetrodotoxin (TTX)-resistant action potentials and it has been shown DRG neurons from patients with neuropatic pain to be characterized by spontaneous action potentials insensitive to 300 nM TTX (Liu *et al*., 2006). Regarding $Na_V1.9$ isoform, an up-regulation has been demonstrated during inflammation process and seems to be the isoform related to sensory neuronal hyperexcitability associated with inflammatory pain but doesn't play a major role in nerve injury-induced hyperalgesia (Liu *et al*., 2006). Studies on this isoform are difficult to perform because of its extremely difficult functional expression in heterologous expression systems (Cummins *et al*., 2007).

$Na_V1.8$ contribute substantially to the inward current underlying action potential of small-sized DRG neurons, and it is likely TTX-R currents described in the majority of *in vitro* studies are conducted by $Na_V1.8$ channels (Catterall *et al*., 2005; Liu *et al*., 2006; Cummins *et al*., 2007). $Na_V1.8$ has a specialized role in nociceptors for perception of cold pain and pain in the cold, since at low temperatures $Na_V1.8$ remains the only isoform producing action potential in nociceptors and $Na_V1.8$-null mice show negligible responses to noxious cold and mechanical stimulation at low temperatures (Zimmermann *et al*., 2007). Moreover, $Na_V1.8$ isoform has a well demonstrated role in pain sensation. $Na_V1.8$ is up-regulated in some models of inflammatory pain and $Na_V1.8$-null mice exhibit delayed development of inflammatory hyperalgesia, reduced pain responses to noxious mechanical stimuli, and lower sensitivity in several models of visceral pain (Catterall *et al*., 2005; Liu *et al*., 2006) and in nerve-growth factor-induced thermal hyperalgesia (Liu *et al*., 2006). Antisense oligonucleotides $Na_V1.8$ knockdown prevented hyperalgesia, reversed tactile and thermal allodynia induced by spinal nerve injury (Liu *et al*., 2006; Cummins *et al*., 2007) and decreased hyperalgesia induced by inflammatory agent prostaglandine E2 (PGE2) (Liu *et al*.,

2006). This in agreement with Liu *et al*. recent findings (2010) of PGE2 increased trafficking and protein level on cell surface of $Na_V1.8$.

**Voltage-gated sodium channel neurotoxins**

The receptor sites on the α subunits of pharmacological agents and natural toxins acting on sodium channels have been identified (Catterall *et al*., 2005). Thus far, at least eight distinct receptor sites for neurotoxins and one receptor site for local anaesthetics and related drugs have been identified (Cestèle and Catterall, 2000; Wang and Wang, 2003) and their corresponding affect on the channel described (summarized in the the following table and figure).

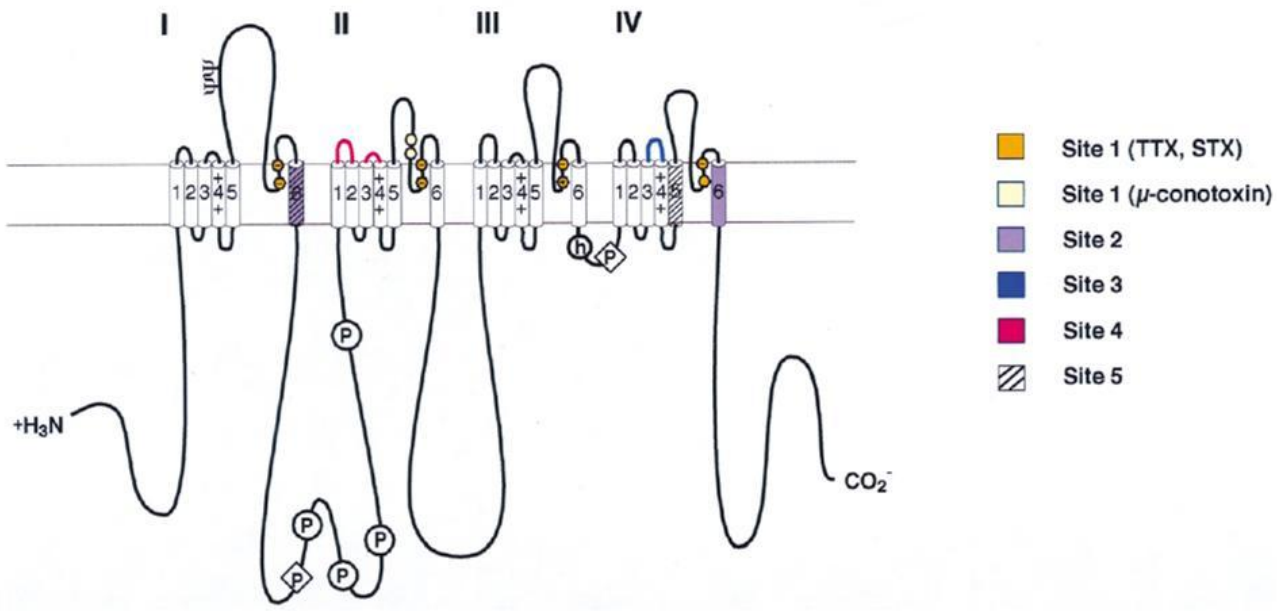


**Figure 23:**
**neurotoxins binding sites on $Na^+_V$ α-subunit**
(Cestèle and Catterall, 2000).

**Table 5:**

**receptor sites on voltage gated sodium channels α-subunit**

| Receptor site | Toxin or drug | Domains | Physiological effects |
|---|---|---|---|
| **Neurotoxin site 1** | tetrodotoxin and saxitoxin; μ-conotoxin | IS2-S6, IIS2-S6, IIIS2-S6, IVS2-S6 | inhibition/block conductance |
| **Neurotoxin site 2** | veratridine; batrachotoxin; grayanotoxin; aconitine | I-IVS6 | persistent activation, repetitive firing |
| **Neurotoxin site 3** | α-scorpion toxins; sea anemone toxins; spider toxins | IS5-IS6, IVS3-S4, IVS5-S6 loops | inhibition inactivation, enhanced persistent activation |
| **Neurotoxin site 4** | β-scorpion toxins | IIS1-S2, IIS3-S4 loop | shifted activation, repetitive firing |
| **Neurotoxin site 5** | brevetoxins; ciguatoxins | IS6, IVS5 | enhanced persistent activation, inhibited inactivation, repetitive firing |
| **Neurotoxin site 6** | δ-conotoxins; | nd | enhanced persistent activation, repetitive firing |
| **Neurotoxin site 7** | pyrethroids; DDT | I, II and IIIS6 | persistent activation, depolarization of resting potential |
| **Neurotoxin site 8** | Conus stratius toxin | nd | prolonged channel opening |
| **Site 9** | local anaesthetic, antiarrythmic, antidepressants and antiepileptic drugs | IS6-IIIS6, IVS6 | inhibition of $Na^+$ permeability |

*In vivo*, ion channels do not exist in isolation but instead associate in complex with other plasma membrane, extracellular matrix and intracellular proteins that participates in cell adhesion, cytoskeletal anchoring and signal transduction. Molecular composition of a particular complex can have significant influence on channel function, localization and

cellular excitability. A given channel pore-forming subunit may behave very differently depending on its associated proteins (Meadows and Isom, 2005). However, when expressed in mammalian cells as heterologous expression systems, α-subunit alone can form functional voltage-gated $Na^+$ channels with current kinetics and activation, ion selectivity, ion flow and inactivation processes comparable to their native counterparts (Wang and Wang, 2003; Chancey *et al*., 2007).

The critical difference between *in vitro* and *in vivo* studies is channel expression in native cells: in their native environment voltage-gated sodium channel are targeted to specialized subcellular domains where they associate with specific signalling and structural proteins, and where they are exposed to second messengers. Co-expression of α- with β-subunits results in cell type-specific shifts in the voltage-dependence of activation and inactivation and in changes in channel modal gating behaviour with altered rates of activation, inactivation and recovery from inactivation. Channel expression at plasma membrane is increased (Meadows and Isom, 2005).

# AIM OF THE STUDY

Brevetoxins' and ciguatoxins' parent molecules and their metabolites are a suite of voltage-gated sodium channel specific neurotoxins sharing a similar polyether chemical structure and mode of action. They are respectively responsible for two different human food-borne illnesses, Neurotoxic shellfish poisoning (NSP) and Ciguatera fish poisoning (CFP), characterized by particular peripheral neurological symptoms of distortion of oral and peripheral temperature sensation, with reversal of hot/cold temperature perception (paradoxical dysaesthesia) and diffuse pain syndrome.

The voltage-gated sodium channels $Na_V1.8$ in sensory neurons has a specialized role in nociceptors for perception of cold pain and a well demonstrated role in pain sensation (Zimmermann *et al*., 2007, Catterall *et al*., 2005; Liu *et al*., 2006; Cummins *et al*., 2007) and the P-CTX-3C was recently found to preferentially affect $Na_V1.8$ than $Na_V1.2$.

This study proposed to further investigate those findings by comparing various polyether site-5 neurotoxin potencies on the peripheral sensory neuron $Na_V1.8$ isoform and the central neuron $Na_V1.2$ isoform using a cytotoxicity assay. Toxins of choice were type A and type B brevetoxins, a Caribbean and two Pacific ciguatoxins.

**Plan of action:**

a) Create stable clones of human embryonic kidney cell line (HEK293) expressing $Na_V$ channels;

b) Assess the relative potency of brevetoxins and ciguatoxins on $Na_V1.8$ channel isoform and compare it to that on 1.2.

# MATERIALS & METHODS

**HEK-293 cell line culture**

Human embryonic kidney cell line (HEK-293) was purchased from American Type Culture Collection (ATCC). Cultures were grown in a humidified atmosphere of 5% $CO_2$, 95% air, at 37 °C in Dulbecco's Modified Eagle Medium (DMEM) high glucose+GlutaMAX™-1 supplemented with 10% fetal bovine serum (FBS). Geneticin G418 antibiotic solution was also added to a final concentration of 500 µg/mL in the selective medium or to a final concentration of 250 µg/mL in the maintenance medium. At confluence, cultures were passaged by a rinse with PBS, detached with an incubation in a trypsin enzyme solution (TrypLE™ Express) for 10 minutes at 37 °C and subcultured in the same medium. For cytotoxicity assays, cells were harvested at 70-80% confluence.

Clones were stored under liquid nitrogen in growth medium with 10% dimethyl sulfoxide (DMSO) and 20% FBS until use. Only cultures with passage number (<50) were used.

**Stable cell transfection**

To induce stable expression of either human $Na_V1.2$ or $Na_V1.8$, HEK cells were transfected with channel alpha subunits gene inserted in a TrueClone pCMV6-Neo plasmid. This expression vector has a Cytomegalovirus (CMV) promoter capable of driving heterologous gene expression in a variety of mammalian cell lines in culture and codes for the neomycin resistance gene allowing the growth in a selective medium to clones with a cDNA stably integrated in their genome. Plasmid DNA was dissolved in 100 µL of sterile deionized water to a final concentration of 100 ng/µL. The tube was let sit at 4 °C overnight, vortex mixed and used for the transfection the day after. Remaining solution was stored at -20 °C.

The method of choice was a chemical transfection technique with artificial cationic liposomes which electrostatically associate to and cover nucleic acid negative charges. This complex results in a closer association of the DNA with the negatively charged cell membrane, followed by its endocytosis or fusion with the plasma membrane and its trapping in endosomes and lysosomes. How the DNA or the DNA/liposome complex enters into the nucleus is not yet known.

Cells were seeded into 24-well plates to achieve 50% confluence 24 h (90.000 cells/$cm^2$) or 48 h (50.000 cells/$cm^2$) before the transfection day. Transfection mixture was prepared with serum-free medium without antibiotics and pre-warmed at 37 °C by adding different amounts of DNA

(0.25, 0.5 and 0.75 µg/well) and the TransFast™ Transfection reagent (3.0 µL/µg DNA). The mixture was incubated for 15 minutes at room temperature (RT), briefly and gently vortex mixed and then used to replace the growth medium on the cells (200 µL/well). Cells were incubated for 1 h at 37 °C in a 5% $CO_2$ incubator, then overlaid with warm complete medium (1 mL/well) and let rest for 48 hours. Cells were then trypsinized and plated at increasing dilution factors (1:20 up to 1:500) into 60 mm Petri dishes with selective medium containing a concentration of geneticin (G418) founded to kill the 90% of the non transfected cells in 7 days (500 µg/mL). Medium was then changed every 3-4 days to remove cell debris and dead cells for about 14 days, until small clusters of 20-30 cells of each surviving clone were obtained.

Each isolated growing clone was then subcultured into a 24-well plate in complete growth medium with a maintenance dose of G418 (250 µg/mL). From each transfection an average of 30 geneticin-resistant clones were obtained and subcloned to finally select by N2a cytotoxicity assay the most sensitive one to 1 µM PbTx-3 for both $Na_V$ isoforms.

**RNA extraction and clean-up**

The integration of the plasmid was verified by the isolation of total RNA from the cells and the amplification of its complementary DNA (cDNA) by two step Real-Time Polymerase Chain Reaction (RT-PCR).

Total RNA was isolated from confluent 75 $cm^2$ flasks of both transfected and non transfected cell lines using TRI Reagent® isolation reagent. Flasks were rinsed with PBS and trypsinized as routine culture protocol, and trypsin enzyme was stopped by the addition of warm complete medium. Cell suspension was centrifuged (Thermo IEC Centra CL2, Thermo Fisher Scientific Inc.) at 170*g* for 1 minute at RT and supernatant was discarded. Cells pellet was then re-suspended in a 15 mL tube with TRI Reagent (2 mL/confluent 75 $cm^2$ flask), mixed and incubated at RT for 5 minutes. Chloroform was added (0.4 mL/tube), shaked for 15 times and let sat at RT for 2 minutes. Tubes were then centrifuged (Thermo Electron Corporation, IEC MultiRF centrifuge) at 12,000*g* for 15 minutes at 4 °C and supernatant was then transferred into a pre-chilled RNase/DNase free microcentrifuge tube to add isopropanol (0.5 mL/tube) to precipitate RNA, vortex mixing briefly. Then, either RNA extraction was stopped and samples were stored at -80 °C, or continued after sat samples for 5 minutes at RT. Supernatant obtained

by centrifugation at 12,000*g* for 8 minutes at 4 °C (Eppendorf centrifuge 5417R) was discarded by vacuum aspiration and the RNA pellet was washed by vortex mixing with 1 mL of cold 75% ethanol and centrifuged again at 7,500*g* for 5 minutes at 4 °C. Ethanol wash was removed and the pellet was air-dried for 10 to 15 minutes. RNase-free water (100 µL) supplemented by Rnasein inhibitor (0.8 µL) was then added to each tube to dissolve the pellet.

RNA clean-up was performed with Qiagen's RNeasy Mini Kit. According to manufacturer protocol, buffer RLT was added to each tube (350 µL), mixing and adding 100% ethanol (250 µL/tube), and mixed by pipetting. Samples were collected into columns and spin at 8,000*g* for 15 seconds, flow-through was discarded and buffer RW1 was then added (350 µL), to spin as above. Flow-through was discarded and DNase I incubation mix (10 µL DNase I stock solution into 70 µL buffer RDD) was added directly to the columns and left at RT for 15 minutes to remove genomic DNA. Buffer RW1 (350 µL/column) was then added and centrifuged at 8,000*g* for 15 seconds, flow-through was discarded, buffer RPE was added (500 µL/column) and spun as previously described, flow through was damped and buffer RPE was added to spin at 8,000*g* for 2 minutes. Flow-through was discarded and samples were centrifuged at 8,000*g* for 1 minute. Columns were placed in new collection tubes, nuclease free water (30 µL/column) was added and let stand 1 minute. Samples were spun at 8,000*g* for 1 minute, water was then added again to repeat the spin. Clean RNA extracted was quantified with 2 µL samples by a NanoDrop ND-1000 spectrophotometer (3.3 software version). Samples were stored at -80 °C until reverse transcription.

**Reverse transcription**

Total RNA samples were diluted in nuclease-free water to a final RNA concentration of 500 ng/µL. Complementary DNA template for PCR amplification was synthesized with RETROScript® kit as follows: for each sample, 500 ng of RNA extracted were placed in a tube, adding oligo(dT) primers (50 µM, 2 µL/tube) and bringing to a final volume of 12 µL with nuclease-free water. Tubes were heated at 70-85 °C for 3 minutes to heat denature the RNA to remove secondary structure, and then placed on ice. 10X RT buffer (500 mM Tris-HCl, pH 8.3, 750 mM KCl, 30 mM $MgCl_2$, 50 mM DTT) (2 µL/tube), 4 deoxynucleotide triphosphates mixed (2.5 mM each, 4 µL/tube), RNase inhibitor (10 units/µL, 1 µL/tube) and Moloney murine

leukemia virus (MMLV) reverse transcriptase (100 units/µL, 1 µL/tube) were added to the tubes and mixture was incubated at 42-44 °C for 1 hour. Tubes were then incubated at 92 °C for 10 minutes to inactivate the reverse transcriptase and stored at 4 °C until use.

**Real Time PCR**

Primers sequences for RT-PCR were the same as reported by Yarowsky *et al*. (1991) for HEK-$Na_V1.2$ clone (named as primer pair B) and by Jo *et al*. (2004) for HEK-$Na_V1.8$ clone and are summarized in table 6. Sequences were synthesized by IDT, Integrated DNA Technologies. Oligonucleotides were dissolved in nuclease-free water up to a 100 µM final concentration and used without further purification.

Experiments were conducted in triplicate for each clone, HEK control cell line and a no template control to exclude a DNA contamination in the PCR reagents. Power SYBR Green PCR Master Mix (25 µL), nuclease-free water (21 µL), primer pair (2 µL, prepared by mixing 80 µL of nuclease-free water and 10 µL of each primer solution) and either the cDNA template or nuclease-free water for the no-template control (2 µL) were added to each tube in this order.

As shown in figure 24, PCR was run with an initial heat denaturation at 95 °C for 10 minutes (stage 1), followed by cooling to 94 °C for 15 seconds and to 60 °C for 40 seconds to anneal template and primers, finally heating to 72 °C for 1 minute for optimal amplification, repeated 40 times (stage 2). Final dissociation was then performed by heating to 95 °C for 15 seconds, cooling to 60 °C for 1 minute and re-heating to 95 °C for 15 seconds (stage 3). RT-PCR was performed with an Applied Biosystems 7500 Real-Time PCR System.

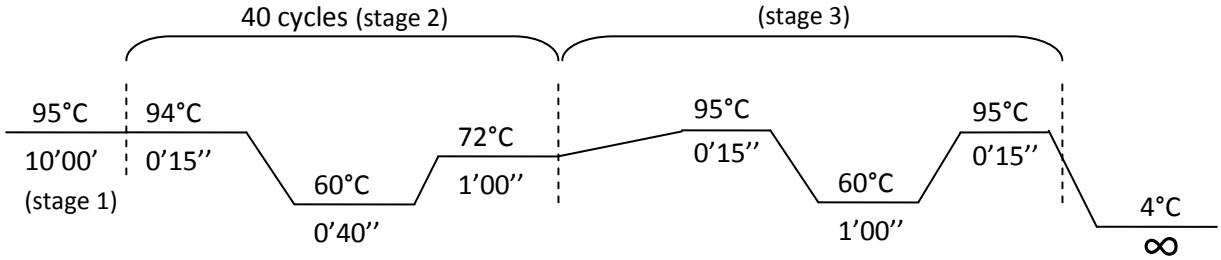


**Figure 24: Real Time PCR settings for HEK-$Na_V1.2$ and HEK-$Na_V1.8$ clones**

| CHANNEL | SIZE (bp) | SEQUENCE (5'-3') |
|---|---|---|
| **$Na_v1.2$** | 626 | **Forward: CATTCCTCCAGAGATGGTGTC**<br>**Reverse: TTCATGGGCAACCTGAGGAATA** |
| **$Na_v1.8$** | 453 | **Forward: CTTGGGCTTTCCTCTCACTG**<br>**Reverse: AGGCGAGGCCIAGAAAAGAC** |

**Table 6: primers used for Real Time PCR amplification of $Na_V1.2$ and $Na_V1.8$ genes**

**Real Time PCR products bio sizing and quantification**

RT-PCR products were size-fractionated and quantified by an Agilent 2100 Bioanalyzer (Agilent Technologies, Waldbronn, Germany) with Agilent DNA 1000 reagents. DNA dye concentrate and DNA gel matrix mixture were prepared according to manufacturer's protocol and stored at 4 °C in the dark up to 4 weeks. The DNA chip was loaded with gel-dye mix (9 µL) at the bottom of the first well marked 'G' and pressurized with the appropriate syringe for 60 seconds. After 5 seconds gel-dye mix was pipetted in each of the wells marked. DNA marker (5 µL) was pipette into both ladder and samples wells, adding then 1 µL of either DNA ladder or sample. Chip was then vortex mixed at 2400 rpm for 1 minute and the run started within 5 minutes into the Agilent 2100 Bioanalyzer (Version A.02.12 SI292).

**Real Time PCR products clean up**

PCR products were cleaned for sequencing with the QIAquick® PCR Purification kit. For each sample, 60 µL of PCR product were mixed with 5 volumes of Buffer PB (300 µL) into a spin column in a collection tube to spin at 17,800*g*, for 45 seconds at RT (Eppendorf centrifuge 5417R). Flow-through was discarded and tubes were spun as above again after the addition of Buffer PE (750 µL) to wash. Flow-through was discarded and tubes were spun again as before for 1 minute. Columns were then placed in new 1.5 mL microcentrifuge tubes and nuclease-free water (50 µL/tube) was added directly to each membrane and samples were spun as above to elute DNA.

**Real Time PCR products sequencing**

HEK-$Na_V1.2$ clone cDNA product and relative primers were shipped to SeqWright DNA Technology Services (SeqWright Inc., Houston, TX, USA, www.seqwright.com) for sequencing.

**Cytotoxicity assay**

The cytotoxicity assay consists of exposing cells to $Na_V$ modulator toxins in presence of both veratridine and ouabain. Veratridine was prepared as 1 mM stock solution in pH 2 water and ouabain was prepared as 10 mM stock solution in water and kept protected from light. Both solutions were sterilized by filtration and stored at 4 °C for no longer than 10 weeks. Toxins were serially diluted in 100% methanol to concentrations ranging from 100 µg/mL to 0.001 µg/mL for brevetoxins (PbTx-1, PbTx-3 and PbTx-7) and from 1 ng/mL to 0.000001 ng/mL for ciguatoxins (P-CTX-1, C-CTX-1 and C-CTX-3C) and stored at -20 °C.

Cells were seeded in 96-well plates (40.000 cells/well) in DMEM+GlutaMAX™-1 supplemented with 10% FBS (100 µL/well) 24 hours before starting the exposure to the toxins to reach 50-70% confluence. Incubation started adding to each well both veratridine (50 µM for HEK-$Na_V1.2$ clones and non transfected cells, 100 µM for HEK-$Na_V1.8$ clones) and ouabain (0.05 µM), followed by the addition of serially diluted toxins stock solutions (1 µL/well) or of 100% methanol (1 µL/well) to vehicle control wells. After 24 hours of exposure cell viability was estimated with the CellTiter 96® $AQ_{ueous}$ One Solution Cell Proliferation Assay added directly to each well (20 µL/well) and incubated for 3 hours at 37 °C. Absorbance of produced formazan crystals was measured at 544 nm wavelength by an automated microplate-based plate reader FLUOstar spectrophotometer (BMG Labtechnology).

Each experimental point was run in duplicate and repeated two-six times.

**Amino acid sequences comparison**

Clones $Na_V$ alpha subunit amino acid sequences were compared to each other as well as to the putative brevetoxin receptor site 5 sequences identified by Trainer *et al*. (1994).

Amino acid sequences for both clone alpha subunit isoforms were obtained from mRNA accession number by a nucleotide Megablast (blastn) and sequences were compared by a protein-protein BLAST (blastp) with NCBI Blast (www. http://blast.ncbi.nlm.nih.gov/Blast.cgi).

## Data analysis

Results were graphed with GraphPad Prism version 4.0 (GraphPad Software Inc., San Diego, CA, USA). RT-PCR products were automatically size-fractionated and quantified by an Agilent 2100 Bioanalyzer (Version A.02.12 SI292).

Data from cytotoxicity experiments were analyzed as absorbance raw values by sigmoidal concentration-response curve regression with GraphPad Prism software. Values of 50% effective concentration ($EC_{50}$) from cytotoxicity curves were then determined as mol/L for each experiment and data are reported as means ±standard deviations (SD). Student *t*-test was performed to calculate *p* values.

## Chemicals

**Agilent Technologies (Waldbronn, Germany):** Agilent DNA 1000.

**Applied Biosystems/Ambion® (Austin, TX, USA):** RETROScript® kit, Power SYBR Green PCR Master Mix.

**Costar (Cambridge, MA, USA):** 24- and 96-well tissue culture plates, 60 mm Petri dishes, 75 $cm^2$ flasks.

**Gibco BRL/Life Technology (Carlsbad, CA, USA)–Grand Island, NY**: DMEM high glucose+GlutaMAX™-1, FBS, TrypLE™ Express.

**IDT Integrated DNA Technologies, Inc.** (Coralville, IA, USA): $Na_V1.2$ and $Na_V1.8$ α-subunits primer pairs.

**Promega (Madison, WI, USA):** TransFast™ Transfection reagent, CellTiter 96® $AQ_{ueous}$ One Solution Cell Proliferation Assay.

**Sigma Chemical Company (St Louis, MO, USA):** G418 disulfate salt solution, DMSO, veratridine, ouabain, chloroform, isopropanol, ethanol, methanol.

**Origene (Rockville, MD, USA):** TrueClone™ human full-length cDNA clones: accession numbers NM_021007.1 (human 1.2 alpha subunit) and NM_006514.2 (human 1.8 alpha subunit).

**Molecular Research Center, Inc (Cincinnati, OH, USA):** TRI Reagent®-RNA/DNA/protein isolation reagent.

**QIAGEN Sciences (Maryland, USA):** RNeasy® Mini Kit, QIAquick® PCR Purification kit.

**Calbiochem-Novabiochem Corporation (La Jolla, CA, USA):** Brevetoxins PbTx-1, PbTx-3 and PbTx-7.

**Other toxins employed in this study:** P-CTX-1 was purchased from Doctor Richard Lewis (Institute for Molecular Bioscience, The University of Queensland, Brisbane, Qld 4072, Australia), C-CTX-1 was generously given by Doctor Robert Dickey (US FDA) and P-CTX-3C was a kind gift of Professor Takeshi Yasumoto (Tama Laboratory, Japan Food Research Laboratories, Tama, Tokyo, Japan).

# *RESULTS*

## Expression of $Na_V1.2$ and $Na_V1.8$ VGSC alpha subunit mRNA in HEK clones

### *Real time PCR*

Real Time PCR performed on the two clones and on non-transfected HEK-293 cells demonstrated the selective mRNA production of both VGSC isoforms in transfected cells.
Figure 25 shows for each sample the corresponding threshold cycle (Ct) value, a measure of the cycle number at which the fluorescent signal of the reaction crosses the threshold, becoming statistically significant with respect to the calculated baseline signal. Ct value is inversely related to the amount of starting template. Ct values had an average of 23.85 ±0.32 cycles for the $Na_V1.2$ clone and 16.64 ±0.37 cycles for the $Na_V1.8$ clone. The non-transfected HEK-293 control cell line had Ct values of 32.74 ±1.23 cycles for the 1.2 VGSC alpha subunit and 37.92 ±1.41 cycles for the $Na_V1.8$ alpha subunit, suggesting a very low specific mRNA expression or a non-specific product amplification in these samples.

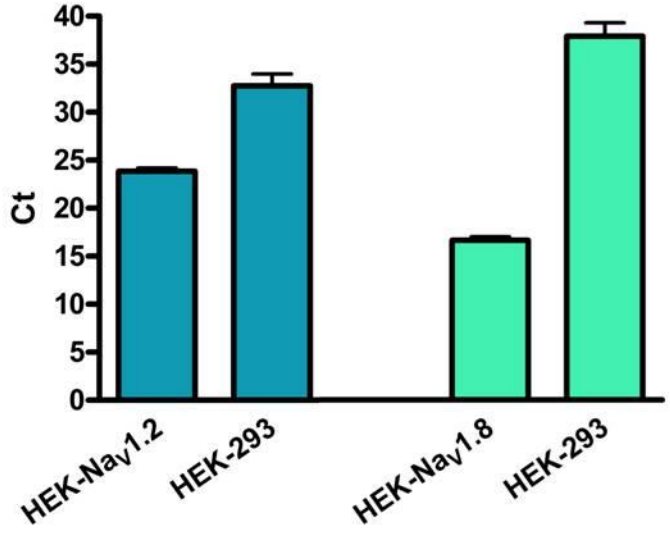


**Figure 25: Real Time PCR analysis of $Na_V1.2$ and $Na_V1.8$ alpha subunit mRNA synthesis in transfected and non-transfected cells.**
Data are reported as corresponding threshold cycle (Ct) values (means ±SD, *n*=3) of PCR-amplified samples.

### *Real Time PCR products bio sizing and quantification*

Complementary DNA size-fractionation showed products with a size of 566 bp, at a concentration of 1.5 ng/µL for the $Na_V1.2$ VGSC clone and of 427 bp, at a concentration of 5.8 ng/µL for the $Na_V1.8$ VGSC clone cDNA. These values are similar to the size expected for both isoforms, reported to be 626 bp and 453 bp, respectively, for the $Na_V1.2$ and $Na_V1.8$ isoforms (Yarowsky *et al*., 1991; Jo *et al*., 2004) (see figure 26).

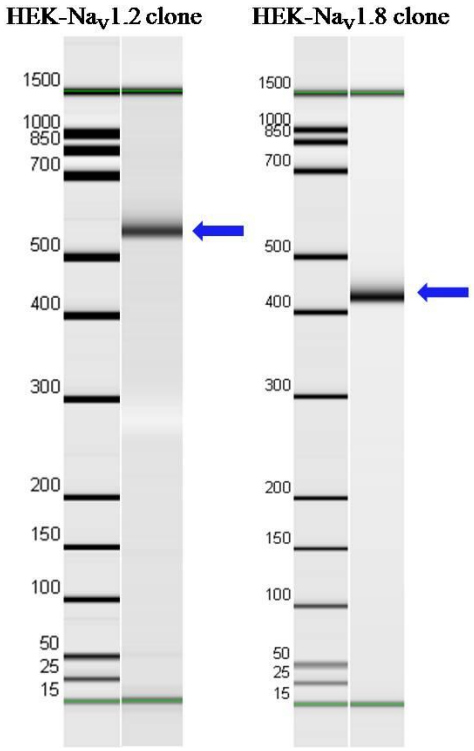


**Figure 26: cDNA products bio sizing**
Results are visualized as a band of cDNA product (right lanes) for which the size, in bp, is estimated using the standardized ladder bands (left lanes).

### *Real Time PCR product sequencing*

The HEK-$Na_V1.2$ clone cDNA product as analyzed by Seqwright DNA Technology Services (Houston, TX, USA) showed a maximum identity of 93 % (by forward primer) and 94 % (by

reverse primer) with *Mus musculus* voltage gated type II alpha1 (Scn2a1) sodium channel subunit mRNA (accession number NM_001099298.2).

## Brevetoxin and ciguatoxin toxicity on HEK-$Na_V1.2$ and -$Na_V1.8$ clones and on HEK-non transfected cells

### *Dose-response curves*

The relative potencies of ciguatoxins and brevetoxins on $Na_V$ were assessed by a cytotoxicity assay using cell viability as an end point. The cells were exposed overnight to the site-2 sodium channel activator veratridine and the $Na^+/K^+$ ATPase pump inhibitor ouabain in the presence of increasing concentrations of neurotoxins, ranging from 0.001 µM up to 100 µM for the BTXs (PbTx-1, PbTx-7 and PbTx-3), or from 0.000001 µM up to 1 µM for the CTXs (P-CTX-1, P-CTX-3C and C-CTX-1). The most toxic response to the polyether toxins was obtained with a ouabain concentration of 0.05 µM, along with the addition of veratridine at final concentration of 50 µM for HEK-$Na_V1.2$ and 100 µM for HEK-$Na_V1.8$. Figure 27 represents the toxin cytotoxicity on HEK-$Na_V1.2$ (figure 27A) and HEK-$Na_V1.8$ (figure 27B) reporting the toxin concentration as $Log_{10}$ g/mL on X axis, and the cell viability expressed as a percentage of ouabain/veratridine treated control cells on Y axis. Data were best fitted using a sigmoidal regression curve with a slope of 1. The maximum cell death observed, estimated by the bottom value of the curve, of the ouabain-veratridine treated control cells averaged at ~26% with HEK-$Na_V1.2$ and ~31% with HEK-$Na_V1.8$. On the other hand, no reduction in cell viability was observed when non-transfected cells were incubated with ouabain (0.05 µM), veratridine (50 µM) and toxin concentration ranging from 0.001 µM up to 100 µM for the BTXs (PbTx-1, PbTx-7 and PbTx-3), or from 0.000001 µM up to 1 µM for the CTXs (P-CTX-1, P-CTX-3C and C-CTX-1) (figure 28).

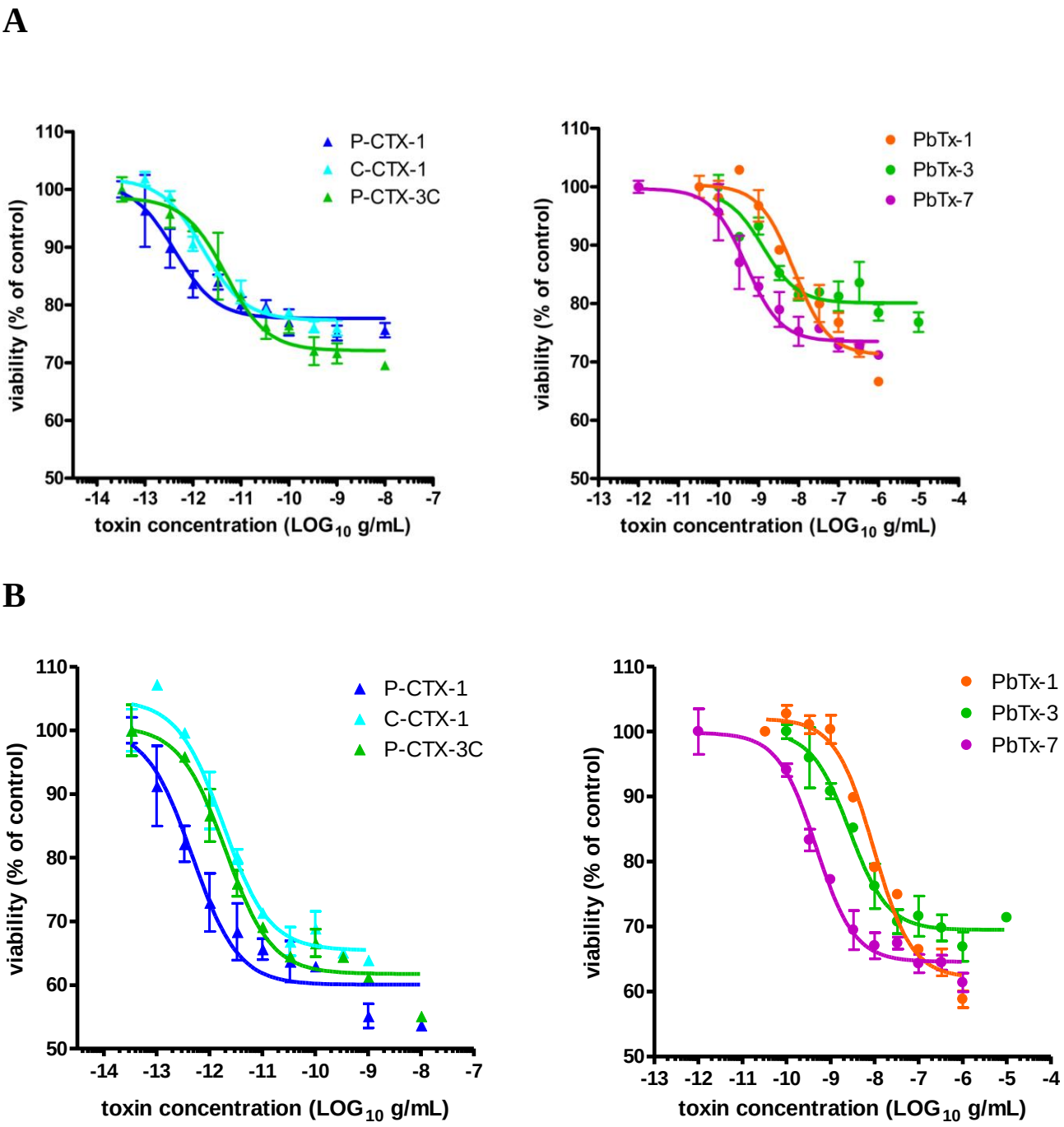


**Figure 27: CTXs and BTXs cytotoxicity on (A) HEK-$Na_V1.2$ and (B) HEK-$Na_V1.8$**

Data are reported as mean ±SD. Viability is expressed as the percent absorbance of viable cells relative to ouabain/veratridine control (*n=6*). Each experimental point was run in duplicate wells and repeated two to four times.

$EC_{50}$ values for each curve are reported in table 7.

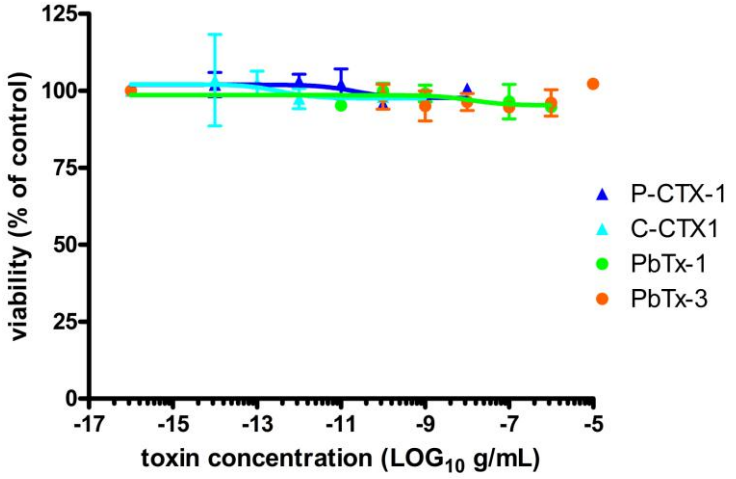


**Figure 28: CTXs and BTXs cytotoxicity on non-transfected HEK-293 cells**
Data are reported as mean ±SD. Viability is expressed as percent absorbance of viable cells relative to ouabain/veratridine control. Each experimental point was run in duplicate.

### *Comparison of brevetoxin and ciguatoxin $EC_{50}$ values in $Na_V1.2$ and $Na_V1.8$ clones*

The effective concentration at 50 % ($EC_{50}$) values for the CTX and BTX treatments for both HEK clones are reported in the table 7. Values compared by Student *t*-test found a significant difference between P-CTX-1 and both C-CTX-1 ($p<0.05$) and P-CTX-3C ($p<0.001$), and between PbTx-1 and both PbTx-3 ($p<0.05$) and PbTx-7 ($p<0.01$) in the HEK-$Na_V1.2$ clone. A significant difference was found between P-CTX-1 and C-CTX-1 ($p<0.05$) and between PbTx-7 and both PbTx-1 and PbTx-3 ($p<0.05$) in the HEK-$Na_V1.8$ clone. In both $Na_V1.2$ and $Na_V1.8$ clones, the most potent CTX was P-CTX-1 with $EC_{50}$ values ~5-fold lower than that of C-CTX-1 and ~8-fold lower than that of P-CTX-3C. Similarly, the most potent BTX was PbTx-7 with $EC_{50}$ values 7-fold lower than PbTx-1 and ~3-fold lower than PbTx-3.

| | HEK-$Na_V1.2$ | | HEK-$Na_V1.8$ | |
|---|---|---|---|---|
| | $EC_{50}$ | relative potency | $EC_{50}$ | relative potency |
| **P-CTX-1** | $4.81 \times 10^{-13}$ ($\pm 1.89 \times 10^{-13}$) | 1 | $4.60 \times 10^{-13}$ ($\pm 1.63 \times 10^{-15}$) | 1 |
| **C-CTX-1** | $2.69 \times 10^{-12}$ ($\pm 1.55 \times 10^{-12}$) | 5.8 * | $1.75 \times 10^{-12}$ ($\pm 7.37 \times 10^{-13}$) | 3.9 * |
| **P-CTX-3C** | $4.67 \times 10^{-12}$ ($\pm 5.30 \times 10^{-13}$) | 9.7 *** | $3.27 \times 10^{-12}$ ($\pm 2.24 \times 10^{-12}$) | 7.1 |
| **PbTx-1** | $7.73 \times 10^{-9}$ ($\pm 1.73 \times 10^{-9}$) | 7.4 * | $3.86 \times 10^{-9}$ ($\pm 3.53 \times 10^{-9}$) | 7.0 * |
| **PbTx-3** | $2.73 \times 10^{-9}$ ($\pm 1.99 \times 10^{-9}$) | 2.7 | $1.76 \times 10^{-9}$ ($\pm 4.83 \times 10^{-10}$) | 3.3 * |
| **PbTx-7** | $1.04 \times 10^{-9}$ ($\pm 8.41 \times 10^{-10}$) | 1 | $5.48 \times 10^{-10}$($\pm 3.18 \times 10^{-10}$) | 1 |

**Table 7: Summary of toxin potency on HEK-$Na_V1.2$ and HEK-$Na_V1.8$ VGSC clones**
Data are reported as mean ±SD of molar $EC_{50}$ values obtained by sigmoid curve regression of experiments performed in duplicate, repeated two to six times. Averaged values were compared as relative P-CTX-1 potency *vs* both C-CTX-1 and P-CTX-3C, and PbTx-7 *vs* both PbTx-1 and PbTx-3.
* $p<0.05$; *** $p<0.001$ (Student *t*-test).

### Amino acid sequences comparison

Amino acid sequences of the alpha subunit clones were compared by NCBI Blast to the two putative brevetoxin receptor site 5 sequences identified by Trainer *et al*. (1994) on VGSC domain I and domain IV. Figure 29 reports data on the Y axis as score bits to compare alignment scores from different searches, and on the X axis the name of the single domain compared to each alpha subunit.

Blast system significance is reported as expectation value E: the lower the E value, the more significant the score. $Na_V1.2$ sequence showed an identity of 97 % (E=3e-55, 197 score bits) with the domain I sequence and an identity of 94 % (E=1e-57, 206 score bits) with the domain IV sequence. The 1.8 VGSC alpha subunit sequence showed an identity of 71 % (E=2e-40, 148 score bits) with the domain I sequence and an identity of 74 % (E=1e-42, 156 score bits) with the domain IV sequence.

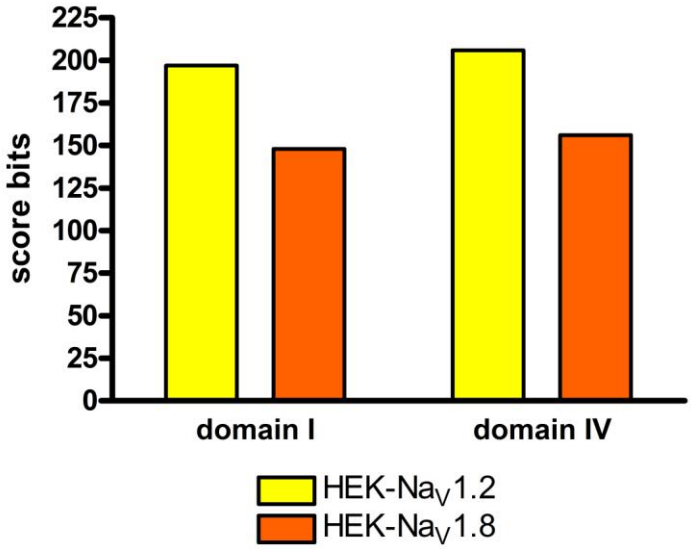


**Figure 29: Comparison between alpha subunits and putative brevetoxin receptor site 5 amino acid sequences.** Values were calculated by NCBI blast system and reported as score bits.

# DISCUSSION

The typical sensory abnormalities observed in CFP particularly in the Pacific suggest that the site-5 neurotoxins may have a unique interaction with voltage gated sodium channel ($Na_V$) isoforms from sensory neurons. In this study we have examined the effects of three ciguatoxins (P-CTX-1, P-CTX-3C and C-CTX-1) and three brevetoxins (PbTx-1, PbTx-7, and PbTx-3) on the peripheral sensory neuron $Na_V1.8$ isoform and compared it to that on the central nervous $Na_V1.2$ isoform.

Human embryonic kidney (HEK) cells were transfected by a chemical approach with $Na_V\alpha$-subunits cDNA gene however without the auxiliary $Na_V\beta$-subunit, and two stable cell lines expressing either $Na_V1.2$ or $Na_V1.8$ were successfully constructed to conduct this study. Real time-PCR analysis confirmed the expression of specific $Na_V1.2$ or $Na_V1.8$ mRNA in the two HEK stable cell line produced while a very low or non-specific mRNA product amplification was measured in non transfected HEK cells. It is worth noting that since the primer pair used for $Na_V1.2$ had broad-selectivity for the four brain isoforms $Na_V1.1$, $Na_V1.2$, $Na_V1.2a$ and $Na_V1.3$, which confirms the previous report of their absence in HEK cell line (Liu *et al*. 2006).

Toxin potencies and thus evaluation of $Na_V$ functionality in the two clones were assessed using a cytotoxicity assay that was first described for mouse neuroblastoma N2a cells (Kogure *et al*. 1988), and successively modified (Jellett *et al*., 1992; Manger *et al*., 1993, 1995; Dickey *et al*., 1999) and adapted to the HEK cell line as an heterologous system for high copy stably expressed homologous target receptors (Fairey *et al*., 2001). Using this method, the best toxic response to the polyether toxins was obtained with a ouabain $Na^+/K^+$ ATPase pump inhibitor concentration of 0.05 μM, along with the addition of site-2 sodium channel activator veratridine at final concentration of 50 and 100 μM for HEK-$Na_V1.2$ and HEK-$Na_V1.8$, respectively. As previously reported (Fairey *et al*., 2001; Bottein Dechraoui and Ramsdell, 2003) the HEK clones appeared highly sensitive to ouabain which was used at concentration four order magnitudes lower than that used in the original neuroblastoma cells assay. The use of a higher veratridine concentration for the HEK-$Na_V1.8$ clone was also in agreement with other studies showing a reduced sensitivity of the rat $Na_V1.8$ to veratridine relative to the rat $Na_V1.2a$ or the human $Na_V1.5$ expressed in F-11, CHO and 293-EBNA cells, respectively (Vickery *et al*., 2004), and a lower agonist effect of veratridine on human $Na_V1.8$ than $Na_V1.5$ and $Na_V1.7$ (Liu *et al*., 2006).

Overall our assay condition resulted in a low to moderate reduction of cell viability (with an averaged maximum loss of ~26% with HEK-$Na_V1.2$; and ~31% with HEK-$Na_V1.8$).

Yet the observed dose-dependent cytotoxic effect confirmed the presence of $Na_V$ proteins at the cell membranes and revealed the susceptibility of both the peripheral and the central sodium channel isoforms to the polyether toxins. Further analysis of the sigmoidal dose-response parameters revealed similar toxin's relative potencies within the two clones. Among the three ciguatoxins backbone tested (i.e. type 1 and 2 Pacific CTX P-CTX-1 and P-CTX-3, respectively and a Caribbean CTX the C-CTX-1), the P-CTX-1 appeared the most potent while no significant differences in the $EC_{50}$ values were observed within the C-CTX-1 and the P-CTX-3C. Among all brevetoxins tested the type A alcohol brevetoxin (PbTx-7) was the most potent with an $EC_{50}$ value 7-fold lower than its parental type A aldehyde (PbTx-1), and 3-fold lower than its corresponding type B alcohol (PbTx-3), in both HEK-$Na_V$1.2 and -$Na_V$1.8 clones.

Along with previous study of the effects and affinity on $Na_V$ to a wide panel of polyether toxins and their newly discovered metabolites the new results provided here are providing useful information to better assess toxin's structure-activity relationship. As such, the hydroxyl groups at the extremities of the CTX molecule are proposed to promote a more stable interaction with binding site (i.e. by creation of hydrogen bonds within the binding site), although structural differences at the CTX M-ring may lead to slight differences in potency indicating that the ring contributes to, but is not critical for, high affinity binding to $Na_V$ (Lewis *et al*., 1993). As well Dechraoui *et al*. (1999) reported that ciguatoxins affinity and toxicity seemed related to hydroxylation of the A-ring. For the brevetoxins, the important role shown in this study is the polarity induced by the hydroxyl group on the K-ring side-chain on toxin potency which confirms previous findings comparing the BTX type B alcohol (PbTx-3) with its aldehyde parental (PbTx-2) toxin (Gawley *et al*., 1992; Poli *et al*., 1986; Bottein Dechraoui and Ramsdell, 2003; Bottein Dechraoui *et al*., 2006; Cao *et al*., 2008, Atchinson *et al*. 1986). As well, our result confirms the lower potency of the more rigid type B brevetoxin backbone observed by others (Baden *et al*., 1988; Gawley *et al*., 1992; Cao *et al*., 2008).

An additional level of understanding of CTXs and BTXs interaction with their molecular binding site is provided by comparative studies of site-5 toxins' activity within $Na_V$ isoforms. Different primary and/or tertiary protein structure can greatly alter ligand interaction with the channel and small changes such as a single amino acid substitution have been shown to importantly affect neurotoxin site affinity/sensitivity of an isoform to ligand

toxins (Satin *et al*., 1992; Favre *et al*., 1995; Cummins *et al*., 2002; Xue *et al*., 2003; Haverinen *et al*., 2007), although high identity among isoforms does not always implicate the same or similar sensitivity (Denac *et al*., 2002). Within the putative brevetoxin receptor binding site identified by Trainer *et al*. (1994) on the $Na_V$, the primary structure of $Na_V1.2$ respectively shows 91%, 76% and 74% identities against $Na_V1.4$, $Na_V1.5$ and $Na_V1.8$ (NCBI blast). Hence, a previous study comparing site-5 toxins' relative potency and affinity on $Na_V1.4$, 1.5 and 1.2 reported a tissue selectivity of the BTX type B PbTx-3 and PbTx-2 which was found neither for the BTX type A PbTx-1 nor the CTX P-CTX-3C (Dechraoui and Ramsdell, 2003); BTX type B toxins were showing a uniquely lower affinity and toxicity for the cardiac $Na_V1.5$ sodium channel. These findings were consistent with electrophysiological recordings using a patch clamp method and P-CTX-3C on the three isoform $Na_V1.2$, $Na_V1.4$ or $Na_V1.5$ isoforms (Yamaoka *et al*. 2004, 2009).

In the present study, the direct comparison of the susceptibility of the HEK-$Na_V1.8$ to -$Na_V1.2$ to the site-5 toxins was limited by the probable variation in receptor expression level and the fact that the assay conditions were different for the two clones. Nonetheless the $EC_{50}$ values for each toxin were similar for both clones (in the low pM range for CTXs and low nM range for BTXs) which was not in agreement with the electrophysiological recent findings from Yamaoka (2009) showing a greater effect of the P-CTX-3C on the rat $Na_V1.8$ (transiently expressed in ND7-23 cells) compared to that on $Na_V1.2$ and 1.4 (transiently expressed in HEK). These divergent observations could reside in the expression of a dysfunctional sodium channel. Indeed in the 2009 Yamaoka *et al*. studies, $Na_V1.8$ in HEK cells were found not functional whilst two chimeric mutants from both $Na_V1.4$ and $Na_V1.8$ were successfully expressed when co-transfected with auxiliary $Na_V\beta1$-subunit. The 2004 report highlighted the higher toxin concentrations, in the μM range, needed to give electrophysiological responses, when low nM range were found to be effective in previous studies, suggesting that a unique channel conformation due to the presence of other proteins not provided in HEK cells such as auxiliary subunits could be responsible for channel higher sensitivity to the toxin. In an earlier study using TSA 201 cells transiently transfected with the rat $Na_V1.2$ α with the $Na_V\beta1$ subunits, the binding for both brevetoxin and saxitoxin was found directly related to the molar ratio of β1 to α subunit (Trainer *et al*., 1996).

In heterologous expression systems, host cell do not always provides proteins essential for function or stability, i.e. chaperone, anchoring proteins, scaffold proteins for intracellular signalling (Thomas and Smart, 2005; Holst *et al*., 2009). The importance of the auxiliary β-

subunits in the expression and stabilization of $Na_V$ α-subunit in the membrane as well as their role as structures of contact with cytoskeletal or extracellular matrix proteins have been well demonstrated (Moran *et al*., 2003). However no mRNA for subunit β1 has been found in HEK cells (Moran *et al*., 2000; Young and Caldwell, 2005), and although abundant mRNA encoding for the $Na_V$ auxiliary $Na_V\beta2$, $Na_V\beta3$, $Na_V\beta4$, $Na_V\beta1A$ and $Na_V\beta1B$ splice variants (Moran *et al*., 2000; Shah *et al*., 2004; Young and Caldwell, 2005), and very low levels of $Na_V\beta1$ and $Na_V\beta2$ subunits (Shah *et al*., 2004) were reported, recent Western blots analyses (Aman *et al*., 2009) found no detectable expression of $Na_V\beta1A$, $Na_V\beta2$, $Na_V\beta3$ and $Na_V\beta4$. The lack of cofactors such as β-subunits in HEK heterologous expression system could lead to missing interactions and altered channel conformation in a region important for toxin sensitivity (Moran *et al*., 2003, Kamiya *et al*., 2004; Yamaoka *et al*., 2009). This may be the case particularly for $Na_V1.8$ which is mainly localized intracellularly in the cytoplasmic pool and has to be recruited to the plasma membrane to exert its function (Djouhri *et al*., 2003).

**Conclusions**

The present study compared the potency of several ciguatoxins (P-CTX-1; C-CTX-1; P-CTX-3C) and brevetoxins (PbTx-1, PbTx-7, PbTx-3) on human voltage-gated sodium channel of either central $Na_V1.2$ or peripheral $Na_V1.8$ nervous system expressed in HEK cells.

High level of $Na_V$ mRNA were found in the HEK clones and a dose-dependent cytotoxic effect of the polyether toxins confirmed the presence of functional $Na_V$ proteins at the cell membranes.

The peripheral as well as the central sodium channel isoforms were similarly susceptible to site-5 toxins.

A better understanding of the specific neurologic in particular cutaneous effect of the ciguatoxins may require further investigation of $Na_V1.9$ or $Na_V1.6$ susceptibility.

# REFERENCES

Abraham W.M., Bourdelais A.J., Sabater J.R., Ahmed A., Lee T.A., Serebriakov I., Baden D.G. 2005. Airway responses to aerosolized brevetoxins in an animal model of asthma. Am J Respir Crit Care Med 171(1): 26-34.

Aman T.K., Grieco-Calub T.M., Chen C., Rusconi R., Slat E.A., Isom L.L., Raman I.M. 2009. Regulation of persistent $Na^+$ current by interactions between β subunits of voltage-gated Na channels. J Neurosci 29(7): 2027-2042.

Atchison W.D., Scruggs L.V., Narahashi T., Vogel S.M. 1986. Nerve membrane sodium channels as the target site of brevetoxins at neuromuscular junctions. Br J Pharmac 89: 731-738.

Baden D.G. 1989. Brevetoxins: unique polyether dinoflagellates toxins. FASEB J 3: 1807-1817.

Baden D.G., Bikhazi G., Decker S.J., Foldes F.F., Leung I. 1984. Neuromuscolar blocking action of two brevetoxins from the Florida red tide organism *Ptychodiscus brevis*. Toxicon 22(1): 75-84.

Baden D.G., Bourdelais A.J., Jacocks H., Michelliza S., Naar J. 2005. Natural and derivative brevetoxins: hystorical background, moltiplicity and effects. Environ Health Perspect 113(5): 621-625.

Baden D.G. and Mende T.J. 1982. Toxicity of two toxins from the Florida red tide marine dinoflagellates *Ptychodiscus brevis*. Toxicon 20(2): 457-461.

Baden D.G., Mende T.J., Szmant A.M., Trainer V.L., Edwards R.A., Roszell L.E. 1988. Brevetoxin binding: molecular pharmacology versus immunoassay. Toxicon 26(1): 97-103.

Bagnis R., Chanteau S., Chungue E., Hurtel J.M., Yasumoto T., Inoue A. 1980. Origins of ciguatera fish poisoning: a new dinoflagellates, *Gambierdiscus toxicus* Adachi and Fukuyo, definitely involved as a causal agent. Toxicon 18(2): 199-208.

Bentur Y., Spanier E. 2007. Ciguatoxin-like substances in edible fish on the eastern Mediterranean. Clin Toxicol (Phila) 45(6): 695-700.

Bidard J.N., Vijverberg H.P.M., Frelin C., Chunguell E., Legrand A.M., Bagnis R., Lazdunski M. 1984. Ciguatoxin is a novel type of $Na^+$ channel toxin. J Biol Chem 259 (13): 8353-8357.

Birinyi-Strachan L.C., Gunning S.J., Lewis R.J., Nicholson G.M. 2005. Block of voltage-gated potassium channels by Pacific ciguatoxins-1 contributes to increased neuronal excitability in rat sensory neurons. Toxicol Appl Pharmacol 204(2): 175-186.

Bottein Dechraoui M.Y. and Ramsdell J.S. 2003. Type B brevetoxins show tissue selectivity for voltage-gated sodium channels: comparison of brain, skeletal muscle and cardiac sodium channels. Toxicon 41: 919-927.

Bottein Dechraoui M.Y., Wacksman J.J., Ramsdell J.S. 2006. Species selective resistance of cardiac muscle voltage gated sodium channels: characterization of brevetoxin and ciguatoxins binding sites in rats and fish. Toxicon 48: 702-712.

Bourdelais A.J., Campbell S., Jacocks H., Naar J., Wright J.L.C., Carsi J., Baden D.G. 2004. Brevenal is a natural inhibitor of brevetoxin action in sodium channel receptor binding assays. Cell Mol Neurobiol 24(4): 553-563.

Brock J.A., McLachlan E.M., Jobling P., Lewis R.J. 1995. Electrical activity in rat tail artery during asynchronous activation of postganglionic nerve terminals by ciguatoxins-1. Br J Pharmacol 116(4): 2213-2220.

Cao Z., George J., Gerwick W.H., Baden D.G., Rainier J.D., Murray T.F. 2008. Influence of lipid-soluble gating modifier toxins on sodium influx in neocortical neurons. J Pharmacol Exp Therapeut 326(2): 604-613.

Catterall W.A., Cestèle S., Yarov-Yarovoy V., Yu F.H., Konoki K., Scheuer T. 2007. Voltage-gated ion channels and gating modifier toxins. Toxicon 49: 124-141.

Catterall W.A., Chandy K.G., Gutman G.A. 2002. The IUPHAR compendium of voltage-gated ion channels. Ed Girdlestone D. Published by IUPHAR Media, University of Leeds, Leeds LS2 9JT, UK. pp 11-30.

Catterall W.A., Goldin A.L., Waxmax S.G. 2005. International Union of Pharmacology. XLVII. Nomenclature and structure-function relationships of voltage-gated sodium channels. Pharmacol Rev 57(4): 397-409.

Cestèle S., Catterall W.A. 2000. Molecular mechanisms of neurotoxin action on voltage-gated sodium channels. Biochimie 82: 883-892.

Chancey H.J., Shockett P.E., O'Reilly J.P. 2007. Relative resistance to slow inactivation of human cardiac $Na^+$ channel $hNa_V1.5$ is reversed by lysine or glutamine substitution at V930 in D2-S6. Am J Physiol Cell Physiol 293: C1895-C1905.

Cummins T.R., Aglieco F., Dib-Hajj S.D. 2002. Critical molecular determinants of voltage-gated sodium channel sensitivity to μ-Conotoxins GIIIA/B. Mol Pharmacol 61(5): 1192-1201.

Cummins T.R., Sheets P.L., Waxman S.G. 2007. The roles of sodium channels in nociception: implications for mechanisms of pain. Pain. 131(3): 243-257.

Cuypers E., Abdel-Mottaleb Y., Kopljar I., Rainier J.D., Raes A.L., Snyders D.J., Tytgat J. 2008. Gambierol, a toxin produced by the dinoflagellates *Gambierdiscus toxicus*, is a potent blocker of voltage-gated potassium channels. Toxicon 51(6): 974-983.

David L.S., Plakas S.M., El Said K.R., Jester E.L., Dickey R.W., Nicholson R.A. 2003 A rapid assay for the brevetoxin group of sodium channel activators based on fluorescence monitoring of synaptoneurosomal membrane potential. Toxicon 42(2): 191-198.

Dechraoui, M.Y., Naar, J., Pauillac, S., Legrand, A.M. 1999. Ciguatoxins and brevetoxins, neurotoxic polyether compounds active on sodium channels. Toxicon 37: 125-143.

Denac H., Mevissen M., Kühn F.J.P., Kühn C., Guionaud C.T., Scholtysik G., Greeff N.G. 2002. Molecular cloning and functional characterization of a unique mammalian cardiac $Na_V$ channel isoform with low sensitivity to the synthetic inactivation inhibitor (-)-(S)-6-amino-α-[(4-diphenylmethyl-1-piperazinyl)-methyl]-9H-purine-9-ethanol (SDZ 211-939). J Pharmacol Exp Therapeut 303(1): 89-98.

Dickey R., Jester E., Granade R., Mowdy D., Moncreiff C., Rebarchik D. et al. 1999. Monitoring brevetoxins during a *Gymnodinium breve* red tide: comparison of sodium channel specific cytotoxicity assay and mouse bioassay for determination of neurotoxic shellfish toxins in shellfish extracts. Nat Toxins 7(4): 157-165.

Diss J.K., Fraser S.P., Djamgoz M.B. 2004. Voltage-gated $Na^+$ channels: multiplicity of expression, plasticity, functional implications and pathophysiological aspects. Eur Biophys J 33(3): 180-193.

Djouhri L., Fang X., Okuse K., Wood J.N., Berry C.M., Lawson S.N. 2003. The TTX-resistant sodium channel Nav1.8 (SNS/PN3): expression and correlation with membrane properties in rat nociceptive primary afferent neurons. J Physiol 550.3: 739-752.

Dortch Q., Moncreiff C.A., Mendenhall W.M., Parsons M.L., Franks J.S., Hemphill K.W. 1998. Spread of *Gymnodinium breve* into the northern Gulf of Mexico. In: Reguera B., Blanco J., Fernandez M.L., Wyatt T. Harmful Algae. Xunta de Galicia and intergovernmental oceanographic commissiono f UNESCO, Vigo, Spain pp. 143-144.

Ellis S., Spikes J.J., Johnson G.L. 1979. Respiratory and cardiovascular effects of *G. Breve* toxin in dogs. In: Proceedings of the second international conference on toxic dinoflagellates blooms. Taylor D.L. Seliger H.H. Eds. Elsevier, New York, North Holland. pp 431-434.

Fairey E.R., Bottein Dechraoui M.Y., Sheets M.F., Ramsdell J.S. 2001. Modification of the cell based assay for brevetoxins using human cardiac voltage dependent sodium channels expressed in HEK-293 cells. Biosens Bioelectr 16: 579-586.

Favre I., Moczydlowski E., Schild L. 1995. Specificity for block by saxitoxin and divalent cations at a residue which determines sensitivity of sodium channel subtypes to guanidinium toxins. J Gen Physiol 106: 203-229.

Flewelling L.J., Naar J.P., Abbott J.P., Baden D.G., Barros N.B., Bossart G.D., Bottein M.Y., Hammond D.G., Haubold E.M., Heil C.A., Henry M.S., Jacocks H.M., Leighfield T.A., Pierce R.H., Pitchford T.D., Rommel S.A., Scott P.S., Steidinger K.A., Truby E.W., Van Dolah F.M., Landsberg J.H. 2005. Brevetoxicosis: red tides and marine mammal mortalities. Nature 435(7043): 755-756.

Friedman MA, Fleming LE, Fernandez M, Bienfang P, Schrank K, Dickey R, Bottein MY, Backer L, Ayyar R, Weisman R, Watkins S, Granade R, Reich A. 2008. Ciguatera fish poisoning: treatment, prevention and management. Mar Drugs 6(3): 456-479.

Gallagher R.T. and Shinnick-Gallagher P. 1980. Effect of *Gymnodinium breve* toxin in the rat phrenic nerve diaphragm preparation. Br J Pharmacol 69(3): 367-372.

Gawley R.E., Rein K.S., Jeglitsch G., Adams D.J., Theodorakis E.A., Tiebes J., Nicolaou K.C., Baden D.G. 1995. The relationship of brevetoxin 'length' and A-ring functionality to binding and activity in neuronal sodium channels. Chem Biol 2: 533-541.

Gawley R.E., Rein K.S., Kinoshita M., Baden D.G. 1992. Binding of brevetoxins and ciguatoxins to the voltage-sensitive sodium channel and conformational analysis of brevetoxin B. Toxicon 30(7): 780-785.

Ghiaroni V., Sasaki M., Fuwa H., Rossini G.P., Scalera G., Yasumoto T., Pietra P., Bigiani A. 2005. Inhibition of voltage-gated potassium currents by gambierol in mouse taste cells. Toxicol Sci 85(1): 657-665.

Goldin A.L., Barchi R.L., Caldwell J.H., Hofmann F., Howe J.R., Hunter J.C., Kallen R.G., Mandel G., Meisler M.H., Netter Y.B., Noda M., Tamkun M.M., Waxman S.G., Wood J.N., Catterall W.A. 2000. Nomenclature of voltage-gated sodium channels. Neuron 28(2): 365-368.

Hamilton B., Whittle N., Shaw G., Eaglesham G., Moore M.R., Lewis R.J. 2009. Human fatality associated with Pacific ciguatoxins contaminated fish. Toxicon. doi:10.1016/j.toxicon.2009.06.007.

Haverinen J., Hassinen M., Vornanen M. 2007. Fish cardiac sodium channels are tetrodotoxin sensitive. Acta Physiol 191: 197-204.

Hidalgo J., Liberona J.L., Molgó J., Jaimovich E. 2002. Pacific ciguatoxin-1b effect over $Na^+$ and $K^+$ currents, inositol 1,4,5-triphosphate content and intracellular $Ca^{2+}$ signals in cultured rat myotubes. Br J Pharmacol 137(7): 1055-1062.

Hogg R.C., Lewis R.J., Adams D.J. 1998. Ciguatoxin (CTX-1) modulates single tetrodotoxin-sensitive sodium channels in rat parasympathetic neurones. Neurosci Lett 252(2): 103-106.

Holst A.G., Calloe K., Jespersen T., Cedergreen P., Winkel B.G., Jensen H.K., Leren T.P., Haunso S., Svendsen J.H., Tfelt-Hansen J. 2009. A novel SCN5A mutation in a patient with coexistence of brugada syndrome traits and ischaemic heart disease. Case Report Med doi:10.1155/2009/963645.

Huang J.M., Wu C.H., Baden D.G., 1984. Depolarizing action of a red-tide dinoflagellates brevetoxin on axonal membranes. J Pharmacol Exp Therap 229(2): 615-621.

Inoue M., Hirama M., Satake M., Sugiyama K., Yasumoto T. 2003. Inhibition of brevetoxin binding to the voltage-gated sodium channel by gambierol and gambieric acid-A. Toxicon 41: 469-474.

Jeglitsch G., Rein K., Baden D.G., Adams D.J. 1998. Brevetoxin-3 (PbTx-3) and its derivatives modulate single tetrodotoxin-sensitive sodium channels in rat sensory neurons. J Pharmacol Experiment Therapeut 284(2): 516-525.

Jellett J.F., Marks L.J., Stewart J.E., Dorey M.L., Watson-Wright W., Lawrence J.F. 1992. Paralytic shellfish poison (saxitoxin family) bioassays: automated endpoint determination and standardization of the *in vitro* tissue culture bioassay, and comparison with the standard mouse bioassay. Toxicon 30(10): 1143-1156.

Jo T., Nagata T., Iida H., Imuta H., Iwasawa K., Ma J., Hara K., Omata M., Nagai R., Takizawa H., Nagase T., Nakajima T. 2004. Voltage-gated sodium channel expressed in cultured human smooth muscle cells: involvement of SCN9A. FEBS Lett 567: 339-343.

Johnson G.L., Spikes J.J., Ellis S. 1985. Cardiovascular effects of brevetoxins in dogs. Toxicon. 23(3): 505-515.

Kamiya K., Kaneda M., Sugawara T., Mazaki E., Okamura N., Montal M., Makita N., Tanaka M., Fukushima K., Fujiwara T., Inoue Y., Yamakawa K. 2004. A nonsense mutation of the sodium channel gene SCN2A in a patient with intractable epilepsy and mental decline. J Neurosci 24(11): 2690-2698.

Kogure K., Tamplin M.L., Simidu U., Colwell R.R. 1988. A tissue culture assay for tetrodotoxin, saxitoxin and related toxins. Toxicon 26(2): 191-197.

Kopljar I., Labro A.J., Cuypers E., Johnson H.W., Rainier J.D., Tytgat J., Snyders D.J. 2009. A polyether biotoxin binding site on the lipid-exposed face of the pore domain of $K_V$ channels revealed by the marine toxin gambierol. Proc Natl Acad Sci USA 106(24): 9896-9901.

Lewis R.J. 2001. The changing face of ciguatera. Toxicon. 39(1): 97-106.

Lewis R.J. 2006. Ciguatera: Australian perspectives on a global problem. Toxicon. 48(7): 799-809.

Lewis R.J., Endean R. 1984. Mode of action of ciguatoxins from the Spanish Mackerel, Scomberomorus commersoni, on the guinea-pig ileum and vas deferens. J Pharmacol Exp Ther 228(3): 756-760.

Lewis R.J., Endean R. 1986. Direct and indirect effects of ciguatoxin on guinea-pig atria and papillary muscles. Naunyn Schmiedebergs Arch Pharmacol 334(3): 313-322.

Lewis R.J., Holmes M.J. 1993. Origin and transfer of toxins involved in ciguatera. Comp Biochem Physiol 106(3): 615-628.

Lewis R.J., Hoy A.W. 1993. Comparative action of three major ciguatoxins on guinea-pig atria and ilea. Toxicon 31(4): 437-446.
Lewis R.J., Hoy A.W., McGiffin D.C. 1992. Action of ciguatoxins on human atrial trabeculae. Toxicon 30(8): 907-914.

Lewis R.J., Norton R.S., Brereton I.M., Eccles C.D. 1993. Ciguatoxin-2 is a distereomer of ciguatoxins-3. Toxicon 31(5): 637-643.

Lin Y-Y, Risk M, Ray SM, Van Engen D, Clardy J, Golik J, et al. 1981. Isolation and structure of brevetoxin B from the "red tide" dinoflagellate *Ptychodiscus brevis* (*Gymnodinium breve*). J Am Chem Soc 103: 6773-6775.

Liu C., Li Q., Su Y., Bao L. 2010. Prostaglandin E2 promotes Nav1.8 trafficking via its intracellular RRR motif through the protein kinase a pathway. Traffic 11: 405-417.

Liu C.J., Priest B.T., Bugianesi R.M., Dulski P.M., Felix J.P., Dick I.E., Brochu R.M., Knaus H.G., Middleton R.E., Kaczorowski G.J., Slaughter R.S., Garcia M.L., Köhler M.G. 2006. A high-capacity membrane potential FRET-based assay for $Na_V1.8$ channels. Assay Drug Dev Technol 4(1): 37-48.

Lombet, A., Bidard, J.-N., Ladzunski, M., 1987. Ciguatoxin and brevetoxins share a common receptor site on the neuronal voltage-dependent $Na^+$ channel. FEBS Lett 219: 355-359.

Manger R.L., Leja L.S., Lee S.Y., Hungerford J.M., Wekell M.M. 1993. Tetrazolium-based cell bioassay for neurotoxins active on voltage-sensitive sodium channels: semiautomated assay for saxitoxins, brevetoxins, and ciguatoxins. Anal Biochem 214(1): 190-194.

Manger R.L., Leja L.S., Lee S.Y., Hungerford J.M., Hokama Y., Dickey R.W., Granade H.R., Lewis R., Yasumoto T., Wekell M.M. 1995. Detection of sodium channel toxins: directed cytotoxicity assays of purified ciguatoxins, brevetoxins, saxitoxins, and seafood extracts. J AOAC Int 78(2): 521-527.

Marquais M. and Sauviat M.P. 1999. Effect of ciguatoxins on the cardiocirculatory system. J Soc Biol 193(6): 495-504.

Mattei C, Molgó J, Legrand AM, Benoit E. 1999. Ciguatoxins and brevetoxins: dissection of the neurobiological actions. J Soc Biol 193(3): 329-344.

Mattei C., Marquais M., Schlumberger S., Molgó J., Vernoux J.P., Lewis R.J., Benoit E. 2009. Analysis of Caribbean ciguatoxins-1 effects on frog myelinated axons and the neuromuscular junction. Toxicon doi: 10.1016/j.toxicon.2009.07.026.

Mattei C., Wen P.J., Nguyen-Huu T.D., Alvarez M., Benoit E., Bourdelais A.J., Lewis R.J., Baden D.J., Molgó J., Meunier F.A. 2008. Brevenal inhibits Pacific ciguatoxin-1B-induced neurosecretion from bovine chromaffin cells. PLoS ONE 3(10) doi10.1371/journal.pone.0003448.

McCormick K.A., Srinivasan J., White K., Scheuer T., Catterall W.A. 1999. The extracellular domain of the beta subunit is both necessary and sufficient for beta 1-like modulation of sodium channel gating. J Biol Chem 274: 32638-32646.

Meadows L.S., Isom L.L. 2005. Sodium channels as macromolecular complexes: implications for inherited arrhythmia syndromes. Cardiovasc Res 67(3): 448-458.

Miyahara J.T., Akau C.K., Yasumoto T. 1979. Effects of ciguatoxins and maitotoxin on the isolated guinea pig atria. Res Commun Chem Pathol Pharmacol 25(1): 177-180.

Molgó J., Gaudry-Talarmain Y.M., Legrand A.M., Moulian N. 1993. Ciguatoxins extracted from poisonous moray eels Gymnothorax javanicus triggers acetylcholine release from Torpedo cholinergic synaptosomes via reversed $Na^{+}$-$Ca^{2+}$ exchange. Neurosci Lett 160(1): 65-68.

Molgó J., Shimahara T., Gaudry-Talarmain Y.M., Comella J.X., Legrand A.M. 1992. Ciguatoxin-induced changes in acetylcholine release and in cytosolic calcium levels. Bull Soc Pathol Exot 85(5 Pt2): 486-488.

Moran O., Conti F., Tammaro P. 2003. Sodium channel heterologous expression in mammalian cells and the role of the endogenous β1-subunits. Neurosci Lett 336: 175-179.

Moran O., Nizzari M., Conti F. 2000. Endogenous expression of the β1A sodium channel subunit in HEK-293 cells. FEBS Lett 473: 132-134.

Murata, M., Legrand, A.-M., Ishibashi, Y., Yasumoto, T. 1989. Structures of ciguatoxin and its congener. J Am Chem Soc 111: 8929-8931.

Music S.I., Howell J.T., Brumback C.L. 1973. Red tide. Its public health implications. J Fla Med Assoc 60(11): 27-29.

Naar JP, Flewelling LJ, Lenzi A, Abbott JP, Granholm A, Jacocks HM, Gannon D, Henry M, Pierce R, Baden DG, Wolny J, Landsberg JH. 2007. Brevetoxins, like ciguatoxins, are potent ichthyotoxic neurotoxins that accumulate in fish. Toxicon 50(5): 707-723.

Nguyen-Huu T.D., Mattei C., Wen P.J., Bourdelais A.J., Lewis R.J., Benoit E., Baden D.G., Molgó J., Meunier F.A. 2009. Ciguatoxin-induced catecholamine secretion in bovine chromaffin cells: Mechanism of action and reversible inhibition by brevenal. Toxicon doi: 10.1016/j.toxicon.2009.08.002.

Ohizumi Y., Ishida Y., Shibata S. 1982. Mode of the ciguatoxin-induced supersensitivity in the guinea-pig vas deferens. J Pharmacol Exp Ther 221(3): 748-752.

Ohizumi Y., Shibata S., Tachibana K. 1981. Mode of the excitatory and inhibitory actions of ciguatoxin in the guinea-pig vas deferens. J Pharmacol Exp Ther 217(2): 475-480.

Ohshika H. 1971. Marine toxins from the Pacific. IX. Some effects of ciguatoxins on isolated mammalian atria. Toxicon 9(4): 337-343.

Parmentier J.L., Narahashi T., Wilson W.A., Trieff N.M., Sadagopa Ramanujam V.M., Risk M., Ray S.M. 1978. Electrophysiological and biochemical characteristics of *Gymnodinium breve* toxins. Toxicon 16(3): 235-244.

Plakas S.M. and Dickey R.W. 2009. Advances in monitoring and toxicity assessment of brevetoxins in molluscan shellfish. Toxicon doi: 10.1016/j.toxicon.2009.11.007.

Pierce R.H. 1986. Red tide (Ptychodiscus brevis) toxin aerosols: a review. Toxicon. 24(10): 955-965

Poli, M. A., Mende, T. J., Baden, D. G., 1986. Brevetoxins, unique activators of voltage-sensitive sodium channels, bind to specific sites in rat brain synaptosomes. Mol Pharmacol 30: 129-135.

Pottier I., Vernoux J.P. 2003. Evaluation of Antilles fish ciguatoxicity by mouse or chick bioassays. Bull Soc Pathol Exot 96(1): 24-28.

Pottier I., Vernoux J.P., Jones A., Lewis R.J. 2002. Charactherization of multiple Caribbean ciguatoxins and congeners in individual specimens of horse-eye jack (Caranx latus) by high performance liquid chromatography/mass spectrometry. Toxicon 40(7): 929-939.
Purkerson-Parker S.L., Fieber L.A., Rein K.S., Podona T., Baden D.G. 2000. Brevetoxin derivatives that inhibit toxin activity. Chem Biol 7: 385-393.

Radwan F.F., Ramsdell J.S. 2006 Characterization of *in vitro* oxidative and conjugative metabolic pathways for brevetoxin (PbTx-2). Toxicol Sci 89(1): 57-65.

Rayner M.D. 1972. Mode of action of ciguatoxins. Fed Proc 31(3): 1139-1145.

Rayner M.D. and Kosaki T.I. 1970. Ciguatoxin: effects on Na fluxes in frog muscle. Fed Proc Fed Am Soc Exp Biol 29: 548.

Rein K.S., Baden D.G., Gaw1ey R.E. 1994. Conformational analysis of the sodium channel modulator, brevetoxin A, comparison with brevetoxin B conformations, and a hypothesis about the common pharmacophore of the 'site 5' toxins. J Org Chem 59: 2101-2106.

Richards I.S. and Bourgeois M. 2010. Red tide toxin produces *in vitro* depolarization of human airway smooth muscle. Clin Toxicol (Phila) doi: 10.3109/15563650903476483.

Risk M., Norris P.J., Coutinho-Netto J., Bradford H.F. 1982. Actions of *Ptychodiscus brevis* red tide toxin on metabolic and transmitter-releasing properties of synaptosomes. J Neurochem 39: 1485-1488.

Sasner J. J. 1965. A study of the effects of a toxin produced by the Florida red tide dinoflagellate *Gymnodinium breve* Davis, Ph.D. Thesis, University of California, Los Angeles, 1965.

Satake, M., Fukui, M., Legrand, A.-M., Cruchet, P., Yasumoto, T., 1998. Isolation and structures of new ciguatoxin analogs, 2,3-dihydroxyCTX3C and 51-hydroxyCTX3C, accumulated in tropical reef fish. Tetr Lett 39: 1197-1198.

Satake, M., Murata, M., Yasumoto, T., 1993. The structure of CTX3C, a ciguatoxin congener isolated from cultured *Gambierdiscus toxicus*. Tetr Lett 34: 1975-1978.

Satin J., Kyle J.W., Chen M., Bell P., Cribbs L.L., Fozzard H.A., Rogart R.B. 1992. A mutant of TTX-resistant cardiac sodium channels with TTX-sensitive properties. Science 256(5060): 1202-1205.

Sauviat M-P, Marquais M., Vernoux J.P. 2002. Muscarinic effects of the Caribbean ciguatoxin C-CTX-1 on frog atrial heart muscle. Toxicon 40: 1155-1163.

Schlumberger S., Mattei C., Molgó J., Benoit E. 2009. Dual action of a dinoflagellate-derived precursor of Pacific ciguatoxins (P-CTX-4B) on voltage-dependent $K^+$ and $Na^+$ channels of single myelinated axons. Toxicon doi: 10.1016/j.toxicon.2009.06.035.

Schreibmayer W. and Jeglitsch G. 1992. The sodium channel activator Brevetoxin-3 uncovers a multiplicity of different open states of the cardiac sodium channel. Biochim Biophys Acta 1104: 233-252.

Seino A., Kobayashi M., Momose K., Yasumoto T., Ohizumi Y. 1988. The mode of inotropic action of ciguatoxin on guinea-pig cardiac muscle. Br J Pharmacol 95: 876-882.

Shah B.S., Rush A.M., Liu S., Tyrrell L., Black J.A., Dib-Hajj S.D., Waxman S.G. 2004. Contactin associates with sodium channel $Na_V1.3$ in native tissues and increases channel density at the cell surface. J Neurosci 24(33): 7387-7399.

Shimizu Y, Chou HN, Bando H. 1986. Structure of brevetoxin A (GB-1 toxin), the most potent toxin in the Florida red tide organism *Gymnodinium breve* (*Ptychodiscus brevis*). J Am Chem Soc 108: 514-515.
Shinnick-Gallagher P. 1980. Possible mechanisms of action of *Gymnodinium breve* toxin at the mammalian neuromuscular junction. Br J Pharmacol 69(3): 373-378.

Shoukimas J. J., Siger A., Abbott B.C. 1979. The action of *G. breve* neurotoxin on membrane conductance. In Toxic Dinoflagellate Blooms, Eds. D. L. Taylor and H. H. Seliger, Elsevier/North Holland, New York, pp 425-430.

Sims JK. 1987. A theoretical discourse on the pharmacology of toxic marine ingestions. Ann Emerg Med. 16(9): 1006-1015.

Strachan L.C., Lewis R.J., Nicholson G.M. 1999. Differential actions of pacific ciguatoxin-1 on sodium channel subtypes in mammalian sensory neurons. J Pharmacol Exp Ther 288(1): 379-388.

Sun H., Varela D., Chartier D., Ruben P.C., Nattel S., Zamponi G.W., Leblanc N. 2008. Differential interactions of $Na^+$ channel toxins with T-type $Ca^{2+}$ channels. J Gen Physiol 132(1): 101-113.

Thomas P. and Smart T.G. 2005. HEK293 cell line: a vehicle for the expression of recombinant proteins. J Pharmacolog Toxicolog Meth 51: 187-200.

Trainer, V.L., Baden, D.G., 1999. High affinity binding of red tide neurotoxins to marine mammal brain. Aquatic Toxicol 46: 139-148.

Trainer, V.L., Baden, D.G., Catterall, W.A., 1994. Identification of peptide components of the brevetoxin receptor site of rat brain sodium channels. J Biol Chem 269: 19904-19909.

Trainer V.L., Baden D.G., Catterall W.A. 1996. Brevetoxin and saxitoxin binding to sodium channel transiently expressed in human kidney cells. In Harmful and Toxic Algal Blooms, Yasumoto T., Oshima Y., Fukuyo Y. Eds. Intergovernmental Oceanographic Commission of UNESCO, pp 467-470.

Trainer VL, Thomsen WJ, Catterall WA, Baden DG. 1991. Photoaffinity labeling of the brevetoxin receptor on sodium channels in rat brain synaptosomes. Mol Pharmacol 40(6): 988-994.

Ueda H. 2006. Molecular mechanisms of neuropathic pain–phenotypic switch and initiation mechanisms. Pharmacol Therapeut 109: 57-77.

Vernoux J.P., Lewis R.J. 1997. Isolation and characterisation of Caribbean ciguatoxins from the horse-eye jack (Caranx latus). Toxicon 35(6): 889-900.

Vernoux J.P, Magras L.P., Abbad el Andaloussi S., Riyeche N. 1986. Evaluation of different stage levels of ciguatera toxicity of the marine food fish chain found around Saint Barthélemy Island in French Antilles. Bull Soc Pathol Exot Filiales 79(2): 275-283.

Vickery R.G., Amagasu S.M., Chang R., Mai N., Kaufman E., Martin J., Hembrador J., O'Keefe M.D., Gee C., Marquess D., Smith J.A. 2004. Comparison of the pharmacological properties of rat Na(V)1.8 with rat Na(V)1.2a and human Na(V)1.5 voltage-gated sodium channel subtypes using a membrane potential sensitive dye and FLIPR. Recept Chann 10(1): 11-23.

Vogel S.M., Atchinson W.D., Narahashi T. 1982. Neuromuscular blocking actions of a purified toxin from the dinoflagellate *Ptychodiscu.s brevis*. Fed Proc 41: 1721.

Wang S.Y., Wang G.K. 2003. Voltage-gated sodium channels as primary targets of diverse lipid-soluble neurotoxins. Cell Signall 15: 151-159.

Westerfield M., Moore J.W., Kim Y.S., Padilla G.M. 1977. How *Gymnodinium breve* red tide toxin(s) produces repetitive firing in squid axons. Am J Physiol 232: C23-C29.

Wu C.H., Huang J.M., Vogel S.M., Luke V.S., Atchison W.D., Narahashi T. 1985. Actions of *Ptychodiscus brevis* toxins on nerve and muscle membranes. Toxicon 23(3): 481-487.

Xue T., Ennis I.L., Sato K., French R.J., Li R.A. 2003. Novel interactions identified between μ-conotoxin and the $Na^+$ channel domain I P-loop: implications for toxin-pore binding geometry. Biophys J 85: 2299-2310.

Yamaoka K., Inoue M., Miyahara H., Miyazaki K., Hirama M. 2004. A quantitative and comparative study of the effects of a synthetic ciguatoxin CTX3C on the kinetic properties of voltage-dependent sodium channels. Br J Pharmacol 142(5): 879-889.

Yamaoka K., Inoue M., Miyazaki K., Hirama M., Kondo C., Kinoshita E., Miyoshi H., Seyama I. 2009. Synthetic ciguatoxins selectively activate $Na_V1.8$-derived chimeric sodium channels expressed in HEK293 cells. J Biol Chem 284(12): 7597-7605.

Yarowsky P.J., Kruegert B.K., Olson C.E., Clevingert E.C., Koos R.D. 1991. Brain and heart sodium channel subtype mRNA expression in rat cerebral cortex. Proc Nat Acad Sci USA Neurobiology 88: 9453-9457.

Young K.A. and Caldwell J.H. 2005. Modulation of skeletal and cardiac voltage-gated sodium channels by calmodulin. J Physiol 565(2): 349-370.

Zimmermann K., Leffler A., Babes A., Cendan C.M., Carr R.W., Kobayashi J.-i., Nau C., Wood J.N., Reeh P.W. 2007. Sensory neuron sodium channel $Na_V1.8$ is essential for pain at low temperatures. Nature 447: 855-859.